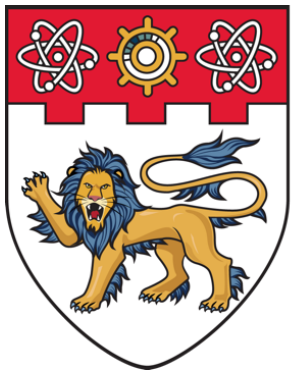

NANYANG TECHNOLOGICAL UNIVERSITY
SINGAPORE

MULTILAYERED SIRNA NANOPARTICLES AS A DELIVERY SYSTEM FOR EXTENDED GENE SILENCING EFFECT

NG JIE YING ALICE

SCHOOL OF MATERIALS SCIENCE AND ENGINEERING

2019

MULTILAYERED SIRNA NANOPARTICLES AS A DELIVERY SYSTEM FOR EXTENDED GENE SILENCING EFFECT

NG JIE YING ALICE

SCHOOL OF MATERIALS SCIENCE AND ENGINEERING

A thesis submitted to the Nanyang Technological University
in partial fulfilment of the requirement for the degree of
Master of Materials Science and Engineering

2019

Statement of Originality

I hereby certify that the work embodied in this thesis is the result of original research, is free of plagiarised materials, and has not been submitted for a higher degree to any other University or Institution.

6th August 2019 *alice ng*

. . . . . .
Date

. . . . . .
Ng Jie Ying Alice

Supervisor Declaration Statement

I have reviewed the content and presentation style of this thesis and declare it is free of plagiarism and of sufficient grammatical clarity to be examined. To the best of my knowledge, the research and writing are those of the candidate except as acknowledged in the Author Attribution Statement. I confirm that the investigations were conducted in accord with the ethics policies and integrity standards of Nanyang Technological University and that the research data are presented honestly and without prejudice.

6th August 2019

. . . . . .
Date

. . . . . .
Professor Subbu Venkatraman

Authorship Attribution Statement

This thesis **does not** contain any materials from papers published in peer-reviewed journals or from papers accepted at conferences in which I am listed as an author.

This thesis includes content where I received support from my supervisor and mentor as follows:

- Professor Subbu Venkatraman and Dr Tan Yang Fei provided the initial project direction.
- I prepared the final thesis. Revisions and advice were taken from Professor Subbu Venkatraman, Dr Tan Yang Fei and Dr Wong Yee Shan.
- I co-designed the study with Dr Tan Yang Fei and Dr Wong Yee Shan.
- I performed all experiments, sample processing and data analysis in Ocular Therapeutics Engineering Centre (OTEC) at the School of Material Science and Engineering (MSE).
- Dr Tan Yang Fei conducted the Confocal laser scanning microscopy (CLSM) imaging for the qualitative investigation on the cellular internalization of 7 layered LbL NPs.
- Jenndy conducted the X-ray Powder Diffraction (XRD) of HAp at the Facility for Analysis, Characterization, Testing and Simulation (FACTS) laboratory. I collected the X-ray diffraction patterns of HAp and conducted data evaluation with guidance rendered to me by Dr Liu Weiling from FACTS laboratory.
- Lim Pei Qi conducted the Transmission electron micrographs (TEM) of the HAp NPs, 3 layered, 5 layered and 7 layered nanoparticles.

6th August 2019 *alice ng*

. . . .

Date Ng Jie Ying Alice

Abstract

At present, various diseases occur without an effective mode of treatment. The production of undesirable proteins leads to the onset of many diseases. For instance, an elevated expression of secreted protein acidic and rich in cysteine (SPARC) is linked with fibrosis and the inhibition of *SPARC* expression reduces fibrosis. This work reports on the successful development of an optimized multilayered nanoparticles (NPs) system, utilizing fibrosis as a model to evaluate the effectiveness of the system in releasing siRNA within cell cytoplasm and the suppression of protein production over 3 weeks. The significance of utilizing the layer by layer (LbL) system is to protect the siRNA from degradation by cellular enzymes and to increase its cell internalization property. The multilayered NPs system contains hydroxyapatite (HAp) NPs as the core material, with alternating layers of the cationic polyelectrolyte poly-L-arginine (PLR) and the SPARC siRNA. The 7 layered LbL NPs coated with PLR >70 000 Da and loaded with 3 layers of siRNA demonstrated the highest total siRNA content compared to other prototypes (lower PLR M_w and lesser siRNA layers) and it was employed for the subsequent *in vitro* tests. The 7 layered LbL NPs of HAp | PLR | siRNA | PLR | siRNA | PLR | siRNA | PLR configuration was 431.30 nm in hydrodynamic diameter with positive surface charge of 42.13 mV. The *in vitro* study showed that the NPs treatment did not cause toxic effects to the Human retroperitoneal fibroblast (HuRPF) cells. The qualitative and quantitative cellular internalization of LbL NPs showed the presence of 6FAM GFP-labelled NPs in HuRPF cells over 21 days. Further, the 7L LbL NPs ability to escape from the endosome to release siRNA in the cytoplasm (site of action of siRNA) was investigated. The amount of free siRNA within HuRPF cells and the *SPARC* knockdown study were evaluated over 21 days. It is important to note that the siRNA was present within the cells and was able to elicit a significant *SPARC* knockdown activity over 21 days. Moreover, the siRNA release profile (within the cells and in PBS medium) showed similar release behavior over 21 days. This suggests the disassembly of LbL NPs through a layer by layer 'onion effect' (starting with the outermost layer) leading to the constant release of siRNA in the cell cytoplasm. This is the first time a study was done to investigate the multilayered delivery system releasing siRNA within

the cells/cytoplasm to cause an effective and prolonged gene silencing effect over 3 weeks with just a single application.

Lay Summary

Currently, various diseases occur without an effective mode of treatment. Additionally, the huge production of certain proteins leads to continued persistence of some diseases. siRNA is a class of double-stranded RNA molecules that suppress the protein production but there is limitation due to the lack of suitable systems to deliver it safely into the cell cytoplasm for its mode of action. This work reports on the successful development of an optimized multilayered nanoparticles (NPs) system utilizing fibrosis as a model to study its effectiveness in releasing siRNA within cell cytoplasm and the suppression of protein production over 3 weeks. The multilayered NPs system utilizes HAp NPs as the core, with alternating layers of the polyelectrolyte (poly-L-arginine, PLR) and the SPARC (secreted protein acidic and rich in cysteine) siRNA. The advantages of utilizing the multilayered NPs system that has a positively charged outermost layer is to facilitate its entry into the cells and to protect the siRNA from degradation by biological molecules. The SPARC siRNA suppresses the production of *SPARC* protein (a protein responsible for the occurrence of fibrosis) and ensuring that only the *SPARC* protein is suppressed for 3 weeks. Studies conducted using *in vitro* (an artificial environment for the growth of cells) methods showed that a single application of the multilayered NPs system suppressed the *SPARC* protein production over 3 weeks. In addition, the NPs treatment did not cause toxic effects to the cells. The study focuses on the investigation of the siRNA amount released within the cell cytoplasm and the suppression of *SPARC* protein production over 3 weeks. The study concludes that the multilayered NPs system disassemble and release siRNA in the cell cytoplasm through a layer by layer 'onion effect' (starting with the outermost layer). This leads to the suppression of *SPARC* protein production over 3 weeks with just a single application. This is the first time a study was done to investigate the multilayered delivery system releasing siRNA within the cell cytoplasm to cause an effective and prolonged suppression of *SPARC* protein production over 3 weeks with just a single application.

Acknowledgements

This dissertation would not have been possible without funding from the NTU-Northwestern Institute for Nanomedicine.

Special thanks are conveyed to my research project supervisor Professor Subbu Venkatraman for his continual guidance, support and wisdom imparted upon me that has been a great asset throughout my Master's degree. I am especially grateful to my mentor and close friend Dr Tan Yang Fei for his patience and incisive recommendations concerning the scope of the research and for his expertise and intelligence with constant encouragement and motivation that has inspired me to new stages of opportunity and strength.

This thesis greatly benefited from the input of Dr Wong Yee Shan who patiently reviewed on the scope of the research and provided her valuable advice and further improvements in the research project.

I am filled with gratitude for all the assistance rendered to me by my peers and friends Dr Liu Weiling, Dr Debasish Mondal, Anastasia Darwitan, Chan Jing Ni, Jenndy, Lim Pei Qi, Shaun Lim Wen Zheng and Toong Wee Yee Daniel when I was conducting some of my experiments at Ocular Therapeutics Engineering Centre (OTEC) and for making my postgraduate journey memorable and smooth so far.

Also, I would like to show my appreciation to Revathy Selvi, Anjanei Dhayalan, Aminuddin, Chaw Su Yin, Ong Boon Chong and Jeremy Lim for their tremendous support and friendship.

Lastly, I would like to thank my family for their everlasting encouragement, love and care which have been a powerful source of support and energy.

Table of Contents

Table Captions

Figure Captions

concentrations, with Ex/Em of 480/520 nm). The samples in the dialysis tubing that were submerged in the glass container was replenished with fresh 10 mL PBS (pH 7.40) for the subsequent timepoints. All samples were prepared and readings measured in triplicates.

Figure 4.3: Cumulative siRNA percent release of 3 layered LbL NPs (loaded with different PLR M_w >70 kDa) in PBS (pH 7.40) medium over a period of 28 days. At the respective timepoint (days 1, 3, 5, 7, 14, 21 and 28), the samples were collected and measured with the microplate reader to observe the amount of 6FAM siRNA percent release (compared against a series of 6FAM siRNA of known concentrations, with Ex/Em of 480/520 nm). The samples in the dialysis tubing that were submerged in the glass container was replenished with fresh 10 mL PBS (pH 7.40) for the subsequent timepoints. All samples were prepared and readings measured in triplicates.

Figure 4.4: Cumulative siRNA release profile of 3 layered, 5 layered and 7 layered LbL NPs (loaded with PLR M_w >70 kDa) in PBS (pH 7.40) medium over a period of 28 days. At the respective timepoint (days 1, 3, 5, 7, 14, 21 and 28), the samples were collected and measured with the microplate reader to observe the amount of 6FAM siRNA release (compared against a series of 6FAM siRNA of known concentrations, with Ex/Em of 480/520 nm). The samples in the dialysis tubing that were submerged in the glass container was replenished with fresh 10 mL PBS (pH 7.40) for the subsequent timepoints. All samples were prepared and readings measured in triplicates.

Figure 4.5: Cumulative siRNA percent release of 3, 5 and 7 layered LbL NPs (loaded with PLR M_w >70 kDa) in PBS (pH 7.40) medium over a period of 28 days. At the respective timepoint (days 1, 3, 5, 7, 14, 21 and 28), the samples were collected and measured with the microplate reader to observe the amount of 6FAM siRNA percent release (compared against a series of 6FAM siRNA of known concentrations, with Ex/Em of 480/520 nm). The samples in the dialysis tubing that were submerged in the glass container was replenished with fresh 10 mL PBS (pH 7.40) for the subsequent timepoints. All samples were prepared and readings measured in triplicates.

Figure 4.6: TEM images of (A) HAp only NPs, (B) 3 layered LbL NPs, (C) 5 layered LbL NPs and (D) 7 layered LbL NPs.

Figure 4.7: MTT assay tracking the cell viability of 500 HuRPF cells after treatment with 7 layered LbL NPs at dosages of 258 μg, 129 μg and 64.50 μg over a span of 2 days (siSPARC = NPs loaded with SPARC siRNA). Measurements were taken using the microplate reader with an absorbance wavelength at 595 nm. All samples were prepared and readings measured in triplicates.

Figure 4.8: Confocal microscopic images of the cellular entry of 7 layered LbL NPs with FITC-labelled HAp. (A) The cell nuclei were visualized by the staining of vectashield with DAPI. (B) Green fluorescence from the 7 layered LbL NPs with FITC-labelled HAp. (C) Brightfield image of the HuRPF cells. (D) Internalization of 7 layered LbL NPs with FITC-labelled HAp in the HuRPF cells as shown in the overlay image. The images were taken at 40X magnification and 4.3X zoom. The sample cells were compared against control cells (without NPs treatment).

Figure 4.9: Flow cytometry analysis of HuRPF cells containing the 7 layered 6FAM siRNA loaded LbL NPs at the respective time interval of day 1, day 3, day 5, day 7, day 14 and day 21. There were 80 % to 90 % of cells containing the 6FAM siRNA loaded LbL NPs for 7 days before a sudden drop was experienced in the cells containing the 6FAM siRNA loaded LbL NPs from day 7 to day 21. All samples were prepared and readings measured in triplicates.

Figure 5.0: Effect of 6FAM siRNA in PBS and in the lysis buffer. The gradients ($y = mx$) remained similar for both the standard curve which suggest that the lysis buffer will not degrade the 6FAM siRNA.

Figure 5.1: Graphical representation of the amount of free siRNA within cells (represented by the orange bar) after the treatment of 7 layered 6FAM siRNA loaded LbL NPs to HuRPF cells at the respective time interval of day 1, day 3, day 5, day 7, day 14 and day 21. The

siRNA remained in NPs (represented by the blue bar) and the siRNA consumed/degraded (represented by the grey bar) at each time interval could also be evaluated. The total amount of siRNA loaded in 50 000 HuRPF cells was 618.13 (± 3.97) pmol. The samples were collected and measured with the microplate reader (compared against a series of 6FAM siRNA of known concentrations, with Ex/Em of 480/520 nm). All samples were prepared and readings measured in triplicates.

Figure 5.2: Immunoblotting analysis of 7 layered siRNA loaded LbL NPs in HuRPF cells at the respective time interval of day 1, day 3, day 5, day 7, day 14 and day 21. (A) Protein separation and antibody treatment over 21 days using Biorad Chemidoc system. siScram-LbL was added into 50 000 HuRPF cells as a negative control in comparison with the siSparc-LbL sample that was added into 50 000 HuRPF cells. (B) Percentage knockdown of *SPARC* over 21 days. All samples were prepared and readings measured in triplicates.

Figure 5.3: *In vitro* cumulative/consumed siRNA release profile within the cells and the cumulative siRNA release profile in PBS (pH 7.40) release medium. The release of siRNA in the cells was higher than the release of siRNA in PBS (pH 7.40) release medium. This could be due to certain interaction of the cellular components in the cytoplasm with the particle system. Hence, induces the higher release profile within the cells. However, the release behavior (within the cells and in PBS medium) were similar over 21 days. All samples were prepared and readings measured in triplicates.

Abbreviations

Ago2	Argonaute 2
BMP-2	Bone morphogenetic protein
$CaCO_3$	Calcium carbonate
CLSM	Confocal Laser Scanning Microscope
DOX	Doxorubicin
DLS	Dynamic light scattering
DDS	Drug delivery system
ECM	Extracellular matrix
ELS	Electrophoretic light scattering
E.E.	Encapsulation efficiency
FTIR	Fourier Transform Infrared Spectroscopy
FITC	Fluorescein isothiocyanate
FRET	Fluorescence resonance energy transfer
GRAS	Generally regarded as safe
GFP	Green fluorescent protein
GPC	Gel permeation chromatography
GAPDH	Glyceraldehyde 3-phosphate dehydrogenase
HAp	Hydroxyapatite
HuRPF	Human retroperitoneal fibroblast
ICSD	Inorganic crystal structure database
LbL	Layer by layer
M_w	Molecular Weight
NPs	Nanoparticles
NaCl	Sodium chloride
PLR	poly-L-arginine
PEG	Polyethylene glycol
PLL	poly-L-lysine
PLH	poly-L-histidine
PEI	Polyethyleneimine

PBS	Phosphate buffered saline
PE	Polyelectrolyte
pI	Isoelectric point
PSC	Pancreatic stellate cells
PSS	Polystyrene sulfonate
PAH	Poly-allyl amine hydrochloride
RFP	Red fluorescent protein
RNAi	RNA interference
ROS	Reactive oxygen species
RISC	RNA-induced silencing complex
shRNA	Short hairpin RNA
SiO_2	Silicon dioxide
siRNA	Small interfering RNA
SPARC	Secreted protein acidic and rich in cysteine
SCMC	Sodium carboxymethyl cellulose
T2DM	Type 2 diabetes mellitus
TEM	Transmission electron microscopy
TRITC	Tetramethylrhodamine
XRD	X-ray diffraction
6-FAM	6-Carboxyfluorescein

Chapter 1

Introduction

This chapter briefly introduces the significance of fabricating the layer by layer (LbL) polymeric nanoparticle (NPs) system utilizing RNAi therapy as an approach in combating against various diseases. Hydroxyapatite (HAp) NPs will be used as the core material of the LbL system, coated with poly-L-arginine (PLR) in its bilayer. siRNA will then be loaded in the LbL system which provides a safe and effective delivery of siRNA into the cells. It briefly describes the advantages of the system in delivering a sustained and extended release of siRNA in vitro for the efficient and prolonged gene silencing effect. Optimization of the LbL NPs system (i.e. the effect of PLR and siRNA amount, the different PLR M_w *and the number of siRNA layers loaded on the LbL NPs system) could be done to increase the total siRNA content in the particles and extend its gene silencing effect. Following this, in vitro studies should be done to investigate the cellular internalization of the particles, the amount of free siRNA released within cells and the gene silencing effect of the LbL NPs for a period of 21 days.*

1.1 Background

The discovery of RNA interference (RNAi) in the year 1998 by Fire *et al.* [1], and the proof by Elbashir *et al.* demonstrating the role of synthetic small interfering RNA (siRNA) resulting in sequence-specific knockdown of targeted gene in cultured mammalian cells [2], have led to extensive efforts in the development of siRNA therapeutics for the various prevention and treatment of disease targets. The therapeutic effect of synthetic siRNA usually lasts several weeks until the siRNA reaches the therapeutic threshold [3]. However, since siRNA are 'naked', they are subjected to degradation by endogenous enzymes such as nucleases inside the cell [4] and the negatively charged surfaces of the siRNA prevent their optimal cellular entry [5]. Thus, the administration and the incorporation of siRNAs in LbL NPs (with selection of biodegradable delivery system that exhibit low toxicity) can safely deliver and increase the transfection efficiency of siRNAs into the cell cytoplasm for their therapeutic treatment of various diseases [6].

The utilization of core-shell NPs for drug delivery often show transient effects, for instance, Cao *et al.* reported that the drugs encapsulated in the Poly Lactic-co-Glycolic Acid (PLGA) core-shell NPs were observed to release more than 50 % of the drug within 12 hours in 37 °C PBS (pH 7.40) release medium [7]. Furthermore, an article published by Fan *et al.* has shown that the rate of release for its raw anti-tumor drug doxorubicin (DOX) was 80.90 % within 6 hours in 37 °C PBS (pH 7.40) release medium, whereas the release of DOX encapsulated within alternate layers of the layer by layer (LbL) NPs resulted in a more sustained releasing rate under 60 % after 72 hours [8]. This suggests that the release behavior is dependent on the distribution of drugs and characteristics of the polymer/external polyelectrolyte (PE) shell used as the drug delivery carrier. Acharya and Park reviewed drug-eluting stents (DES) for drug delivery and proposed that the ability of sustained and prolonged release of drugs encapsulated in LbL NPs depends on the biodegradability of the polymer used [9]. The review also highlighted the controlled release of ionized drugs including nucleic acids (i.e. DNA and RNA) that has made recent advances in the layer by layer (LbL) assembly of NPs.

The LbL approach allows the loading of charged drugs in its bilayers by electrostatic interactions between the alternation of cationic and anionic charged PE [10]. It was found that the multilayered NPs provided a sustained and prolonged release of drugs at physiological pH condition [11]. Another study by Lee *et al.* observed that the multilayered NPs fabricated with oppositely charged poly-L-lysine (PLL) and siRNA in its bilayers demonstrate gradual siRNA release due to the slow degradation of PLL [12]. This suggests that the polymer/external polyelectrolyte (PE) shell of the LbL NPs should be biodegradable for slow degradation of the PE layer in order to achieve a sustained and prolonged release of therapeutic agents under physiological pH condition. Furthermore, the same study also showed extended gene silencing effect with an increased number of siRNA layers loaded. Also, a study conducted by Eltoukhy *et al.* on the effect of polymer molecular weight (M_w) on DNA transfection in HeLa cells shows that the transfection activity increased with the polymer M_w and this could lead to the increase in gene silencing activity [13].

Over the years, the LbL NPs incorporation of siRNA has been investigated to deduce the maximal duration of siRNA delivery in the cells. For instance, Castleberry *et al.* did a study on the degradation and sustained release profile of 3 layered LbL siRNA NPs and found that the release of siRNA from the NPs lasted for 10 days [14]. This suggests the possibility that with additional siRNA layers encapsulated on the LbL NPs, it could result in a more sustained and prolonged siRNA release profile *in vitro*. Thus, the duration of siRNA release could depend on the length of time needed for the therapeutic effects to actuate, thereby dictating the construction of respective number of layers of siRNA incorporated in the LbL NPs.

Presently, various diseases occur without an effective mode of treatment and the huge production of certain proteins leads to continued persistence of some diseases. For instance, fibrosis occurs due to the excessive secretion and deposition of extracellular matrix (ECM) present in tissues that leads to the onset of various diseases such as interstitial pulmonary fibrosis, chronic inflammation and in diabetes [15]. An elevated expression of secreted protein acidic and rich in cysteine (SPARC) in fibrosis is often reported in various studies

and the inhibition of SPARC expression reduces fibrosis [16, 17]. Therefore, the problem of fibrosis could be overcome by using SPARC siRNA to silence SPARC gene in the cytoplasm (which will in turn control fibrosis) [18]. The layer by layer (LbL) self-assembly system could be used to load the anionic siRNA with alternating layers of cationic PE to protect the siRNA from degradation by cellular enzymes and to increase its internalization into cells. This is expected to reduce fibrosis by the sustained release behavior of the LbL system for an extended therapeutic delivery effect *in vitro.* In a previous study conducted by Tan *et al.*, it was investigated that the LbL NPs system incorporating SPARC siRNA with alternating layers of poly-L-arginine (PLR) were coated efficiently onto HAp particles as the core material. It was found that the internalization into Human Foreskin Fibroblast (FibroGRO) cells was by endocytosis and the LbL NPs were able to escape from the endosomal complex into the cytoplasm for gene silencing of SPARC by 60 % (96 hours post NPs treatment) using one layer of SPARC siRNA loaded LbL system [19]. Furthermore, the LbL SPARC siRNA NPs system was proven to be non-toxic to FibroGRO cells which provides an optimistic approach as a safe and systemic delivery platform for the non-viral vector development of siRNA therapy that reduces the occurrence of fibrosis.

In this thesis, the LbL NPs system incorporating SPARC siRNA was utilized to investigate the effects of some parameters of the LbL-coated HAp nanoparticles for increasing the total siRNA content to provide an efficient and prolonged gene silencing effect over 21 days with a single application. It was found that the multilayered NPs coated with more layers of siRNA were able to maximize the total siRNA content and release the most amount of siRNA at each time interval for an extended period of time. Releasing more amount of siRNA at each time interval could result in a greater gene silencing effect to cause a significant amount of gene knockdown [20, 21]. Currently, there are limited studies done to evaluate the siRNA release within cells/cytoplasm to cause an efficient and prolonged gene silencing effect. Therefore, *in vitro* studies were done in this thesis to investigate the cellular internalization of LbL NPs, the disassembly of LbL NPs in the cells and the amount of siRNA release within cells, as well as to validate the efficient and prolonged release of siRNA to cause significant gene silencing effect over 21 days.

1.2 Problem Statement

A number of therapeutic gene silencing agents based on siRNA have been discovered. However, their prolonged action inside diseased cells have been limited to a few hours or days due to lack of control over their release. This thesis describes and validates the fabrication of layer by layer (LbL) NPs system incorporating multiple layers of siRNA to effectively deliver siRNA into the cells for an efficient and prolonged gene silencing effect.

1.3 Hypothesis

Varying the characteristics of the poly-L-arginine used in the layers of an LbL-coated hydroxyapatite nanoparticle leads to high loadings of siRNA and to extended duration of release of the siRNA.

1.4 Objective and Scope

The objective of this study is to quantify the effects of some parameters of the LbL-coated hydroxyapatite (HAp) nanoparticles on the following:

(a) siRNA loading per particle
(b) Prolonged release of the loaded siRNA *in vitro* and inside cells
(c) Prolonged gene silencing effect in cells *in vitro*

HAp will be used as the anionic core material of the LbL system. Poly-L-arginine (PLR) will be used as the positively charged linear polymer layer in the synthesis of the LbL nanoparticles (NPs) followed by the loading of negatively charged SPARC siRNA layer to generate the LbL NPs system. Human retroperitoneal fibroblast (HuRPF) cells will be used for the *in vitro* tests. The focus of this study illustrates the effectiveness of the optimized particle designed as a siRNA delivery vehicle with a prolonged effect over 21 days.

1.5 Dissertation Overview

The dissertation is organized into the following 6 chapters.

Chapter 1 briefly introduces the significance of fabricating and optimizing the layer by layer (LbL) polymeric nanoparticle (NPs) system utilizing RNAi therapy to safely deliver siRNA into cells for the efficient and prolonged gene silencing effect. This chapter briefly describes the *in vitro* studies to be done for investigating the cellular internalization of LbL NPs, how LbL NPs breakdown in the cells, the amount of siRNA released within cells and the efficient and prolonged release of siRNA which enables the significant gene silencing effect over 21 days. The hypothesis, objective and scope are presented in this chapter.

Chapter 2 summarizes the background and current research related to the work in this thesis. The chapter discusses the use of RNAi technology and provides detailed information on the advantages of utilizing the LbL NPs system as an ideal siRNA delivery carrier. It addresses the current research and challenges of fibrosis which will be used as a model to study the effectiveness of the LbL NPs system. This chapter also describes the advantages of using the various reagents for the fabrication of the LbL delivery system. The effects of the various parameters on the cellular internalization and release profile of LbL NPs *in vitro* (both in PBS medium and in the cells) for extended gene knockdown will also be discussed.

Chapter 3 defines the materials and methods adopted in this thesis.

Chapter 4 reports the results and discussion on the characterization and optimization of the LbL NPs with the aim of maximizing the total amount of siRNA that can be loaded in the LbL NPs system to cause an effective and prolonged gene silencing effect over 21 days. The effect on the amount of poly-L-arginine (PLR) and siRNA on LbL NPs were evaluated and it was found that there was no significant difference to the total amount of siRNA content in the particles. Following this, the effect on the fabrication of LbL NPs with different PLR molecular weight (M_w) was carried out. It was observed that the particles

coated with the highest PLR M_w showed the most amount of total siRNA content and released the fastest and highest amount of siRNA (in PBS medium) at each time interval over 28 days. Moving on, the NPs coated with the highest PLR M_w was further optimized with additional layers of siRNA loading. It was found that the LbL NPs loaded with the greatest number of siRNA layers exhibited the most amount of total siRNA content and released the fastest and highest amount of siRNA (in PBS medium) at each time interval over 28 days. The optimized multilayered NPs were tested for their cell viability followed by investigating the particles' internalization into cells. Finally, the study proceeded to find out the amount of free siRNA and its release within the cells, as well as the gene silencing effect of utilizing the LbL NPs system incorporating the RNAi technology. It was observed that the LbL NPs system was able to effectively deliver siRNA into the cells, where the siRNA escaped from the endosome into the cytoplasm, to cause a significant amount of gene silencing effect over 21 days. All in all, the study shows that the developed multilayered siRNA loaded particle could sustained release of siRNA within the cytoplasm and elicit prolonged gene silencing effect with just a single application over 3 weeks.

Chapter 5 proposes the future possibility of utilizing the multilayered NPs system by modification of the HAp core material to increase the overall negative surface potential. The increased negative surface potential of the core material could in turn allow the binding of more cationic poly-L-arginine (PLR) layers, hence compensating the loss of the PLR layers from the necessary washing steps during the fabrication process. The chapter also proposes the utilization of the designed system to incorporate other types of therapeutic agents (i.e. loading of different kind of siRNA) for gene silencing of a wide variety of diseases with just a single application. Further investigations could be done to examine the mRNA levels in the cell cytoplasm which could correlate with the gene knockdown study. *In vivo* studies could also be done to test the effect of the LbL NPs system on diseased animals and the possibility of introducing this system into clinical trials in future.

Chapter 6 presents the conclusion from all the above findings and to extend the focus on when and how the nanoparticles release siRNA within cells and their correlation with the efficient and prolonged gene silencing effect for a period of 21 days. The chapter also

concludes that further investigations on the future work of utilizing the same multilayered NPs system will be fruitful.

1.6 Findings and Outcomes/Originality

This research has led to several novel outcomes:

1. Fabricated an optimized layer by layer NPs system incorporating RNAi therapy to maximize the loading of total siRNA content in the particles. To safely deliver siRNA into HuRPF cells for the efficient and prolonged gene silencing effect over 21 days with just a single application.
2. The release profile of the LbL NPs loaded with siRNA was done to observe its release behavior in PBS medium and in the HuRPF cells. The amount of siRNA within cells was evaluated and it was shown to correlate with the amount of gene knockdown over 21 days. This provides an insight on the prolonged gene silencing effect.
3. The flexibility to modify the LbL NPs system to cater to different disease targets.

References

[1] Andrew Fire, S.X., Mary K. Montgomery, Steven A. Kostas, Samuel E. Driver & Craig C. Mello, *Potent and specific genetic interference by double-stranded RNA in Caenorhabditis elegans.* Nature, 1998. **391**(6669): p. 806-811.

[2] Sayda M. Elbashir, J.H., Winfried Lendeckel, Abdullah Yalcin, Klaus Weber and Thomas Tuschl, *Duplexes of 21-nucleotide RNAs mediate RNA interference in cultured mammalian cells.* Nature, 2001. **411**(6836): p. 494-498.

[3] Davis, D.W.B.a.M.E., *Insights into the kinetics of siRNA-mediated gene silencing from live-cell and live-animal bioluminescent imaging.* Nucleic Acids Research, 2006. **34**(1): p. 322–333

[4] Rosemary L Kanasty, K.A.W., Arturo J Vegas and Daniel G Anderson, *Action and Reaction: The Biological Response to siRNA and Its Delivery Vehicles.* Molecular Therapy, 2012. **20**(3): p. 513–524.

[5] Jie Wang, Z.L., M. Guillaume Wientjes, and Jessie L.-S. Au, *Delivery of siRNA Therapeutics: Barriers and Carriers.* The AAPS Journal, 2010. **12**(4): p. 492-503.

[6] Katyayani Tatiparti, S.S., Sushil Kumar Kashaw and Arun K. Iyer, *siRNA Delivery Strategies: A Comprehensive Review of Recent Developments.* Nanomaterials, 2017. **7**(77): p. 1-17.

[7] Yang Cao, B.W., Yazhou Wang, Deshuai Lou, *Dual Drug Release from Core–Shell Nanoparticles with Distinct Release Profiles.* Journal of Pharmaceutical Sciences, 2014. **103**(10): p. 3205-3216.

[8] Jingqian Fan, R.L., Yuangang Liu, Shibin Wang, Yulu Liu, Ran Zhang and Ranjith Kumar Kankala *Synthesis and characterization of innovative poly(lactide-co-glycolide)-(poly-L-ornithine/ fucoidan) core–shell nanocarriers by layer-by-layer self-assembly.* RSC Adv., 2017. **7**(52): p. 32786–32794.

[9] Ghanashyam Acharya, K.P., *Mechanisms of controlled drug release from drug-eluting stents.* Advanced Drug Delivery Reviews, 2006. **58**(3): p. 387–401.

[10] M. Keeney, X.Y.J., M. Yamane, M. Lee, S. Goodman, and F. Yang, *Nanocoating for biomolecule delivery using layer-by-layer self-assembly.* J Mater Chem B Mater Biol Med. , 2015. **3**(45): p. 8757-8770.

[11] Mehrotra S, L.D., Maloney R, Pawelec KM, Tuszynski MH, Lee I, Chan C, Sakamoto J., *Time Controlled Protein Release from Layer-by-Layer Assembled Multilayer Functionalized Agarose Hydrogels.* Adv Funct Mater, 2010. **20**(2): p. 247–258.

[12] Dr. Seung Koo Lee, M.S.H., Dr. Subashini Asokan, and Prof. Ching-Hsuan Tung, *Effective Gene Silencing by Multilayered siRNA Coated Gold Nanoparticles.* Small, 2011. **7**(3): p. 364–370.

[13] Ahmed A. Eltoukhy, D.J.S., Christopher A. Alabib, Jay S. Rajand, Robert Langer, and Daniel G. Anderson, *Effect of molecular weight of amine end-modified poly(β-amino ester)s on gene delivery efficiency and toxicity.* Biomaterials, 2012. **33**(13): p. 3594–3603.

[14] Steven Castleberry, M.W.a.P.T.H., *Nano-Layered siRNA Dressing for Sustained Localized Knockdown.* ACS Nano. , 2013 **7**(6): p. 1-20.

[15] Wynn, T., *Cellular and molecular mechanisms of fibrosis.* J Pathol., 2008. **214**(2): p. 199–210.

[16] Bradshaw, J.T.-e.a.A.D., *The Function of SPARC as a Mediator of Fibrosis.* The Open Rheumatology Journal, 2012. **6**: p. 146-155.

[17] Jiu-CunWang, S.L., Xinjian Guo, Xuefeng Zhang, Benoit de Crombrugghe, Sonali Sonnylal, Frank C Arnett and Xiaodong Zhou, *Attenuation of fibrosis in vitro and in vivo with SPARC siRNA.* Arthritis Research & Therapy 2010. **12**(2): p. 1-9.

[18] Catalina Atorrasagasti, J.B.A., Leonardo Hofman, Laura Alaniz, Mariana Malvicini, Mariana Garcia, Lorena Benedetti, Scott L. Friedman, Osvaldo Podhajcer, and Guillermo Mazzolini, *SPARC downregulation attenuates the profibrogenic response of hepatic stellate cells induced by TGF-β1 and PDGF.* Am J Physiol Gastrointest Liver Physiol, 2011. **300**(5): p. G739–G748.

[19] Yang Fei Tan, R.C.M., Min Hui Averil Chen, Jacqueline Lessig, Björn Neu, Subbu S. Venkatraman, and Tina T. Wong, *Layer-by-Layer Nanoparticles as an Efficient siRNA Delivery Vehicle for SPARC Silencing.* Small, 2014. **10**(9): p. 1790–1798.

[20] Cheol Am Hong, H.Y.S.a.Y.S.N., *Layer-by-layer siRNA/poly(L-lysine) Multilayers on Polydopamine-coated Surface for Efficient Cell Adhesion and Gene Silencing.* Scientific Reports, 2018. **8**(7738): p. 1-7.

[21] Betul Bozdogan, O.A., Ekin Çelik, Mustafa Turk and Emir Baki Denkbas, *Novel layer-by-layer self-assembled peptide nanocarriers for siRNA delivery.* RSC Adv., 2017. **7**: p. 47592–47601.

Chapter 2

Literature Review

This review discusses the fabrication of layer by layer (LbL) nanoparticles (NPs) system incorporating RNAi technology, with the effects of various parameters on the cellular entry and release profile of LbL NPs in vitro (both in PBS medium and inside the cells) for an efficient and prolonged gene knockdown effect. This chapter also addresses the current research and challenges of fibrosis which will be used as a model to study the effectiveness of the LbL NPs system.

2.1 The occurrence of fibrosis

Fibrosis is the development of excessive connective tissues that cause scarring and affect organs of the body and the skin. There is a wide variety of fibrotic diseases, including atherosclerosis, asthma, cirrhosis and diabetes mellitus [1]. For instance, diabetes mellitus is currently one of the main causes of concern affecting public health globally. That is characterized by a group of metabolic diseases due to hyperglycemia as the body is unable to produce insulin and consequently, leads to abnormally high levels of glucose in the bloodstream. As the disease progresses, it results in chronic hyperglycemia that leads to failure and damage of various organs such as the eyes, kidney and heart in the long-term [2]. Epidemiological researchers have reported that 285 million people worldwide were diagnosed with diabetes in the year 2010, and the disease is expected to increase by the year 2030 to 439 million people worldwide [3].

An example of such fibrosis is type 2 diabetes mellitus (T2DM) which usually occurs as a result of the dysfunction of pancreatic β-cells in the body due to the lack of insulin production. The body is resistant to the effects of insulin and do not respond or produce enough insulin to regulate the normal homeostasis processes. Hence, this leads to the build-up of glucose in the bloodstream [4]. Islet fibrosis happens when clusters of cells in the pancreas experienced an inflammatory reaction that leads to an excessive deposition of extracellular matrix components. Islet fibrosis was observed in rat models and in T2DM patients. Pancreatic stellate cells (PSC) were found located in the islets in which PSC activation is associated with the length of islet fibrosis [5, 6]. The activation of PSC occurs when it is transformed from an inactive state to an activated form, which is responsible for the production of extracellular matrix (ECM) proteins such as collagens, elastin, fibronectins, etc. [7]. Therefore, PSC in its activated form would lead to the synthesis of ECM proteins and upregulate a variety of factors to cause the occurrence of fibrosis in islet cells.

2.1.1 Therapies for fibrosis and its limitations

Over the years, there have been a wide variety of drugs developed as anti-fibrotic agents. The TGFβ pathway is known to be the main mediator of fibrosis initiation in various fibrotic diseases and an antagonism of this pathway is essential for the treatment of fibrosis [8, 9]. Another example as mentioned earlier was the pancreatic stellate cells (PSCs), among other factors such as insulitis and islet inflammation, are associated with fibrosis in diabetes mellitus [10]. Researchers have been studying the effects of using anti-fibrotic agents, gene therapy and receptor antagonist to counter the activation of PSCs, inflammation and fibrosis in islet and β-cells. For instance, Lee *et al.* conducted a study on rat PSCs cultured with high glucose content for 4 days. It was found that there was an increase in cell proliferation rates and also in the release of collagen. However, treatment with Pirfenidone (anti-fibrotic agent) was found to attenuate these effects, and also in the *in vivo* study it showed that the rats injected with Pirfenidone exhibited a lower degree of islet fibrosis in comparison with control rats [6]. Another *in vivo* study conducted by Lacraz *et al.* found that certain genes involved in endothelial cell activation, inflammation, etc., showed an upregulation in islet cells. However, a downregulation of the genes was observed after interleukin-1 (IL-1) receptor antagonist (IL-1Ra) treatment. This means that IL-1Ra could be used to counter the effect of inflammation on islet endothelial cell, and hence mediate fibrosis [11].

However, despite the use of anti-fibrotic agents, gene therapy and receptor antagonist could aid in the anti-fibrotic activities, they might not result in a controlled and prolonged effect of the therapeutics. For instance, the use of unmodified siRNA may be able to elicit a gene silencing effect but it is fragile and subjected to degradation by nucleases, and with their negatively charged surface it prevents the optimal entry into the cells. Therefore, it is unable to sustain and prolong these therapeutic activities [12, 13].

2.1.2 Proposed idea to overcome the limitations

The aim of this project is to focus on the effect of various parameters in the construction of a layer by layer (LbL) technique and with the incorporation of RNA interference (RNAi) technology, that provides a more efficient and prolonged therapeutic effect over an

extended period of 3 weeks. siRNA is fragile and is subjected to degradation by cellular nucleases, coupled with their negatively charged surface it prevents the optimal internalization into cells. The LbL nanoparticles (NPs) system is an important technique to be applied in this project such that the system will serve as a delivery carrier, transporting the siRNA safely into the cells/cytoplasm to initiate gene silencing. The LbL NPs system contains a core material which will be fabricated with the alternating layers of positively charged polyelectrolyte and the negatively charged siRNA.

With utilizing the LbL NPs system, a greater amount of polyelectrolyte and siRNA could be loaded in the NPs per layer to examine a potential increase in the total siRNA content. The NPs fabricated could be coated with different PLR molecular weight (M_w) and also with the additional layers of siRNA to maximize its total siRNA loading capacity. The siRNA release behavior (in PBS release medium) could be evaluated. A greater amount of total siRNA content in the LbL NPs could lead to a higher and faster siRNA release. This would result in an efficient and prolonged therapeutic effect, reducing the number of NPs treatment to the cells. More siRNA could be packed in between the layers of the NPs with a single application. It is important to carry out this study so as to maximize the NPs ability to cause an efficient and prolonged gene silencing effect with low toxicity in a single application. This could be further validated by the observation of the NPs cellular internalization and its ability to escape from the endosome to the cell cytoplasm, releasing the siRNA for its mode of action. Most NPs are found to accumulate in lysosomes and get digested if they are unable to escape from the endosomes [14]. Hence, by utilizing the LbL system, the outermost polyelectrolyte layer which is highly positively charged, could protect the NPs from lysosomal enzymes through extensive pore formation [15]. Investigations on the amount of siRNA release (within cells/cytoplasm) could be evaluated. Consequently, the effectiveness of the NPs system could be examined by the ability of the system in causing a prolonged and significant gene silencing effect over 3 weeks.

This project will utilize siRNA as the therapeutic agent loaded in the LbL NPs system because it has a huge potential to revolutionize the therapy catered for various diseases.

2.2 RNA interference (RNAi) technology

2.2.1 Mechanism of RNAi

Gene therapy reduces the occurrence of various diseases, through silencing of gene expression using the RNAi technology. This technology is widely known to be an intrinsic cellular process in post-transcriptional gene silencing with therapeutic ability. RNAi plays a role as the key pathway in eukaryotic cells that is triggered by double-stranded (ds) RNA. In turn, they are cleaved into siRNA (small dsRNAs, 20-24 base-pairs in length) by the Dicer9 enzyme. Once siRNA is found to be present in cytoplasm of the cell, it will be incorporated into the RNA-induced silencing complex (RISC) in which the multifunctional protein, Argonaute 2 (Ago2, found within RISC), would unwind the siRNA for the antisense strand to cleave the corresponding mRNA targets which silences their gene expression. The sense strand of siRNA is removed for degradation by cellular nucleases [16].

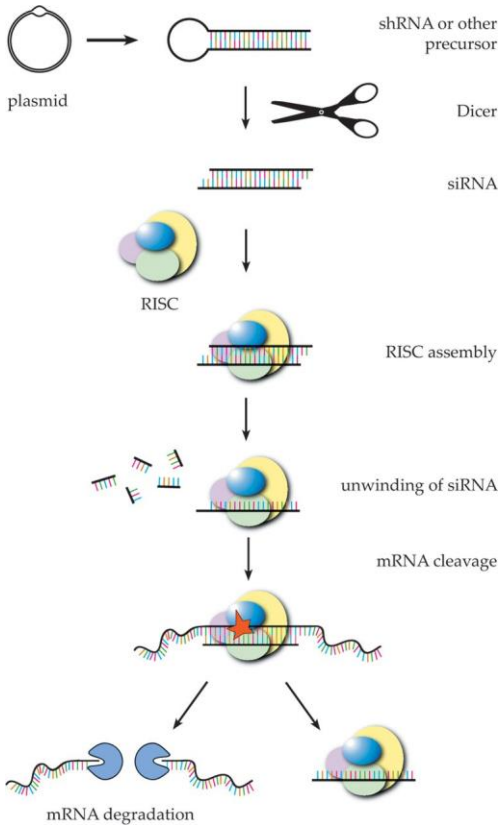

Figure 2.1: Schematic of RNAi mechanism. dsRNA is cleaved into siRNA by Dicer which is then incorporated into RISC complex, followed by unwinding siRNA by Ago2. The sense strand would be removed, and the antisense strand cleaves corresponding mRNA targets to silence the gene expression [17]. [Taken from Cejka *et al.*, 2006]

2.2.2 Advantages and limitations of RNAi technology

Due to its highly specific targeting of genes, RNAi technology has been used to elucidate the roles of individual genes that is involved, especially in diseases. The development of siRNA (specifically target the mRNA for degradation) and shRNA (RNA molecule used for targeted gene silencing) libraries allowed the systematic gene analysis. This is required for various disease processes including cancer which silences the expression of genes. For instance, Rho GTPases (molecular switches controlling variety of signaling transduction pathways in all eukaryotic cells) contributes to various processes that would lead to the progression to cancer, such as the promotion of cancer proliferation, survival, invasion and

metastasis [18]. Pille *et al.* has demonstrated in a study that the anti-RhoA and anti-RhoC siRNA have inhibited cell proliferation and invasion more effectively as compared to conventional drugs *in vitro* and *in vivo* [19].

However, there are also limitations in using RNAi technology such as its off-target effect in which the anti-sense strength might actually interact with other non-targeted strands with similar sequences. This in turn leads to the unintended silencing of non-targeted genes. This could be improved by the design of siRNA incorporating various siRNA duplexes for the silencing of the target gene of interest [20]. Unmodified siRNA could also trigger an activation of the body's immune system and leads to the uncontrolled release of cytokines and other immune-inflammatory effects. Nevertheless, this could be abrogated by a chemical modification of siRNA with the selective use of modified 2'-O-methyl (2'OMe) nucleotides [21]. 'Naked' siRNA would usually be degraded *in vivo* and would not be able to enter into cells due to its large size [22] and negative charged surface [23]. Therefore, a vector or drug delivery system could be introduced to encapsulate and deliver the siRNA into cells safely and to release its content for therapeutic purposes.

2.2.3 Delivery systems for RNAi based gene therapy

Modified 'naked' siRNA can be transferred into cells directly by injection. However, multiple injections would be needed to achieve a higher percentage of total transgenic expression. Further, despite being a safe and simple method, it has a low gene delivery efficiency and accordingly it is more applicable for use in vaccination than the use as a siRNA therapeutics in the treatment of diseases [24, 25].

There are other delivery systems available for RNAi based gene therapy. They can be in the form of viral vectors (utilizing viruses such as retrovirus, adenovirus, lentivirus, etc.) which is one of the most successful systems available to date [26]. The genomes of the viruses have been modified to make them safe and also some viral vectors have been designed with specific receptors that allows the transfer of transgenes to specific cells [27]. However, since these vectors originate from viruses, there are still concerns regarding their

immunogenic and inflammatory effects. Therefore, where clinical applicability is concerned, non-viral vectors would still make a better choice as a siRNA delivery system as compared to viral vectors.

Cationic lipids and cationic polymers are the more frequently used non-viral vectors. Cationic lipids consist of a positively charged head group that binds with negatively charged phosphate group in nucleic acids, forming the lipoplexes [28, 29]. However, its neutralization and rapid elimination from the bloodstream are some drawbacks of this delivery system [30]. Cationic lipids usually accumulate in the Reticuloendothelial System (RES, primary organs associated includes the liver and spleen) and they are prone to clearance by immune cells such as macrophages [31]. Furthermore, the cells present in the RES are part of the innate immune system and this has raised questions on whether the macrophage saturation by cationic lipids will induce immunosuppression and increase the risk of infections [30, 32]. Conjugating the hydrophilic polymer polyethylene glycol (PEG) to the lipid membrane is a strategy to improve its blood circulation times and prevent the clearance by RES [33, 34]. PEGylation creates a concentration of highly hydrated groups which sterically prevents the hydrophobic and electrostatic reactions with the plasma proteins/cells, hence it reduces liposomal uptake by RES [34]. However, there are studies showing that the use of PEG could minimize but does not completely overcome the liposomal uptake by RES [35, 36]. In a recent study by Nunes *et al.* showed that the use of PEG coating on the liposomes did not result in a better *in vivo* profile [37]. The *in vivo* assay showed similar blood clearance and accumulation of the liposomes by RES.

Cationic polymers such as poly-L-arginine (PLR) and poly-L-lysine (PLL) are widely studied polymers with net positive charges. As the molecular weight of these polymers increases, they form more stable complexes, which leads to an increase in polymer adsorption [38]. Polyethyleneimine (PEI) is another cationic polymer that has low cytotoxicity, high transfection activity *in vitro*, with the ability to form toroidal polyplex NPs that are stable and would not form aggregates in physiological conditions [39]. Furthermore, cationic polymers were found to exhibit ‘proton-sponge’ effects with high buffer capacities over a broad range of pH (pH 5 to pH 8). This causes the rupture of

endosomes, allowing the NPs to escape into the cytoplasm, releasing the nucleic acids for their mode of action [40, 41].

2.3 Layer by layer (LbL) nanoparticles (NPs)

2.3.1 LbL NPs synthesis

The LbL NPs synthesis is a well-established technique that provides a wide range of applications such as the utilization as a drug delivery system to protect and transport therapeutic agents (i.e. siRNA) into the cells, in tissue engineering and in biomimetics research [42, 43]. The LbL self-assembly technique is mainly driven by electrostatic interactions, that was first described in 1966 by Iler [44], between oppositely charged polyelectrolytes (PE) on a charged core template NPs, such as polymers, silica, liposomes, etc. [45]. Apart from the electrostatic interactions, the LbL self-assembly can also be driven by hydrogen bonding, covalent bonding, van der Waals forces and bio-specific interactions [46]. The LbL NPs allows the discovery of new NPs with tunable interactions between cells and particles. It also generates a NPs system that enables the sustained release of drugs and siRNA. Further, the thickness of PE used for the formation of LbL NPs would provide information on the final size of LbL NPs.

To synthesize the LbL NPs, a charged core template NP would be immersed in the oppositely charged PE solution. After a certain amount of time, the first layer would be coated onto the core. The NPs would undergo washing steps to remove excess PEs that are uncoated. After that, the PE coated core NPs would then be immersed into the second PE having an opposite surface charge to the previous PE, thus reversing the NPs surface charges. This process would be repeated to achieve the desired layer by layer configuration. (An illustration of the LbL NPs synthesis is shown in Figure 2.2)

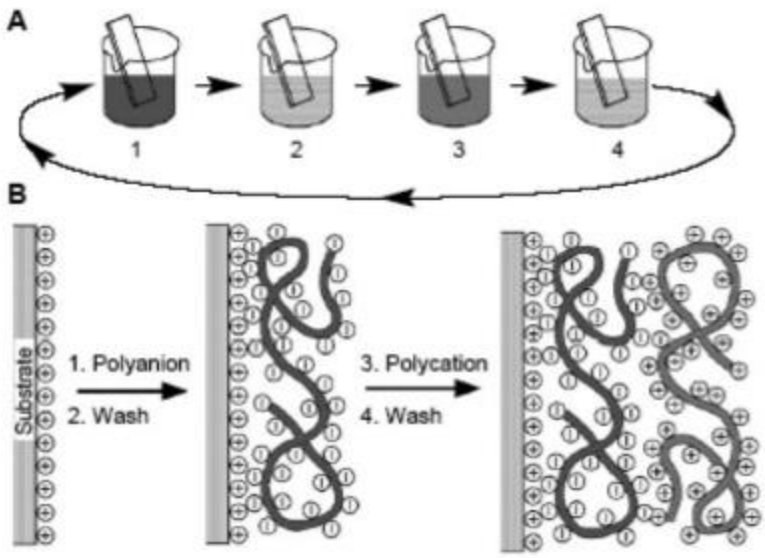

Figure 2.2: Schematic of LbL NPs self-assembly synthesis process via electrostatic interactions. (A) Illustration of deposition of polyelectrolyte film. (B) Illustration of electrostatic interactions of the LbL synthesis [47]. [Taken from Geest *et al.*, 2007]

2.3.2 Advantages of LbL NPs self-assembly technique

The LbL NPs self-assembly technique has been widely used since its discovery, and it has also evolved into the synthesis of novel materials that can be utilized in a wide variety of applications [48]. Additionally, studies have shown that drug loading is dependent on the pH of the solution during the self-assembly process and this could be further tuned according to the drug loaded. This suggests that in order to achieve a stable system, the optimal pH condition of synthesizing the NPs is important for the success of the fabrication process [49]. Finally, the use of LbL NPs system helps to aid in the encapsulation of various therapeutics which in turn increases the potency of drugs administered and eliminates drug resistance. Further, as the synthesis is usually carried out in an aqueous medium, there is very little mechanical force exerted onto the drug or nucleic acid and consequently, they will not be degraded in the process [50]. Given the versatility of this technique, it has been utilized in many different areas, especially in medicine to control and sustain the release of therapeutic drugs.

2.3.3 Application of LbL NPs: Recent development on HER2 gene silencing

Various studies have employed the LbL NPs technique for gene therapies. The most recent findings by Bozdogan *et al.* were arrived at by utilizing this technique to fabricate a siRNA nanocarrier system which consists of the core diphenylalaninamide (FFA) NPs for the silencing of the HER2 gene (commonly overexpressed in breast cancer). The FFA NPs was fabricated with poly-L-lysine (PLL) which is a positively charged polyelectrolyte that increases the stability of core FFA NPs at physiological pH and temperature. The PLL coated NPs were then fabricated with the next layer of polyanionic HER2 siRNA, which were again coated with a second layer of PLL to protect the siRNA and to achieve effective cellular internalization [51]. TEM analysis showed that the size of the FFA NPs was 460 nm with spherical shape morphology. This value corresponded to the dynamic light scattering (DLS) measurement for their mean size to be at 470 nm with zeta potential measurements against water (pH 7) at -13.60 ± 6.40 mV. The gene expression analysis experiment was carried out on two different gene carrier formulations (Batch 1: FFA NPs | PLL | HER2 siRNA | PLL, and, Batch 2: FFA NPs | PLL | HER2 siRNA) to test for their respective abilities to silence HER2 gene in BT-474 breast cancer cell line. It was observed that the gene carrier formulation for Batch 1 results in greater gene silencing as compared to the Batch 2 formulation. This is also validated by previous studies showing that highly positively charged NPs will have a better gene silencing effect [52-54]. This indicates that with the second layer of PLL encapsulating the siRNA, there will be more efficient cellular internalization of NPs because the cellular membrane is negatively charged. Also, the positively charged PLL is able to protect and assist the siRNA cellular internalization and its subsequent release into the cytoplasm through endosomal escape. Therefore, it was concluded that this LbL NPs system has the potential to specifically target the overexpression of the HER2 gene using RNAi technology.

2.3.4 LbL NPs used for RNAi based gene therapy

RNAi based gene therapy was extensively studied in the past decades for its advantages in the treatment of various diseases. The LbL NPs system has the advantage of ensuring the

subsequent re-administration of siRNA based on RNAi gene therapy, by utilizing its ability to form multilayered complexes. This allows for a more controlled and prolonged gene silencing effect. A study conducted by Lee *et al*. described the fabrication of a multilayered NPs system incorporating siRNA for evaluating its gene silencing effect for a prolonged period [55]. The study showed that the multilayered NPs were efficiently internalized into the MDA-MB231 cells by endocytosis and the NPs are gradually releasing siRNA following the degradation of the polypeptide layers. The experiment lasts for 10 days and the gene silencing was still effective even after the cells have undergone cell division. This suggest the ability of LbL NPs system utilizing RNAi gene therapy to cause a prolonged gene silencing effect. However, the study did not report on the number of siRNA layers that was incorporated in the multilayered NPs system that causes the prolonged gene knockdown. It would also be interesting to know the amount of siRNA that is present inside the cells at each time interval for a better correlation between the effectiveness of the NPs system and the subsequent gene silencing effect.

The LbL technique allows the control over the film thickness and the controlled release of the therapeutic agent. This was believed that it may correspond to the degradation/defoliation of the layers from the top-down [56]. Therefore, the consistent release of the therapeutic agent at the stipulated time intervals. Hence, with the advantages of the LbL NPs system incorporating the RNAi technology, the multilayered NPs system will be utilized in this thesis as the carrier for gene therapy for at least two reasons. First, this system has the ability to protect the siRNA. Second, this system is able to achieve an effective cellular internalization that in turn enables a controlled release and prolonged gene silencing effect.

2.4 Design of LbL nanoparticles

2.4.1 Selection of anionic core material

Existing studies on LbL NPs utilizes various core materials to act as the drug delivery carrier and some of the selection criteria of such core material would be for instance, in the

case of this thesis, to have a sufficient negative charge surface so that it will be able to bind to the positively charged PEs. Some of the core materials commonly used includes HAp NPs, silicon dioxide NPs, and calcium carbonate ($CaCO_3$) NPs. For instance, a study by Peng *et al.* utilized multilayered $CaCO_3$ NPs to encapsulate the anti-cancer drug known as etoposide. In that study, it shows that the encapsulated etoposide multilayered NPs were able to achieve a fast and stable release of the drug in response to extra- and intra- cellular stimulus of the acidic environment of tumor cells, and this pH-dependent release is desired for targeting the low pH environment of tumor cells [57]. However, Kim *et al.* conducted the cytotoxicity study and observed that $CaCO_3$ NPs were shown to exhibit cytotoxicity due to the generation of reactive oxygen species (ROS) which causes membrane damage under *in vitro* conditions [58].

Silicon dioxide (SiO_2) is classified as a 'generally regarded as safe' (GRAS) agent by the FDA. Coupled with its biocompatibility and biodegradability, it is one of the commonly used templates for various applications such as in consumer products and the biomedical field [59-61]. However, a recent research study indicated the cytotoxicity of SiO_2 NPs on neural stem cells and the exposure of the cells to SiO_2 NPs results in apoptosis. This inhibits cell proliferation and causes the swelling of the mitochondria where the mitochondria are the major organelle that would clear ROS from the cell. As such, it is evaluated that the damage to the mitochondria caused by SiO_2 NPs would lead to ROS accumulation which consequently results in its cytotoxicity effect [62].

HAp is made up of the main inorganic component of bones and teeth, with similar chemical and structure as bone minerals. HAp is biocompatible, biodegradable and various research studies have indicated that it exhibits low levels of toxicity (although the current knowledge on the exact toxicity of HAp NPs is still unknown) [63, 64]. An *in vitro* study done to investigate the toxicity of HAp NPs of various concentrations was conducted and it was found that the highest concentration of HAp NPs used (at 1000 $\mu g\ cm^{-2}$) exhibited toxic effects. Hence, this indicates that the toxic effect of HAp NPs is dose-dependent [65]. Nevertheless, another research study conducted by Liu *et al.* showed that there were no accumulative toxicity effects observed in rabbit models after the intravenous injection of

HAp NPs and it was therefore suggested that utilizing HAp as a drug carrier in small dosages is safe [66]. Furthermore, initial studies on the cell toxicity of HAp NPs observed the movements of these particles *in vitro* and found that the HAp NPs were dissolved within the lysosomes within 1 day of internalization into cells [67].

Therefore, HAp (having negative electrostatic surface potential) was chosen to be used as the core template material in this thesis for the synthesis of LbL NPs due to its slow dissolution, biocompatibility and low toxicity levels that makes it a promising biomaterial as the drug delivery carrier. Further, it is becoming an important material with extensive use in a variety of research studies [68, 69].

2.4.2 Selection of cationic polyelectrolyte (PE)

The cationic polyelectrolytes (PEs) are positively charged layers of the LbL NPs system which includes polypeptides such as poly-L-arginine (PLR), poly-L-lysine (PLL) and poly-L-histidine (PLH). In this thesis, the positively charged PLR of various molecular weights (according to the information provided by the supplier) – PLR 5000 – 15 000 Da, 15 000 – 70 000 Da and >70 000 Da will be used to evaluate its effect on the release profile of siRNA from the LbL NPs. The repeating units of PLR bear an electrolyte group such that when PLR of a higher M_w is coated on the NPs, the number of 'n' repeats increases. With more repeating units of the PLR, the overall positive charges of the PE could increase. With higher PLR M_W used, a higher amount of siRNA could be loaded in the NPs and with stronger siRNA compaction ability. An illustration of the structure of PLR and its charge location is shown in Figure 2.3.

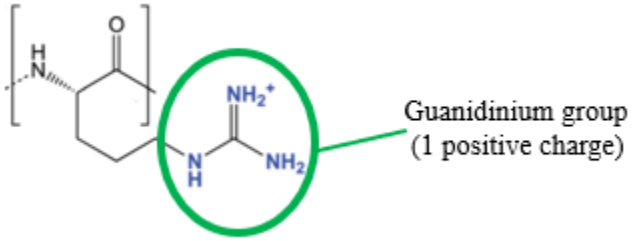

Figure 2.3: Illustration of PLR structure. PLR side chain guanidium group (consist of amine groups) comprise of a positive charge per repeating unit. It can be protonated at pH 7.40, enabling the electrostatic interaction with negatively charged siRNA [70]. [Taken from Danani *et al.*, 2017]

Additionally, PLR is biodegradable [71], has low levels of toxicity and is known to possess a high loading capacity for siRNA (approximately 3500 siRNA molecules per NPs layer), and to be stable at pH 7.40 in PBS buffer over a prolonged period of time with ≤30% siRNA release over the first 24 hours [72]. PLR coated particles have also been observed to possess a higher transfection efficiency as compared to PLL and PLH. Further, with their low cytotoxicity, these PLR coated particles would facilitate the cellular entry of LbL NPs while maintaining the viability of cells [73-75]. The unique features of PLR would hence allow it to protect and provide sustained and prolonged release of siRNA into the cytoplasm, as well as to silence the gene. This would consequently lead to the decrease in occurrence of the targeted disease.

2.4.3 Selection of SPARC siRNA and its association with fibrosis

The layers of positively charged polyelectrolytes would be alternated in the bilayers with negatively charged siRNA to silence the SPARC gene which associated with various fibrotic diseases. SPARC (secreted protein acidic and rich in cysteine), also known as osteonectin or BM-40, is a 32 to 35 kDa multifunctional collagen-interacting protein [76]. An elevated level of SPARC gene expression has been described in various types of fibrosis and the inhibition of SPARC gene expression has been found to reduce type I collagen expression, which in turn leads to a decrease in fibrosis [77-79]. The gene silencing of SPARC takes place at the mRNA process in the cytoplasm. Hence, SPARC siRNA should be present in this compartment to cause gene silencing, and the ability of the LbL NPs to escape from endo-lysosomal complex is essential for the successful delivery of siRNA into the cytoplasm [80, 81].

An emphasis has to be made that the inhibition of SPARC gene would only reduce the spike in collagen expression in respond to an injury and not completely cease the

production of collagen in the biological system as a certain amount of collagen is still needed to maintain the structural integrity of fibroblast cells [82]. Hence, targeting the SPARC gene is an indirect means of reducing collagen levels but at the same time maintaining a certain level of collagen production in the biological system. For instance, a study by Zhou et al. observed that the overexpression of SPARC, COL1A2, COL3A1 and CTGF is present in the fibroblast cells of patients with Systemic Sclerosis (SS), and the use of siRNA to inhibit SPARC showed a reduction in the collagen levels [83]. This further illustrates that the overproduction of collagen in fibroblast cells can be attenuated through the silencing of SPARC.

The phosphate groups along the strands of the siRNA backbone provides the siRNA with a negative charge per base. 'Naked' siRNA is fragile and subjected to degradation by nucleases. Furthermore, they are large in size with negatively charged surface which prevents their optimal internalization into the cells. Thus, the incorporation of SPARC siRNA in LbL NPs with positively charged PEs is required to protect the siRNA, thereby enabling a more efficient and successful cellular internalization, as well as achieving a prolonged gene silencing effect. The PLR side chain guanidinium group binds to the negatively charged phosphate group along the strands of the siRNA backbone. This facilitates the fabrication of the LbL NPs incorporating siRNA, protecting it from degradation by nucleases and transporting the siRNA into the cytoplasm for the gene silencing of SPARC. An illustration of the structure of siRNA and its charge location is shown in Figure 2.4.

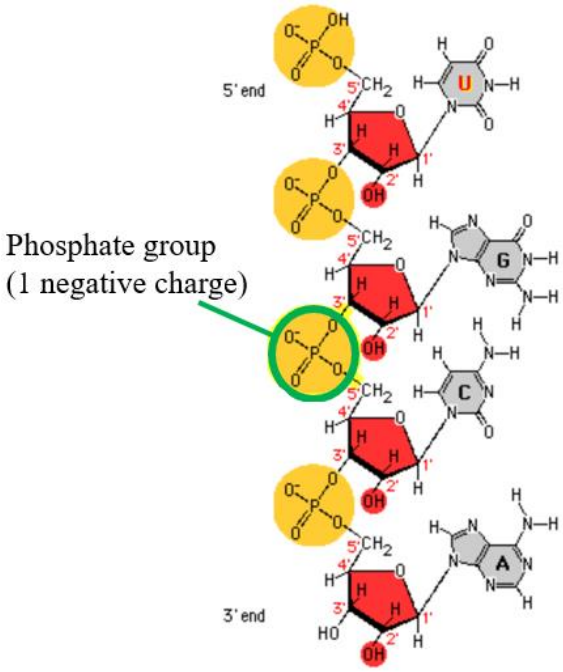

Figure 2.4: Illustration of RNA polynucleotide chain. Phosphate groups along the strands of the siRNA backbone provides the siRNA with a negative charge per base. The PLR side chain guanidinium group bind to the negatively charged phosphate group along the strands of the siRNA backbone [70]. [Taken from Danani *et al.*, 2017]

2.4.4 Optimal pH conditions for fabrication of LbL NPs

The pH value present in the medium used for the LbL synthesis of the polyelectrolyte (PE) bilayers could affect its properties and functionality. Various reviews have investigated on how certain stimuli, such as the pH value of the medium used for LbL NPs synthesis can influence factors such as the cell adhesion capability, thickness, and overall surface potential of the PE. This will in turn determine the success of LbL NPs coating [84, 85]. For instance, Salvi *et al.* have reported that the LbL assembly of PEs (using poly-L-histidine and poly (methacrylic acid)) coatings over the bone morphogenetic protein (BMP-2). A pH dependent release behavior was observed with stable coatings at pH 6 to 7 while the samples that was prepared at more basic pH resulted in a decrease in surface energy. In this

regard, a low surface energy would result in poor adhesion capability while a higher surface energy would provide better adhesion capability [86].

To determine the pH value for the fabrication of LbL NPs, we could first investigate the acid dissociation constant (pKa) values of the selected PE (poly-L-arginine, PLR). Arginine is an amino acid that consists of the carboxyl group with pKa of 2.17, amine group with pKa of 9.04, the R-group side chain having a pKa of 12.48, and the isoelectric point (pI) of arginine could be calculated using these values. The pKa values that oscillate its charges between -1 to +1 will be used for the calculation since the pI represents the pH at which the amino acid does not migrate in an electric field as its net charge is zero. At pKa of 9.04, the charge is at +1 to 0 while at pKa of 12.48, the charge is at 0 to -1. As such, by using these pKa values, the pI of arginine will be 10.76. Therefore, utilizing the pH value below 10.76 will result in a higher incidence of protonation which explains the positively charged surface on arginine (i.e. at pH 7.40) as it becomes protonated due to increased amount of H^+ ion concentration in the solution. This facilitates a strong electrostatic interaction between the alternate depositions of the layers, forming the LbL NPs configuration of HAp | PLR | siRNA | PLR. For instance, as in the case of pH 7.40, at pH 5 the incidence of protonation is expected to be much higher and this will cause the surface charge density to be even more positive. However, since the dominant driving force behind the LbL self-assembly is electrostatic interactions, the decrease in pH value will result in drastic changes and studies have shown that the LbL NPs tend to break down more easily under acidic conditions (i.e. pH 5) than under weak basic conditions (i.e. pH 7.40) [87]. Hence, a higher incidence of protonation caused by the decrease in pH may disturb the configuration of the LbL NPs system. As the outer layer starts acquiring higher charge density, the electrostatic forces may cause the LbL configuration to disintegrate. Due to this instability, it may cause a burst release of siRNA from the LbL NPs. For these reasons, it can be theorized that the fabrication of LbL NPs will be more stable at pH 7.40. Also, S. Nimesh *et al.* studied the pH dependent release of the encapsulant from the nanoparticles. It was observed that the rate of release of the encapsulant from the nanoparticles were slower in pH condition higher and lower than 7.40, with the fastest rate of release at pH

7.40. The authors claimed that the nanoparticles swell in aqueous dispersion and the swelling reaches its maximum at physiological pH [88].

2.5 Disassembly of LbL NPs for investigating total siRNA content

Following the fabrication of LbL NPs incorporating siRNA, it is imperative to know the total amount of siRNA in the particles. Several reports have utilized trypsin (a serine protease that hydrolyzes proteins at carboxyl side of amino acids lysine and arginine) to disassemble the LbL NPs system. For instance, a study was conducted to formulate a nanocarrier system that consisted of diphenylalaninamide (FFA) NPs coated with poly-L-lysine (PLL), made of amino acid lysine, incorporating siRNA to form the 3 layered FFA | PLL | siRNA | PLL NPs complex. 0.25% trypsin-EDTA was utilized to assess the enzymatic effect of trypsin-EDTA on the LbL system and it was observed that the trypsin-EDTA degrades the LbL NPs by digesting the surrounding polyelectrolyte layer [51]. In another study by Radhakrishnan and Raichur, dextran-TRITC labelled microcapsules were treated with trypsin-EDTA and this resulted in the rupturing and release of loaded dextran-labelled TRITC as shown from their scanning electron microscope (SEM) images [89]. Furthermore, it was also observed that the hollow microcapsule with arginine and chondroitin sulfate disintegrated and releases the drugs after treatment with trypsin-EDTA [90].

Therefore, poly-L-arginine (PLR) which is made of the amino acid, arginine, could be degraded by proteases such as trypsin. Hence, 0.25 % trypsin-EDTA could be used in this project for the disassembly of LbL NPs to find out the amount of total siRNA content encapsulated. This can be determined by incubating the LbL NPs with the 0.25 % trypsin-EDTA overnight (to ensure a complete breakdown of the LbL NPs). On the following day, the LbL NPs will be spun down to measure the supernatant containing 6FAM-labelled siRNA with the microplate reader for the total siRNA content in the NPs. In addition, siRNA was not found to be degraded by trypsin-EDTA after the disintegration of the LbL system as observed by Vaissiere *et al* [91]. Hence, this affirms that the true amount of total siRNA is measurable by the microplate reader. All the samples will be compared against a

series of 6FAM siRNA standard curve (Tecan measurements to be taken of 6FAM siRNA of known concentrations).

2.6 siRNA release of NPs fabricated with different PLR M_W

There are various poly-L-arginine (PLR) molecular weight (M_W) commercially available in the market currently. In this thesis, the LbL NPs system could be coated with the different PLR M_W (PLR 5000 – 15 000 Da, PLR 15 000 – 70 000 Da and PLR >70 000 Da) to find out the total siRNA contents and the *in vitro* siRNA release profile (in PBS medium at pH 7.40) of the respective particles over the stipulated time intervals. The pH value at 7.40 mimics the physiological conditions in the cytoplasm [92] and that the swelling of NPs reaches its maximum at physiological pH [88].

For instance, a study was conducted by Qi Lan *et al.* which observed the *in vitro* release behavior of microcapsules (incorporating bovine hemoglobin (Hb), with the different poly-L-arginine (PLR) molecular weight (M_W) forming the polymeric membrane) in PBS medium of neutral pH over 24 hours. The release profile shows that the microcapsules based on the different PLR M_W (125 kDa, 35.50 kDa and 13.30 kDa) coating shared the same release trend and the final cumulative release reached almost 100% over 24 hours [93]. This indicates an obvious burst release of Hb in the study. This could be beneficial for their application in the encapsulation of protein-based drugs (i.e. the need to immediately replenish the deficient protein in the body).

With reference to the above study as an example, *in vitro* investigation on the controlled and prolonged release behavior of the respective particles coated with different PLR M_W in PBS medium (pH 7.40) could be carried out. PLR M_W of >70 000 Da was later selected for used as the polyelectrolyte in the bilayers of LbL NPs system.

2.7 siRNA Release of NPs fabricated with additional siRNA layers

With the NPs coated with PLR M_W >70 000 Da, a 3 layered NPs (containing 1 layer of siRNA), 5 layered NPs (containing 2 layers of siRNA) and 7 layered NPs (containing 3 layers of siRNA) system could be formulated to find out the total siRNA contents and the *in vitro* siRNA release profile (in PBS medium at pH 7.40) of the respective particles over the stipulated time intervals.

In a study by Lee *et al.*, gold nanoparticles (AuNPs) coated with alternating layers of poly-L-lysine (PLL) and siRNA were fabricated into 3 layered NPs (containing 1 layer of siRNA), 5 layered NPs (containing 2 layers of siRNA) and 7 layered NPs (containing 3 layers of siRNA) [94]. These 3 batches of NPs were then subjected to the release study which took about 3 days for the siRNA to be fully released from the 3 layered NPs, 4 days for siRNA to be fully released from 5 layered NPs and 5 days for siRNA to be fully released from 7 layered NPs. This was due to the slow degradation of PLL which led to the gradual release of the incorporated siRNA over an extended period. This validates that the amount of siRNA release depends on the number of layers of siRNA loaded in the NPs and that more siRNA could be carried on a single particle by multiple layering. Further, with more siRNA being carried on a single particle, an extended gene silencing effect could be obtained with just a single application.

An *in vitro* investigation on the controlled and prolonged release behavior of the 3, 5 and 7 layered NPs in PBS medium (pH 7.40) could be carried out. The 7 layered NPs system was later selected for use in subsequent studies of the thesis. Further, in comparison of the proposed layer by layer NPs system with the study that has previously been reported by Lee *et al.* (with coating of PLL in the bilayer of the multilayered NPs system), the proposed system (with coating of PLR in the bilayer of the multilayered NPs system) would be expected to result in a better transfection outcome. As reported by *Zhou et al.*, PLR is known to possess a high loading capacity for siRNA (approximately 3500 siRNA molecules per NPs layer), and to be stable at pH 7.40 in PBS buffer over a prolonged period of time with ≤30% siRNA release over the first 24 hours [72]. Investigation was done in this

study and it was found that significant amount of siRNA was still present in the 7 layered NPs system even at day 21. Whereas, there was a complete release of siRNA from the PLL-coated 7 layered NPs over just a period of 5 days as reported by Lee *et al*. The PLR coated particles have also been observed to possess a higher transfection efficiency as compared to PLL [95]. With a higher transfection efficiency, PLR would be able to protect and provide sustained and prolonged release of siRNA into the cytoplasm, as well as to silence the gene.

All in all, it is important to note that an initial burst release would tend to happen for most controlled release formulations. In which, immediately after placement of the system in the release medium an initial large bolus of drug would be released before the rate of release reaches a stable profile. The initial burst release can have both positive and also negative consequences, depending on the application. For instance, at the beginning of wound treatment, an initial burst release of the drugs would be desirable to provide an immediate relief [96] (in this case, a non-linear release profile would be wanted). However, some researchers would tend to avoid having burst release because the initial high release rate could lead to the concentrations of drug to fall near or above the toxic level *in vivo* [97, 98] (in this case, a linear release profile would be wanted). In any case, after the presence of an initial burst release, it should be followed by prolonged release to promote healing gradually. An ideal prolonged release profile would be one that delivers drug in intervals over an extended period of time. The active ingredients would be released slowly and to provide a continuous supply of drug over a prolonged or an extended period. Again, as mentioned with examples above, it depends on the application of each individual to determine whether if a linear or non-linear profile is desired.

2.8 Nanoparticles entry into cells

Once nanoparticles reached the exterior of cell membrane, they interact with components of the extracellular matrix (ECM) and enter into the cell primarily through endocytosis, which is usually classified into phagocytosis and pinocytosis. Phagocytosis occurs mainly in phagocytes (i.e. macrophages and neutrophils) [99]. Pinocytosis is found to be present in

all cell types in four different forms, for example, in clathrin-dependent endocytosis, caveolin-dependent endocytosis, clathrin/caveolae-independent endocytosis and micropinocytosis [100, 101]. Currently, a majority of the reports propose that positively-charged nanoparticles mainly enter into the cells through clathrin-dependent endocytosis and the electrostatic interactions between the nanoparticles and cell membrane initiates the cellular entry [102]. After the electrostatic interactions, clathrin-1 (cytosolic protein) at the cell membrane polymerizes to allow the internalization of nanoparticles [101]. Subsequently, nanoparticles are wrapped into the cells and the vesicle is pinched off through the activity of GTPase, dynamin, to form clathrin coated vesicles (CCV) [103]. The CCVs then move into the cells by the regulation of actin cytoskeleton. Within the cells, the clathrin coat is shed off and the vesicles fuses with early endosomes and will in turn be sorted into the endo-lysosomal complex [101]. Nanoparticles usually accumulate in the lysosomes and are degraded by lysosomal enzymes. However, it was reported that positively-charged nanoparticles could escape from endosomes to enter into the cytoplasm after cellular internalization due to the 'proton-sponge' effect [40, 41]. Hence, the surface charge of nanoparticles has a dominant effect on the cellular entry and intracellular fate. This is essential as the LbL NPs incorporated with siRNA must escape from the endosomes into the cytoplasm in order to release the siRNA for gene silencing as the mRNA of the targeted protein is found in the cytoplasm.

There are other physicochemical properties of nanoparticles that could affect their cellular internalization. For instance, the NPs' size and shape could determine whether it is able to enter the vesicles. For example, it was reported that smaller-sized particles are able to undergo cellular entry significantly faster as compared to bigger-sized particles [104]. From the reports, it was also shown that the rod-shaped NPs undergo lower cellular entry as compared to the spherical-shaped NPs which could be due to the membrane wrapping of rod-shaped NPs since that takes longer than in the case of spherical NPs [105, 106]. Additionally, once NPs are in contact with biological fluids, they acquire a surface layer made up of proteins and other biomolecules on the NPs' surfaces, known as protein corona. This is an important consideration for NPs' interactions with cells. For instance, whether the NPs will be able to internalize into the cells and the subsequent biological processes.

Notably, when cells are exposed to NPs, they will 'visualize' the NPs/protein corona complexes but not the true form of the NPs itself [107, 108]. The composition of protein corona can change over time and it depends on factors such as the NPs' material, size and surface properties [109-112]. Xia *et al.* have conducted an investigation on the forces that are involved in biological molecules adsorption to the NPs and a weighted nano-descriptor algorithm was developed to deduce the contributions of hydrogen bonding, polarizability, lone-pair interactions, London dispersion and Coulomb forces [113]. However, there has not been any clear findings on the chemical properties that govern the binding of protein to NPs.

2.9 Quantification of siRNA LbL NPs *in vitro*

2.9.1 Quantification of free siRNA/drugs inside the cells

Besides studying the siRNA LbL NPs release profile in PBS (pH 7.40) medium which mimic the physiological condition present in the cytoplasm of the cell, it is also interesting to know the amount of free siRNA that has been released inside the cells, its duration of release and whether the LbL NPs releases siRNA by degradation from the layer by layer 'onion effect' or by the diffusional effect. Further, other than quantifying free siRNA inside the cells, the amount that is still retained within the particle can also be evaluated.

The layer by layer self-assembly technique of nanoparticles fabrication with alternating charges of polyelectrolyte layers provides an opportunity for the release of siRNA or drugs in a controlled manner. This is due to the ability of LbL NPs having high drug loading capacity and the potential of enhancing the stealth properties of nanoparticles. Most studies focus on the release of drugs from LbL NPs *in vitro*, in PBS buffer and in Fetal Bovine Serum (FBS) medium. Further, *in vitro* cell culture studies was conducted to check on the cytotoxic effect of the particles and its cellular entry [114, 115]. There are limited studies conducted on the quantification of total amount of free siRNA inside the cells. In spite of that, a study conducted by Hermle *et al.* have transfected the 293T cells (Human Embryonic Kidney 293 cells, containing SV40 T-antigens) with plasmid HIV (tagged with a fluorescence dye) and at the stipulated time intervals, the medium was removed and the

cells were washed with PBS and incubated in cell lysis buffer for 10 min at room temperature [116]. The cell debris was removed by centrifugation and the supernatant was taken for fluorescence measurement using a multi-plate reader. This would consequently allow the quantification of the release of fluorescence labelled plasmid HIV inside the cells over the stipulated time intervals of the study.

However, the study conducted by Hermle *et al.* did not correlate the release of fluorescence labelled plasmid HIV inside the cells with the total amount of cellular internalization of plasmid HIV. In such a case, the study will not have a thorough understanding on when and how much of the total amount of plasmid HIV has been taken up into the cells and also how much of the total amount is released inside the cells over the stipulated time intervals. Furthermore, there were no experiments conducted to check whether the cell lysis buffer used will have any effect on the plasmid HIV.

There are various positive points of quantifying the total amount of free siRNA or drugs inside the cells. First, it allows for a fundamental understanding of the LbL NPs delivery system and the ability to control and manipulate the delivery of siRNA or drugs in the cells. Further, the number of therapeutic agents that has been released from the particle and how much of such siRNA or drugs is still retained within could be evaluated. Consequently, this provide a thorough understanding of the LbL NPs system, its interaction within the cells and whether the quantity of therapeutic agent used is able to cause an effect to the cells. This could in turn resolve any complications to the biological system which leads to the onset of various diseases. However, there are also some negative points in quantifying the total amount of free siRNA or drugs, such as whether the methods used (i.e. using cell lysis buffer to break open the cells in order to quantify the amount of free siRNA within the cells) will have any effect on the siRNA and the LbL NPs system. Hence, studies can be done to track the NPs cellular internalization process, to quantify the amount of siRNA that has been released from the particle *in vitro* (within the cells) and the amount that is still retained within. Hence, experiments could be conducted to evaluate these negative points. In this regard, it is prudent to make sure that the cell lysis buffer will not degrade

the siRNA and the LbL NPs system before proceeding with this method of quantifying free siRNA inside the cells.

Lastly, this thesis is done to observe and investigate the profile of free siRNA release once the LbL NPs enter into the cell, how the LbL NPs release the free siRNA, and whether if it exhibits the layer by layer 'onion effect' as illustrated by Tan *et al.* on the utilization of the Forster Resonance Energy Transfer (FRET) study. In that study, the defoliation and release experiments conducted gave rise to the observation in respect of the LbL NPs breakdown behavior inside the cells and suggested that the particles disassemble through the layer by layer 'onion effect', starting with the outermost layers [15]. From these findings, the FRET study utilized a FRET pair to evaluate the release behavior of a five-layered LbL NPs system (containing 2 layers of siRNA) and the duration for the 2 layers of siRNA to disassemble from the LbL nanoparticles inside the cells. The siRNA and adjacent Poly-L-Arginine (PLR) layers were tagged with the FRET pair fluorophores and it was found that by day 9, most of the outermost PLR layer has been detached from the outermost siRNA layer. The same was observed for the innermost siRNA and PLR layers. Thus, this affirms the notion that the outermost layer of siRNA disassembles first followed by the innermost layer of siRNA.

Therefore, with information from the FRET study conducted by Tan *et al.*, further evaluation of the LbL NPs inside the cells could be conducted to find out whether the nanoparticles are constantly releasing free siRNA inside the cells. A timepoint study of quantifying the amount of free siRNA inside the cells can be evaluated by lysing the cells using the lysis buffer method, comparing it with the percentage of cells that has taken up the 6FAM-labelled siRNA NPs and conducting the knockdown study to assess the effect of the SPARC siRNA inside the cells. These results could be further analyzed to provide a deeper understanding of the LbL siRNA delivery system *in vitro*.

References

[1] Scott L. Friedman, D.S., Jeremy S. Duffield, Shelia Violette, *Therapy for Fibrotic Diseases: Nearing the Starting Line.* Sci Transl Med, 2013. **5**(167): p. 1-17.

[2] Association, A.D., *Diagnosis and Classification of Diabetes Mellitus.* Diabetes Care, 2014. **3**(1): p. S81-S90.

[3] J.E. Shaw, R.A.S., P.Z. Zimmet, *Global estimates of the prevalence of diabetes for 2010 and 2030.* Diabetes Research and Clinical Practice, 2010. **87** (1): p. 4-14.

[4] McCrimmon, R., *The mechanisms that underlie glucose sensing during hypoglycaemia in diabetes.* Diabet. Med., 2008. **25**: p. 513–522.

[5] Francoise Homo-Delarche, S.C., Jean-Claude Irminger, Marie-Noelle Gangnerau, Josiane Coulaud, Katharina Rickenbach, Manuel Dolz, Philippe Halban, Bernard Portha, and Patricia Serradas, *Islet Inflammation and Fibrosis in a Spontaneous Model of Type 2 Diabetes, the GK Rat.* Diabetes, 2006. **55**(6): p. 1625-33.

[6] Esder Lee, G.R.R., Seung-Hyun Ko, Yu-Bae Ahn, Ki-Ho Song, MD, PhD, *A role of pancreatic stellate cells in islet fibrosis and b-cell dysfunction in type 2 diabetes mellitus.* Biochemical and Biophysical Research Communications 2017. **485** (2): p. 328-334.

[7] MV Apte, P.S.H., T L Applegate, I D Norton, G W McCaughan, MA Korsten, R C Pirola, J S Wilson, *Periacinar stellate shaped cells in rat pancreas: identification, isolation, and culture.* Gut, 1998. **43**(1): p. 128–133.

[8] Dijke, L.J.A.C.H.P.T., *Exploring anti-TGF-β therapies in cancer and fibrosis.* Growth Factors, 2011. **29**(4): p. 140–152.

[9] John Varga, J.R.a.S.A.J., *Transforming growth factor (TGFf) causes a persistent increase in steady-state amounts of type I and type III collagen and fibronectin mRNAs in normal human dermal fibroblasts.* Biochem. J., 1987. **247**(3): p. 597-604.

[10] M. Boni-Schnetzler, J.A.E., M. Faulenbach and M. Y. Donath, *Insulitis in type 2 diabetes.* Diabetes, Obesity and Metabolism, 2008. **10**((Suppl. 4)): p. 201-204.

[11] Gregory Lacraz, M.-H.G., Nadim Kassis, Josiane Coulaud, Anne Galinier, Christophe Noll, Melanie Cornut, Fabien Schmidlin, Jean-Louis Paul, Nathalie Janel, Jean-Claude Irminger, Micheline Kergoat, Bernard Portha, Marc Y. Donath, Jan A. Ehses, Francoise Homo-Delarche, *Islet Endothelial Activation and Oxidative Stress Gene Expression Is*

Reduced by IL-1Ra Treatment in the Type 2 Diabetic GK Rat. PLoS ONE 2009. **4**(9): p. e6963.

[12] Evelina Miele, G.P.S., Ermanno Miele, Enzo Di Fabrizio, Elisabetta Ferretti, Silverio Tomao, Alberto Gulino, *Nanoparticle-based delivery of small interfering RNA: challenges for cancer therapy.* International Journal of Nanomedicine 2012. **7** p. 3637–3657.

[13] Kathryn A. Whitehead, R.L.a.D.G.A., *Knocking down barriers: advances in siRNA delivery.* Nature Reviews Drug Discovery, 2009. **8**(516): p. 129-138.

[14] Fengjuan Wang, A.S.a.P.B., *Lysosome-dependent cell death and deregulated autophagy induced by amine-modified polystyrene nanoparticles.* Open Biol., 2018. **8**(17027): p. 1-13.

[15] Yang Fei Tan, Y.S.L., Li-Fong Seet, Kee Woei Ng, Tina T. Wong and Subbu Venkatraman, *Design and in vitro release study of siRNA loaded Layer by Layer nanoparticles with sustained gene silencing effect.* Expert Opinion on Drug Delivery, 2018. **15**(10): p. 937-949.

[16] Christian Matranga, Y.T., Chanseok Shin, David P. Bartel, and Phillip D. Zamore, *Passenger-Strand Cleavage Facilitates Assembly of siRNA into Ago2-Containing RNAi Enzyme Complexes.* Cell, 2005. **123**(4): p. 607-620.

[17] Daniel Cejka, D.L.a.V.W., *Short interfering RNA (siRNA): tool or therapeutic?* Clinical Science 2006. **110**(1): p. 47–58.

[18] Francisco M. Vega, A.J.R., *Rho GTPases in cancer cell biology.* Febs Letters 2008. **582**(14): p. 2093–2101.

[19] J.-Y. Pille, C.D., J. Varet, J.-R. Bertrand, J. Soria, P. Opolon, H. Lu, L.-L. Pritchard, J.-P. Vannier, C. Malvy, C. Soria, and H. Li, Molecular Therapy 2005. **11**(2): p. 267-274.

[20] Aimee L Jackson, S.R.B., Janell Schelter, Sumire V Kobayashi, Julja Burchard, Mao Mao, Bin Li, Guy Cavet and Peter S Linsley, *Expression profiling reveals off-target gene regulation by RNAi.* Nature Biotechnology 2003. **21**(6): p. 635-638.

[21] Adam D. Judge, G.B., Amy C.H. Lee, Ian MacLachlan, *Design of Noninflammatory Synthetic siRNA Mediating Potent Gene Silencing in Vivo.* Molecular Therapy 2006. **13**(3): p. 494-505.

[22] Cong-fei Xu, J.W., *Delivery systems for siRNA drug development in cancer therapy.* Asian Journal Of Pharmaceutical Sciences 2015. **1** (0): p. 1-12.

[23] Yuan Zhang, A.S.a.L.H., *In Vivo Gene Delivery by Nonviral Vectors: Overcoming Hurdles?* The American Society of Gene & Cell Therapy, 2012. **20**(7): p. 1298–1304.

[24] Audouy SA, D.L.L., Hoekstra D, Molema G., *In vivo characteristics of cationic liposomes as delivery vectors for gene therapy.* Pharm Res. , 2002 **19**(11): p. 1599-605.

[25] Varga CM, H.K., Lauffenburger DA, *Quantitative analysis of synthetic gene delivery vector design properties.* Mol Ther. , 2001. **4**(5): p. 438-46.

[26] YuHuang, X.L., Lanlan Dong, Zhongchun Liu, XiaohuaHe, and Wanhong Liu, *Development of Viral Vectors for Gene Therapy for Chronic Pain.* Pain Res Treat., 2011. **2011**: p. 1-8.

[27] TJ, W., *Ligand-directed targeting of genes to the site of disease.* Nat Med., 2003. **9**: p. 135–139.

[28] Defu Zhi, Y.B., Jian Yang, Shaohui Cui, Yinan Zhao, Huiying Chen, Shubiao Zhang, *A review on cationic lipids with different linkers for gene delivery.* Advances in Colloid and Interface Science, 2018. **253**: p. 117–140.

[29] Kai K. Ewert, A.Z., Ayesha Ahmad, Nathan F. Bouxsein, Heather M. Evans, Christopher S. McAllister, Charles E. Samuel, and Cyrus R. Safinya, *Cationic Lipid–Nucleic Acid Complexes for Gene Delivery and Silencing: Pathways and Mechanisms for Plasmid DNA and siRNA.* Top Curr Chem., 2010. **296**: p. 191–226.

[30] Lisa Sercombe, T.V., Fatemeh Moheimani, Sherry Y. Wu, Anil K. Sood, and Susan Hua, *Advances and Challenges of Liposome Assisted Drug Delivery.* Frontiers in Pharmacology, 2015. **6**(286): p. 1-13.

[31] Chrai, S.S., Murari, R., and Ahmad, I. , *Liposomes (a review): Part two: Drug delivery systems.* BioPharm, 2002. **17**: p. 40–43.

[32] Szebeni J, M.S., *Liposome triggering of innate immune responses: a perspective on benefits and adverse reactions.* J Liposome Res, 2009. **19**(2): p. 85-90.

[33] Oku N, N.Y., *Long-circulating liposomes.* Crit Rev Ther Drug Carrier Syst, 1994. **11**(4): p. 231-70.

[34] Ishida T, H.H., Kiwada H., *Interactions of liposomes with cells in vitro and in vivo: opsonins and receptors.* Curr Drug Metab 2001 **2**(4): p. 397-409.

[35] Sawant, R.R., and Torchilin, V. P. , *Challenges in development of targeted liposomal therapeutics.* AAPSJ, 2012. **14**(2): p. 303–315.

[36] Laverman, P., Carstens, M. G., Storm, G., and Moghimi, S. M. , *Recognition and clearance of methoxypoly(ethyleneglycol)2000-grafted liposomes by macrophages with enhanced phagocytic capacity. Implications in experimental and clinical oncology.* Biochim. Biophys. Acta 2001. **1526**(3): p. 227–229.

[37] Shirleide Santos Nunes, R.S.F., Carolina Henriques Cavalcante, Isabela da Costa César, Elaine Amaral Leite, Sávia Caldeira Araújo Lopes, Alice Ferretti, Domenico Rubello, Danyelle M. Townsend, Mônica Cristina de Oliveira, Valbert Nascimento Cardoso, and André Luís Branco de Barros, *Influence of PEG coating on the biodistribution and tumor accumulation of pH-sensitive liposomes.* Drug Deliv Transl Res, 2019. **9**(1): p. 123–130.

[38] Somasundaran, L.T.L.a.P., *Adsorption of Polyacrylamide on Oxide Minerals.* Langmuir, 1989. **5**(3): p. 854-860.

[39] McKenzie DL, C.W., Rice KG, *Comparative gene transfer efficiency of low molecular weight polylysine DNA-condensing peptides.* J Pept Res. , 1999. **54**(4): p. 311-8.

[40] Gaelle Creusat, A.-S.R., Etienne Weiss, Rkia Elbaghdadi, Jean-Serge Remy, Rita Mulherkar Guy Zuber, *Proton Sponge Trick for pH-Sensitive Disassembly of Polyethylenimine-Based siRNA Delivery Systems.* Bioconjugate Chem. , 2010. **21**(5): p. 994–1002.

[41] Tanja Bus, A.T., Ulrich S. Schubert, *The great escape: How cationic polyplexes overcome the endosomal barrier.* J. Mater. Chem. B, 2018. **6**(43): p. 6904-6918.

[42] YerPeng Tan, U.H.Y., Wei Wei, J. Herbert Waite, and Ali Miserez, *Layer-by-layer polyelectrolyte deposition: a mechanism for forming biocomposite materials.* Biomacromolecules, 2013. **14**(6): p. 1715–1726.

[43] Boudou T, C.T., Ren K, Blin G, Picart C., *Multiple functionalities of polyelectrolyte multilayer films: new biomedical applications.* Adv Mater., 2010. **22**(4): p. 441-67.

[44] RK., I., *Multilayers of colloidal particles.* J Colloid Interface Sci., 1966. **21**(6): p. 569–594.

[45] Santiago Correa, D.K.Y.C., Dr. Erik C. Dreaden, Kasper Renggli, Aria Shi, Dr. Li Gu, Dr. Kevin E. Shopsowitz, Dr. Mohiuddin A. Quadir, Elana Ben-Akiva, and Dr. Paula

T. Hammond, *Highly scalable, closed-loop synthesis of drug-loaded, layer-by-layer nanoparticles.* Adv. Funct. Mater., 2016. **26**(7): p. 991–1003.

[46] Mano, J.B.a.J.F., *Molecular interactions driving the layer-by-layer assembly of multilayers.* Chem. Rev. , 2014. **114**(18): p. 8883–8942.

[47] Bruno G. De Geest, N.N.S., Gleb B. Sukhorukov, Joseph Demeestera and Stefaan C. De Smedt, *Release mechanisms for polyelectrolyte capsules.* Chem. Soc. Rev. , 2007. **36**(4): p. 636–649

[48] Yan Xiang, S.L.a.S.P.J., *Layer-by-layer self-assembly in the development of electrochemical energy conversion and storage devices from fuel cells to supercapacitors.* Chem. Soc. Rev., 2012. **41**: p. 7291–7321.

[49] Bingbing Jiang, J.B.B., Bingyun Li, *Advances in polyelectrolyte multilayer nanofilms as tunable drug delivery systems.* Nanotechnology, Science and Applications 2009. **2**: p. 21–27.

[50] Katsuhiko Ariga, Y.M.L., Kohsaku Kawakami, Qingmin Ji, Jonathan P. Hill, *Layer-by-layer self-assembled shells for drug delivery.* Advanced Drug Delivery Reviews, 2011. **63**(9): p. 762–771.

[51] Betul Bozdogan, O.A., Ekin Çelik, Mustafa Turk and Emir Baki Denkbas, *Novel layer-by-layer self-assembled peptide nanocarriers for siRNA delivery.* RSC Adv., 2017. **7**: p. 47592–47601.

[52] Benter, S.A.a.I.F., *Nonviral delivery of synthetic siRNAs in vivo.* The Journal of Clinical Investigation, 2007. **117**(12): p. 3623-3632.

[53] Joseph Zabner, A.J.F., Tom Moninger, Kristi A. Poellinger, and Michael J. Welsh, *Cellular and Molecular Barriers to Gene Transfer by a Cationic Lipid.* The Journal of Biological Chemistry, 1995. **270**(32): p. 18997-19007.

[54] Ilya Koltover, T.S., Joachim O. Radler, Cyrus R. Safinya, *An Inverted Hexagonal Phase of Cationic Liposome–DNA Complexes Related to DNA Release and Delivery.* Science, 1998. **281**(5373): p. 78-81.

[55] Tung, S.K.L.a.C.-H., *A Fabricated siRNA Nanoparticle for Ultralong Gene Silencing In Vivo.* Adv. Funct. Mater., 2013. **23**(28): p. 3488–3493.

[56] Kris C. Wood, J.Q.B., David M. Lynn, and Paula T. Hammond, *Tunable Drug Release from Hydrolytically Degradable Layer-by-Layer Thin Films.* Langmuir 2005. **21**(4): p. 1603-1609.

[57] Haibao Peng, K.L., Ting Wang, Jin Wang, Jiao Wang, Rongrong Zhu, Dongmei Sun and Shilong Wang, *Preparation of hierarchical mesoporous CaCO3 by a facile binary solvent approach as anticancer drug carrier for etoposide.* Nanoscale Research Letters, 2013. **8**(321): p. 1-11.

[58] Mi-Kyung Kim, J.-A.L., Mi-Rae Jo, Min-Kyu Kim, Hyoung-Mi Kim, Jae-Min Oh, Nam Woong Song and Soo-Jin Choi, *Cytotoxicity, Uptake Behaviors, and Oral Absorption of Food Grade Calcium Carbonate Nanomaterials.* Nanomaterials, 2015. **5**(4): p. 1938-1954.

[59] Shin-Woo Ha, M.N.W.a.G.R.B., Jr. Dental and Skeletal Applications of Silica-Based Nanomaterials. 2013, United States of America: Elsevier.

[60] Norah O'Farrell, A.H., Benjamin R Horrocks, *Silicon nanoparticles: applications in cell biology and medicine.* International Journal of Nanomedicine, 2006. **1**(4): p. 451-472.

[61] Yang Yu, Y.L., Wen Wang, Minghua Jin, Zhongjun Du, Yanbo Li, Junchao Duan, Yongbo Yu, Zhiwei Sun, *Acute Toxicity of Amorphous Silica Nanoparticles in Intravenously Exposed ICR Mice.* PLoS ONE 2013. **8**(4): p. e61346.

[62] Dayu Sun, L.G., Jing Xie, Xiao He, Siyu Chen, Luodan A, Qiyou Li, Zhanjun Gu and Haiwei Xu, *Evaluating the toxicity of silicon dioxide nanoparticles on neural stem cells using RNA-Seq.* RSC Adv. , 2017. **7**(75): p. 47552–47564.

[63] Pau Turon, L.J.d.V., Carlos Alemán, and Jordi Puiggalí *Biodegradable and Biocompatible Systems Based on Hydroxyapatite Nanoparticles.* Appl. Sci. , 2017. **7**(60): p. 1-27.

[64] Liang Chen, J.M.M., James C-M. Lee, and Hao Li, *The role of surface charge on the uptake and biocompatibility of hydroxyapatite nanoparticles with osteoblast cells.* Nanotechnology, 2011. **22**(10): p. 1-19.

[65] E Sonmez, I.C., F Bakan, HTurkez, YI Mohtar, B Togar and AD Stefano, *Toxicity assessment of hydroxyapatite nanoparticles in rat liver cell model in vitro.* Human and Experimental Toxicology, 2016. **35**(10): p. 1073–1083.

[66] Liu LP, X.Y., Xiao ZW, Wang ZB, Li C, Gong X. , *Toxicity of hydroxyapatite nanoparticles on rabbits.* Wei Sheng Yan Jiu, 2005. **34**(4): p. 474-476.

[67] M. Motskin, D.M.W., K. Muller, N. Kyle, T.G. Gard, A.E. Porter, J.N. Skepper, *Hydroxyapatite nano and microparticles: Correlation of particle properties with cytotoxicity and biostability.* Biomaterials, 2009. **30**(19): p. 3307–3317.

[68] M.P. Ferraz, A.Y.M., J.C. Sousa, F.J. Monteiro, *Nanohydroxyapatite microspheres as delivery system for antibiotics: Release kinetics, antimicrobial activity, and interaction with osteoblasts.* J. Biomed. Mater. Res. - Part A, 2007. **81**(4): p. 994–1004.

[69] Vuk Uskokovic, D.P.U., *Nanosized hydroxyapatite and other calcium phosphates: Chemistry of formation and application as drug and gene delivery agents.* Journal of Biomedical Materials Research - Part B Applied Biomaterials, 2011. **96 B**: p. 152–191.

[70] Gianvito Grasso, M.A.D., Viorica Patrulea, Gerrit Borchard, Michael Moller, Andrea Danani, *Free energy landscape of siRNA-polycation complexation: Elucidating the effect of molecular geometry, polymer flexibility, and charge neutralization.* PLoS ONE, 2017. **12**(10): p. e0186816.

[71] X. Zhang, X.P., S.W. Zhang, *Biodegradable medical polymers: fundamental sciences,* X. Zhang, Editor. 2017, Matthew Deans: United Kingdom. p. 1-33.

[72] Zhou J. Deng, S.W.M., Elana Ben-Akiva, Erik C. Dreaden, Kevin E. Shopsowitz, and Paula T. Hammond, *Layer-by-Layer Nanoparticles for Systemic Codelivery of an Anticancer Drug and siRNA for Potential Triple-Negative Breast Cancer Treatment.* ACS Nano, 2013. **7**(11): p. 9571–9584.

[73] Guo-hui Wang, Y.-z.Z., Juan Tan, Shai-hong Zhu, Ke-chao Zhou, *Arginine functionalized hydroxyapatite nanoparticles and its bioactivity for gene delivery.* Trans. Nonferrous Met. Soc. China 2015. **25**(2): p. 490−496.

[74] Tomoko Hashimoto, T.K., Takeshi Nagasaki, Akira Murakami and Tetsuji Yamaoka, *Quantitative comparison between poly(L-arginine) and poly(L-lysine) at each step of polyplex-based gene transfection using a microinjection technique.* Sci. Technol. Adv. Mater., 2012. **13**(015009): p. 1-8.

[75] Xiaoxuan Liu, Q.W., Ling Peng, in *Nanopharmaceutics: The Potential Application of Nanomaterials,* X.-J. Liang, Editor. 2013, World Scientific Publishing Co. Pte. Ltd.: Singapore. p. 173-199.

[76] Wei Han, F.C., Min-bin Chen, Rong-zhu Lu, Hua-bing Wang, Min Yu, Chun-tao Shi, Hou-zhong Ding, *Prognostic Value of SPARC in Patients with Pancreatic Cancer: A Systematic Review and Meta-Analysis.* PLoS ONE, 2016. **11**(1): p. e0145803.

[77] Leigh Vaughan, R.M., Sara Miellet, Paul S. Hartley, *The impact of SPARC on age-related cardiac dysfunction and fibrosis in Drosophila.* Experimental Gerontology, 2017. **109**: p. 1-8.

[78] Hannu Jarvelainen, A.S., Markku Koulu, Thomas N. Wight, and Risto Penttinen, *Extracellular Matrix Molecules: Potential Targets in Pharmacotherapy.* Pharmacol Rev 2009. **61**(2): p. 198–223.

[79] Xiaodong Zhou, F.K.T., Xinjian Guo, Debra Wallis, Dianna M. Milewicz, Sarah Xue, and Frank C. Arnett, *Small Interfering RNA Inhibition of SPARC Attenuates the Profibrotic Effect of Transforming Growth Factor B1 in Cultured Normal Human Fibroblasts.* Arthritis & Rheumatism, 2005. **52**(1): p. 257–261.

[80] Cullen, Y.Z.a.B.R., *RNA interference in human cells is restricted to the cytoplasm.* RNA, 2002. **8**(7): p. 855-860.

[81] Mamta Kapoor, D.J.B., Siddhesh D. Patil, *Physicochemical characterization techniques for lipid based delivery systems for siRNA.* International Journal of Pharmaceutics 2012. **427** (1): p. 35– 57.

[82] Delves, P.J.R., I.M. Fibroblasts ed. I.R. Williams. 1998: Academic Press. 905-912.

[83] Xiaodong Zhou, F.K.T., Xinjian Guo, and Frank C. Arnett, *Attenuation of Collagen Production With Small Interfering RNA of SPARC in Cultured Fibroblasts From the Skin of Patients With Scleroderma.* Arthritis & Rheumatism, 2006. **54**(8): p. 2626–2631.

[84] Sukhishvili, S.A., *Responsive polymer films and capsules via layer-by-layer assembly.* Current Opinion in Colloid & Interface Science, 2005. **10**(1): p. 37-44.

[85] Sato, K.Y., Kentaro Takahashi, Shigehiro Anzai, Jun-ichi, *pH- and sugar-sensitive layer-by-layer films and microcapsules for drug delivery.* Advanced drug delivery reviews, 2011. **63**(9): p. 809-821.

[86] Claire Salvi, X.L., and Amy M. Peterson, *Effect of Assembly pH on Polyelectrolyte Multilayer Surface Properties and BMP-2 Release.* Biomacromolecules, 2016. **17**(6): p. 1949−1958.

[87] Uiyoung Han, Y.S.a.J.H., *Effect of pH on the structure and drug release profiles of layer-by-layer assembled films containing polyelectrolyte, micelles, and graphene oxide.* Scientific Reports, 2016. **6**(24158): p. 1-10.

[88] Surendra Nimesh, R.M., Rupesh Kumar, Amit Saxena, Preeti Chaudhary, Veena Yadav, Subho Mozumdar, Ramesh Chandra, *Preparation, characterization and in vitro drug release studies of novel polymeric nanoparticles.* International Journal of Pharmaceutics, 2006. **323**(1-2): p. 146–152.

[89] Raichur, K.R.a.A.M., *Biologically triggered exploding protein based microcapsules for drug delivery.* Chem. Commun., 2012. **48**(17): p. 2307–2309.

[90] Jaganathan, S., *Bioresorbable polyelectrolytes for smuggling drugs into cells.* Artificial Cells, Nanomedicine, and Biotechnology, 2016. **44**(4): p. 1080–1097.

[91] Anaïs Vaissière, G.A., Karidia Konate, Mattias F. Lindberg, Carole Jourdan, Anthony Telmar, Quentin Seisel, Frédéric Fernandez, Véronique Viguier, Coralie Genevois, Franck Couillaud, Prisca Boisguerin and Sébastien Deshayes, *A retro-inverso cell-penetrating peptide for siRNA delivery.* J Nanobiotechnol, 2017. **15**(34): p. 1-18.

[92] Bright GR, F.G., Rogowska J, Taylor DL, *Fluorescence ratio imaging microscopy: temporal and spatial measurements of cytoplasmic pH.* J Cell Biol, 1987. **104**(4): p. 1019-33.

[93] Qi Lan, Y.W., Shibin Wang, Yuangang Liu, *In Vitro Study of Alginate/Poly-L-Arginine Microcapsules as a Protein or Anticancer Drug Carrier*, in *APCMBE 2008 IFMBE Proceedings*, X.W. Yi Peng, Editor. 2008, Springer-Verlag Berlin Heidelberg: Beijing, China. p. 32–35.

[94] Dr. Seung Koo Lee, M.S.H., Dr. Subashini Asokan, and Prof. Ching-Hsuan Tung, *Effective Gene Silencing by Multilayered siRNA Coated Gold Nanoparticles.* Small, 2011. **7**(3): p. 364–370.

[95] E Alinejad-Mofrad, B.M.-N., L Gholami, SH Mousavi, HR Sadeghnia, M Mohajeri, M Darroudi and RK Oskuee, *Evaluation and comparison of cytotoxicity, genotoxicity, and apoptotic effects of poly-L-lysine/plasmid DNA micro and nanoparticles.* Human and Experimental Toxicology, 2019. **38**(8): p. 983–991.

[96] Xiao Huang, C.S.B., *On the importance and mechanisms of burst release in matrix-controlled drug delivery systems.* Journal of Controlled Release, 2001. **73**(2001): p. 121-136.

[97] B. Jeong, Y.H.B., S.W. Kim, *Drug release from biodegradable injectable thermosensitive hydrogel of PEG-PLGA-PEG triblock copolymers.* J. Control. Release, 2000. **63**(2000): p. 155-163.

[98] M.L. Shively, B.A.C., W.D. Renner, J.L. Southard, A.T. Bennet, *Physiochemical characterization of polymeric injectable implant delivery system.* J. Control. Release, 1995. **33**(1995): p. 237-243.

[99] Aderem A, U.D., *Mechanisms of phagocytosis in macrophages.* Annu Rev Immunol, 1999. **17**: p. 593-623.

[100] Wang J, B.J., Napier ME, DeSimone JM, *More effective nanomedicines through particle design.* Small, 2011. **7**(14): p. 1919-1931.

[101] Rappoport, J.Z., *Focusing on clathrin-mediated endocytosis.* Biochem. J., 2008. **412**(3): p. 415-423.

[102] Conner SD, S.S., *Regulated portals of entry into the cell.* Nature, 2003. **422**(6927): p. 37-44.

[103] Pucadyil TJ, S.S., *Conserved functions of membrane active GTPases in coated vesicle formation.* Science, 2009. **325**(5945): p. 1217–1220.

[104] Ke Li, M.S., *Quantitative evaluation and visualization of size effect on cellular uptake of gold nanoparticles by multiphoton imaging-UV/Vis spectroscopic analysis.* Journal of Biomedical Optics, 2014. **19**(10): p. 1-11.

[105] Chithrani BD, G.A., Chan WC, *Determining the size and shape dependence of gold nanoparticle uptake into mammalian cells.* Nano Lett. , 2006. **6**(4): p. 662-668.

[106] Chithrani BD, C.W., *Elucidating the mechanism of cellular uptake and removal of protein-coated gold nanoparticles of different sizes and shapes.* Nano Lett. , 2007. **7**(6): p. 1542–1550.

[107] P. Aggarwal, J.B.H., C. B. McLeland, M. A. Dobrovolskaia and S. E. McNeil, *Nanoparticle interaction with plasma proteins as it relates to particle biodistribution, biocompatibility and therapeutic efficacy.* Adv. Drug Delivery Rev., 2009. **61**(6): p. 428-437.

[108] M. Mahmoudi, A.M.A., S. Behzadi, J. H. Clement, S. Dutz, M. R. Ejtehadi, R. Hartmann, K. Kantner, U. Linne, P. Maffre, S. Metzler, M. K. Moghadam, C. Pfeiffer, M. Rezaei, P. Ruiz-Lozano, V. Serpooshan, M. A. Shokrgozar, G. U. Nienhaus and W. J. Parak *Temperature: the "ignored" factor at the NanoBio interface* ACS Nano, 2013. **7**(8): p. 6555-6562.

[109] M. Lundqvist, J.S., T. Cedervall, T. Berggard, M. B. Flanagan, I. Lynch, G. Elia and K. Dawson, *The evolution of the protein corona around nanoparticles: a test study.* ACS Nano, 2011. **5**(9): p. 7503-7509.

[110] S. Schottler, K.L.a.V.M., *Controlling the Stealth Effect of Nanocarriers through Understanding the Protein Corona.* Angew. Chem., Int. Ed., 2016. **55**(31): p. 8806-8815.

[111] M. Lundqvist, J.S., G. Elia, I. Lynch, T. Cedervall and K. A. Dawson, *Nanoparticle size and surface properties determine the protein corona with possible implications for biological impacts.* Proc. Natl. Acad. Sci. U. S. A., 2008. **105**(38): p. 14265–14270.

[112] S. Tenzer, D.D., S. Rosfa, A. Wlodarski, J. Kuharev, A. Rekik, S. K. Knauer, C. Bantz, T. Nawroth, C. Bier, J. Sirirattanapan, W. Mann, L. Treuel, R. Zellner, M. Maskos, H. Schild and R. H. Stauber, *Nanoparticle size is a critical physicochemical determinant of the human blood plasma corona: a comprehensive quantitative proteomic analysis.* ACS Nano, 2011, 5, , 2011. **5**(9): p. 7155-7167.

[113] X. R. Xia, N.A.M.-R.a.J.E.R., *An index for characterization of nanomaterials in biological systems.* Nat. Nanotechnol., 2010. **5**(9): p. 671–675.

[114] Gaurav Parekh, P.P., Chaitanya Joshi, Tatsiana Shutava, Mark DeCoster, Tatyana Levchenko, Vladimir Torchilin, and Yuri Lvov, *Layer-by-layer nanoencapsulation of camptothecin with improved activity.* Int J Pharm., 2014. **465**(0): p. 218–227.

[115] Li Zhang, H.Q., Jian Li, Jia-Ni Qiu, Jing-Min Huang, Ming-Chao Li and Yan-Qing Guan, *Preparation and characterization of layer-by-layer hypoglycemic nanoparticles with pH-sensitivity for oral insulin delivery.* J. Mater. Chem. B,, 2018. **6**(7451): p. 7451--7461.

[116] Johannes Hermle, M.A., Anke-Mareil Heuser and Barbara Müller, *A simple fluorescence based assay for quantification of human immunodeficiency virus particle release.* BMC Biotechnology, 2010. **10**(32): p. 1-12.

Chapter 3

Experimental Methodology

This chapter defines the materials and methods adopted to address the problem statement of this thesis, with explanation on the rationale for selection of various materials, the equipment and techniques used in this thesis. Characterization studies of the LbL NPs will be carried out by the use of Malvern Zetasizer for their surface charges and size. X-ray powder diffraction (XRD) was utilized to determine the elemental composition and percent crystallinity of the core material. Gel permeation chromatography (GPC) was employed for the average molecular weight (M_W) distribution of the polyelectrolytes in solution. Transmission Electron Microscopy (TEM) will be done to observe the NPs shape morphology. The effect of poly-L-arginine (PLR) and siRNA amount on the LbL NPs would be evaluated to determine the total siRNA content encapsulated. The release behavior of LbL NPs coated with different PLR M_W, and the release behavior of LbL NPs coated with additional siRNA layers will be measured by using the microplate reader. In vitro studies on the qualitative and quantitative cellular internalization of the LbL NPs, the amount of free siRNA within cells and the percentage knockdown of SPARC will also be assessed.

3.1 Materials

HAp, $Ca_5(OH)(PO_4)_3$, nanopowder of size <200 nm, poly-L-arginine hydrochloride (PLR) with M_w 5000 – 15 000 Da, 15 000 – 70 000 Da and >70 000 Da and phosphate buffered saline (PBS) powder (pH 7.40) were procured from Sigma-Aldrich (USA). 0.25 % Trypsin-EDTA, RPMI 1640 cell culture media, Brazilian Fetal Bovine Serum (FBS) and Penicillin/Streptomycin (antibiotics) were procured from SPD Scientific (Biomedia, Singapore). Negative Control Scrambled siRNA, SPARC siRNA and 6FAM GFP labelled SPARC siRNA with M_w of 13369 g/mol (sense: AAC AAG ACC UUC GAC UCU UUC, anti-sense: GGA AGA GUC GAA GGU CUU GUU) were procured from Simply Science (Bioneer, South Korea).

3.2 Methods

3.2.1 Preparation of LbL NPs

The fabrication of LbL NPs was based on a previously established method [1]. 0.10 M of sodium chloride (NaCl) was prepared and filtered using the 0.20 μm sterile filter unit prior to the synthesis of LbL NPs. The desired amount of poly-L-arginine (PLR) was weighed out and dissolved in 0.10 M NaCl. It was then filtered using 0.20 μm sterile syringe filter in order to prepare sterile PLR solution of 0.50 mg/mL. The HAp nanoparticles (NPs) was weighed out and re-suspended in 1 mL of 0.10 M NaCl as a washing step prior to coating the next layer of PLR on it. The HAp NPs suspension was added to the 0.50 mg/mL of PLR solution (with volume ratio of 1:10) followed by maximum vortex mixing and sonication for 10 minutes. PLR coated HAp NPs were then centrifuged at 12000 rpm for 5 minutes in order to remove unbound PLR and HAp, then it was re-suspended in 0.10 M NaCl. For each layers of SPARC siRNA, 1.20 nmol of siRNA (for every 1 mg worth of HAp) was used for coating the siRNA layer. PLR coated HAp NPs were added into the SPARC siRNA coating solution (with volume ratio of 1:10) followed by an hour of maximum vortex mixing.

The NPs were then washed with 0.10 M NaCl and the coating steps were repeated to achieve particles of the desired LbL NPs configuration. After the fabrication of the LbL NPs, the particles were re-dispersed in sterile 0.10 M of NaCl (25 μL of 0.10 M NaCl for every 1 mg worth of HAp used) and stored in 4 °C before use. The LbL NPs loaded with siSPARC will be termed siSPARC-LbL and those loaded with siSCRAM will be termed siSCRAM-LbL.

3.2.2 Size and zeta potential measurements

Characterization of the LbL NPs using the Malvern zetasizer (Malvern Instruments, Nano 2000, UK) is essential to find out the size and zeta potential of the NPs. Malvern Zetasizer works by employing dynamic light scattering (DLS) and electrophoretic light scattering (ELS) technique to determine the size and zeta potential of particles or polymers in a solution. The size of NPs provides the information on whether the NPs are within the optimal size for cellular entry. DLS from the zetasizer measures the Brownian motion of particles in the solution in which upon irradiation, the monochromatic light is scattered and the intensity of light is detected and relates this to the size of the particles [2]. If the size of the particle is large, the Brownian motion will be slower and vice versa. The zeta potential measurements taken after the synthesis of every layer provides information on whether if the oppositely charged layers has electrostatically self-assembled during the LbL NPs fabrication process. The overall net surface charge of the LbL NPs should be highly positively charged since the outermost layer is composed of PLR, which allows the electrostatic interaction between the LbL NPs to the negatively charged cellular membrane. ELS from the zetasizer measures the zeta potential of the particle in a suspension by the determination of its electrophoretic mobility in which the particles would move towards the opposite chargers of the electrodes and the velocity is determined which in turn can be related to the zeta potential of the particle [3].

3.2.3 X-ray powder diffraction (XRD)

X-ray Powder Diffraction (XRD) is a common technique utilized to observe the crystal structure, atomic spacing, elemental composition and percent crystallinity of the material. XRD works on the basis of constructive interference of monochromatic X-rays and the crystalline sample, the X-rays will be produced by the cathode ray tube that is filtered to create monochromatic radiation that will be directed towards the sample and the constructive interference would be produced once the incident rays interacts with the sample and the diffracted X-rays will then be detected [4]. The goniometer present in the XRD instrument would be used to rotate the sample in the path of the X-ray beam and to maintain the angle, whereas the X-ray detector collects the diffracted X-rays and rotates at an angle of 2theta degree. Studies have observed the relationship between degree of crystallinity and the mechanical properties (i.e. strength, toughness, crack propagation resistance, etc.) of the material, for instance, the greater the crystallinity would result in a hard and strong material, this is because crystallinity reduces the degree of freedom in the movement of its molecular chains [5]. However, although the greater the crystallinity makes a material stronger, but it will also make it brittle if the material is fully crystalline [6].

The XRD (Panalytical X'Pert Pro, UK) instrument is equipped with Cu-Kα radiation operated at 40 kV and 30 mA with vertical high precision goniometer and X'Celerator detector was utilized to find out the elemental composition and percent crystallinity of HAp material. The HAp powder sample were placed into the sample holder and pressed with microscope slide to make a smooth flat surface for analysis with the instrument, it was run for 55 minutes at room temperature over 2theta degree range of 0 - 120° and the data was collected after that. The Match! software was used to identify the space group of HAp in which the elemental composition of the sample can then be retrieved from the inorganic crystal structure database (ICSD). Reference patterns of HAp were also included in the sample data to ensure that the elemental composition of HAp is correctly identified. The percent crystallinity of HAp was calculated by using the TOPAS software in which the area under the diffraction peak is divided by the area under the amorphous hump.

3.2.4 Gel permeation chromatography (GPC)

Gel permeation chromatography (GPC) is a method used for the determination of average molecular weight distribution of a polymer in solution (known as the mobile phase or eluent). GPC separates the polymer based on their size and this is done by injecting a small amount of the polymer solution into a set of columns packed with porous beads. The larger molecules will elute faster than the smaller molecules as the latter can penetrate the pores due to their smaller size. Detectors will be attached to the output of the columns for analysis of the polymers. For analysis of linear polymers, the Differential Refractive Index (DRI) will be employed, while for branched polymers, at least two detectors will be required for their analysis for instance the viscometer (VIS) or a low angle laser light scattering (LALLS) detector. The calibration standards will also be loaded in the system to be measured for generating the calibration curve which can then be compared to the M_w measurement of the polymer sample [7].

This experiment was done to find out the average molecular weight distribution of the three different M_w of poly-L-arginine (PLR) in solution. The eluent used for GPC (Agilent 1260 Infinity GPC/SEC system, USA) measurement of PLR was based on a previously established method [8]. The eluent was prepared which consist of 0.10 % trifluoroacetic acid (TFA), 45 % acetonitrile (ACN) and the remaining with autoclaved DI water, and the pH value adjusted to pH 2. The columns used was PL aquagel-OH 30 and PL aquagel-OH 40 (M_w range from combining both columns is 100 g/mol to 200,000 g/mol) and the calibration standards used is the Agilent EasiVial PEG/PEO 2mL pre-weighed calibration kit (M_w range from 100 g/mol to 1,200,000 g/mol) from Agilent Technologies (USA). Before running the samples, the columns were flushed with autoclaved DI water overnight, followed by the eluent on the next day. This is to wash down any particles or debris left inside the column. The eluent was then used for calibrating the system first, before the start of the sample measurements. 1 mg of the PLR samples were weighed out, dissolved in 2 mL of the eluent and filtered with the 0.22 μm PES syringe filter, and the PEG/PEO calibration standards were dissolved in 2 mL of the eluent. After calibrating the system,

the sample measurement was started with a flow rate of 1 mL/min and each sample (including the standards) were run over 21 minutes with injection volume of 50 μL.

3.2.5 Effect of poly-L-arginine (PLR) and siRNA amount on LbL NPs

The Nanodrop spectrophotometer system were utilized to measure the total siRNA amount present in the LbL NPs fabricated with different loadings of PLR and siRNA. This system is typically used for the quantification of nucleic acid amongst other applications, and it makes use of the sample retention system that relies on surface tension properties of the samples to be measured [9]. In this thesis, LbL NPs were fabricated with different amount of PLR loadings of the following configuration: HAp | **PLR (0.50 mg)** | SPARC siRNA (1.20 nmol) | **PLR (0.50 mg)**, HAp | **PLR (2 mg)** | SPARC siRNA | **PLR (0.50 mg)** and HAp | **PLR (0.50 mg)** | SPARC siRNA | **PLR (2 mg)**. Also, the LbL NPs were fabricated with an increased amount of siRNA loading per layer of the following configuration: HAp | **PLR** (0.50 mg) | **SPARC siRNA (1.20 nmol)** | **PLR** (0.50 mg) and HAp | **PLR** (0.50 mg) | **SPARC siRNA (2.40 nmol)** | **PLR** (0.50 mg).

The rational of conducting this experiment is the speculation that by increasing the amount of PLR and siRNA loading per layer, it could increase the total amount of siRNA content in the LbL NPs. 25 μL (for 1 mg worth of HA) of the respective fabricated LbL NPs was dispersed in 300 μL of 0.25 % Trypsin-EDTA medium and samples were placed in thermoshaker, shaking overnight at 1500 rpm at 37 °C. On the following day, the samples were spun down and the supernatant was measured for total amount of siRNA content present in the respective particles with the Nanodrop system (Thermo Scientific™, Nanodrop™ One, Microvolume UV-VS Spectrophotometer, USA).

3.3 Release behavior of LbL NPs

The release behavior of GFP labelled 6FAM SPARC siRNA LbL NPs was conducted by the use of the microplate reader (iControl Tecan Infinite 200, Austria), with Ex/Em of 480/520 nm. It is a multifunctional instrument that takes measurements of absorbance,

fluorescence and luminescence of the samples, and it is usually used to quantify proteins, expression of genes and various metabolic processes [10]. All sample measurements utilizing the Tecan microplate reader will be compared against a series of 6FAM siRNA standard curve (Tecan measurements to be taken of 6FAM siRNA of known concentrations).

3.3.1 siRNA release behavior of NPs fabricated with different PLR M_W

The nanoparticles were fabricated with PLR M_W 5000 – 15 000 Da, 15 000 – 70 000 Da and >70 000 Da in the 3 layered LbL NPs system. 25 μL (for 1 mg worth of HA) of the respective LbL NPs was dispersed in 300 μL of 0.25 % Trypsin-EDTA medium to test for the total siRNA amount. The respective samples were placed in the thermoshaker, shaking overnight at 1500 rpm at 37 °C. On the following day, the samples were spun down and the supernatant was measured for the total siRNA amount using the microplate reader.

Release study of the respective LbL NPs will be conducted using MWCO of 100 kD dialysis tubing placed in a glass container filled with 10 mL of PBS (pH 7.40). The glass container was placed in the thermoshaker, shaking overnight at 50 rpm at 37 °C over a period of 28 days with the stipulated time intervals of day 1, day 3, day 5, day 7, day 14, day 21 and day 28. At the respective time interval, readings were measured using the microplate reader and the glass container were replenished with fresh 10 mL PBS (pH 7.40) for the subsequent timepoints.

The rational for conducting this experiment is to find out if there will be a greater amount of total siRNA loaded in the 3 layered NPs coated with PLR M_W >70 000 Da. This could in turn lead to a higher amount of release at the respective time interval, as compared to the 3 layered NPs coated with PLR M_W 5000 – 15 000 Da and 15 000 – 70 000 Da. A higher molecular weight of PLR would mean that there will be a greater number of repeating units. Therefore, this could increase the overall net positive charges of the polyelectrolyte layer. Also, this in turn would allow more siRNA to be loaded in the LbL NPs. Based on the total amount of siRNA content and the release profile of the respective

LbL NPs, PLR M_W of >70 000 Da was decided to be used as the polyelectrolyte in the bilayers of the LbL NPs system.

3.3.2 siRNA release behavior of NPs fabricated with additional siRNA layers

The nanoparticles are fabricated with PLR M_w >70 000 Da in 3 layered (containing 1 layer of siRNA), 5 layered (containing 2 layers of siRNA) and 7 layered (containing 3 layers of siRNA) LbL NPs system. 25 μL (for 1 mg worth of HA) of the respective LbL NPs was dispersed in 300 μL of 0.25 % Trypsin-EDTA medium to test for the total siRNA content. The respective samples were placed in the thermoshaker, shaking overnight at 1500 rpm at 37 °C. On the following day, the samples were spun down and the supernatant was measured for the total siRNA content in the respective LbL NPs using the microplate reader.

Release study of the respective LbL NPs will be conducted using MWCO of 100kD dialysis tubing placed in a glass container filled with 10 mL of PBS (pH 7.40). The glass container was placed in the thermoshaker, shaking overnight at 50 rpm at 37 °C over a period of 28 days with the stipulated time interval of day 1, day 3, day 5, day 7, day 14, day 21 and day 28. At the respective time interval, readings were measured using the microplate reader and the glass container were replenished with fresh 10 mL PBS (pH 7.40) for the subsequent timepoints.

The rational for conducting this experiment is to find out if there will be a higher amount of total siRNA loaded in the 7 layered NPs (containing 3 layers of siRNA). Hence, in turn could lead to a higher amount of release at the respective time interval, as compared to the 3 and 5 layered NPs. Additional layers of siRNA loaded in the LbL NPs could increase the total amount of siRNA content in the LbL NPs. Based on the total amount of siRNA content and the release profile of the respective LbL NPs, the 7 layered LbL NPs was decided to be used for the subsequent *in vitro* studies.

3.4 Transmission electron microscope (TEM) imaging

To affirm the shape morphology of the NPs, the fabrication of various batches of LbL NPs (HAp core material, 3 layered, 5 layered and 7 layered) was imaged by Transmission Electron Microscopy (TEM) (Carl Zeiss Libra 120 Plus, Germany). TEM utilizes the transmission of focused beam of highly energetic electrons to examine samples, producing a high resolution of image that will be reflected onto the screen as compared to the conventional light microscopy, hence making it an essential equipment for imaging nanomaterials to acquire qualitative and quantitative analysis of NPs such as the surface features and shape morphology [11]. Samples were prepared in the dilution of 1:100 by adding a drop of sample onto the copper grid and drying overnight before taking the TEM images.

3.5 *In vitro* toxicity study

MTT (methyl-thiazolyldiphenyl-tetrazolium bromide, Sigma-Aldrich, USA) assay, a cell viability assay, is done to assess the viability of cells after treatment with NPs. Actively respiring cells will convert the water-soluble MTT to an insoluble purple formazan which can be solubilized with the addition of DMSO and the fluorescence can then be determined. 500 HuRPF cells were cultured in the 96-wells transparent plate, incubated overnight at 37 °C with 5 % CO_2. On the next day, HuRPF cells was washed with PBS and the respective concentration of the 7 layered siRNA LbL NPs (with concentration of 258 μg, 129 μg and 64.50 μg) was added into the cells. The HuRPF cells were then incubated with the NPs for 24- and 48- hours intervals. At the respective time interval, the cells were assayed for their cell viability with MTT by washing the cells with PBS and 10 μL of the MTT supplemented with 190 μL of PBS was added into each well. After incubation with MTT for 4 hours, at 37 °C with 5 % CO_2, the medium was removed and the cells with the purple formazan crystals were dissolved in DMSO. The fluorescence intensities of the cells were then measured using the microplate reader with an absorbance wavelength of 595 nm. The viability of cells was then calculated in comparison with the control (cells without treatment of NPs).

3.6 *In vitro* cellular entry of LbL NPs

3.6.1 Cell cultures

The Human retroperitoneal fibroblast (HuRPF) cells used in the cell studies were cultured using RPMI 1640 medium supplemented with 10 % FBS and 1 % antibiotics. The cells were then cultured in the incubator at 37 °C with 5 % CO_2 and cultured until confluent before they were used for *in vitro* studies. The samples (cells treated with NPs) were compared against control cells (cells without NPs treatment) for all cell related experiments, whereas for immunoblotting assay the cells will be treated with siSPARC (LbL NPs loaded with SPARC siRNA) and siSCRAM (LbL NPs loaded with SCRAM siRNA as a negative control). All sample measurements involving the use of Tecan microplate reader for measuring the amount of 6FAM siRNA will be compared against a series of 6FAM siRNA standard curve (Tecan measurements to be taken of 6FAM siRNA of known concentrations), with Ex/Em of 480/520 nm.

3.6.2 *In vitro* qualitative cellular entry of LbL NPs

For the qualitative study, the aim of this experiment is to find out whether if the 7 layered LbL NPs are able to internalize into the cells. 5000 HuRPF cells were cultured in the covered glass chamber system (Thermo Scientific™, Nunc™, LAB-TEK™ II Chambered Coverglass, USA) at 37 °C with 5 % CO_2. After 24 hours of incubation, the HuRPF cells was washed with PBS and 0.80 μL of the 7 layered FITC-labelled HAp LbL NPs were added into the chambers. The cells were incubated with the NPs overnight at 37 °C with 5 % CO_2. The cells were washed with PBS on the following day then fixed with 4 % paraformaldehyde (PFA), and incubated at 37 °C with 5 % CO_2 for 10 mins. The 4 % PFA was then removed and replaced with vectashield with DAPI (Vector Laboratories, USA). It was incubated for 4 hours at 37 °C with 5 % CO_2 to stain the cell nuclei. Following this, the cells will be ready for observation using the confocal-laser scanning microscope (CLSM, Leica TCS SP8, Germany) with FITC Ex/Em of 495 nm/519 nm (at magnification

of 40X, Zoom 4.3). The samples were compared against the control cells (without any treatment of particles).

3.6.3 *In vitro* quantitative cellular entry of LbL NPs

For the quantitative study, the aim of this experiment is to find out the percentage of cells with the 7 layered 6FAM-labelled siRNA LbL NPs over various time intervals of day 1, day 3, day 5, day 7, day 14 and day 21. 50 000 HuRPF cells were cultured in the 6-wells plate, incubated at 37 °C with 5 % CO_2. After 24 hours of incubation, the HuRPF cells was washed with PBS and 8 μL of the 7 layered 6FAM-labelled siRNA LbL NPs were added into the wells. The cells were incubated with the NPs at 37 °C with 5 % CO_2, and they were washed with PBS at the respective time intervals then trypsinized and incubated with 0.40 % Trypan blue (Sigma-Aldrich, USA) for 7 minutes at room temperature. Trypan blue is used to quench the surface fluorescence surrounding the cells so that the measurements taken will only reflect the true fluorescence emission from within the cells. The cells will then be spun down at 650 RCF for 5 minutes at 10 °C. Following this, the supernatant was removed and the cell pellet was resuspended in PBS and aliquot into the 96-wells transparent plate for quantitative analysis using the Guava easyCyte Flow Cytometry System. The flow cytometry measures forward and side scattering of light by the cells. A laser beam will be used as the light source to shine upon the cell suspension. As the cell suspension passes through the laser beam, the light will be scattered. Based on the granularity and size of the cell, the direction of light scattering differs. A detector placed in front of the laser beam measures the forward scattering (FS) of light and the side detectors measures the side scattering (SS) of light. The FSC measures amount of laser beam that passes around the cell which provides the relative size of the cell. The SSC measures amount of laser beam that bounces off of the materials inside the cells. Any laser light of the similar wavelength of the laser that bounces off of the materials inside the cells will be collected and recorded as the SSC. The data will then be analyzed using the GuavaExpress Pro software (EMD Millipore, USA). The samples were compared against the control cells (without treatment of NPs).

3.7 Evaluate the amount of free siRNA within HuRPF cells

From the qualitative and the quantitative cellular entry of the 7 layered LbL NPs, further investigation was done to observe the amount of free siRNA that is found within the HuRPF cells. This is essential to know so that the amount of free siRNA within the cells/cytoplasm at the respective time intervals (day 1, day 3, day 5, day 7, day 14 and day 21) could be utilized as a correlation to the percentage gene silencing of SPARC. Also, this information is important as the siRNA release behavior within the cells could then be attained, and also the information on the remaining amount of siRNA that is not present in the cytoplasm (amount of SPARC siRNA that is retained in the NPs and the amount of siRNA that is consumed/degraded) could also be elucidated. The siRNA release behavior within the cells could also be used to correlate with the siRNA release behavior in PBS medium (at pH 7.40). This is to observe whether if the release of siRNA in PBS medium (at pH 7.40) is similar to the release of siRNA within cells.

50 000 HuRPF cells were cultured in the 6-wells plate, incubated at 37 °C with 5 % CO_2. After 24 hours of incubation, the HuRPF cells was washed with PBS and 8 μL of the 7 layered 6FAM-labelled siRNA LbL NPs were added into the wells. The cells were incubated with the NPs at 37 °C with 5 % CO_2, and at the respective time intervals they were washed with PBS. The PBS was then removed completely and the cells were incubated for 10 minutes with 150 μL of cell lysis buffer (to lyze the cells and break open the cell membrane to release the free siRNA found within the cells). Following this, the cells will be scratched and aliquot into a 2 mL microcentrifuge tube, 150 μL of PBS would then be added and vortex to mix well (to prevent any prolonged effect of the lysis buffer on the LbL NPs configuration from within the cells). The samples will then be incubated for 5 minutes at room temperature and after that to be spun down at 15,000 rpm at 10 °C for 5 minutes. The supernatant which contains the free siRNA will be aliquot into the 96-wells black plate to measure using the microplate reader (Ex/Em = 480/520 nm) for the amount of free siRNA within the cells at the respective time interval as compared to the control cells (without treatment of NPs). The cell pellet (contains lyzed cell membrane and the remaining NPs) will be dispersed in 0.25 % trypsin-EDTA, shaking overnight using the

thermoshaker at 37 °C, to break open the LbL NPs and then to measure using the microplate reader (Ex/Em = 480/520 nm) for the remaining siRNA on the NPs (of the respective time intervals) at the following day. All samples will be compared against a series of 6FAM siRNA standard curve (Tecan measurements to be taken of 6FAM siRNA of known concentrations).

Xupeng Mu *et al.* evaluated the encapsulation efficiency of siRNA for their PEG-LP/siRNA NPs by measuring the amount of unencapsulated siRNA in the supernatant, in which the NPs complex fabricated with the 6FAM-labelled siRNA were spun down and the supernatant (containing unencapsulated siRNA) was measured using the microplate reader (Ex/Em = 480/520 nm) [12]. Hence, with reference to the article, it can be assured that in my experiment, the lyzed cells which contains the remaining NPs are being spun down. The measurement of the supernatant will be the true value of the free siRNA within the cells.

3.8 Immunoblotting assay

Immunoblotting assay is performed to find out the percentage of *SPARC* knockdown after administering the HuRPF cells with the 7 layered LbL NPs (siSPARC-LbL and siSCRAM-LbL) for the stipulated time intervals (day 1, day 3, day 5, day 7, day 14 and day 21). 50 000 HuRPF cells were cultured in the 6-wells plate, incubated at 37 °C with 5 % CO_2. After 24 hours of incubation, the HuRPF cells were washed with PBS and 8 μL of the respective 7 layered SPARC-siRNA LbL (siSPARC-LbL) NPs and 7 layered SCRAM-siRNA LbL (siSCRAM-LbL) NPs (negative control) were added into the wells. The cells were incubated with the respective NPs at 37 °C with 5 % CO_2, and at the respective time intervals they were washed with PBS. The PBS was then removed completely followed by the protein extraction of the HuRPF cells treated with siSPARC-LbL and siSCRAM-LbL. The measurement of the protein concentration present in the respective samples were compared with the bovine serum albumin, BSA (Sigma-Aldrich, USA) standards of known concentrations using the microplate reader with an absorbance wavelength of 595 nm. Antibodies against SPARC were purchased from Santa Cruz Biotechnology (California,

USA). Horseradish peroxidase-conjugated secondary antibodies were from Jackson ImmunoResearch Laboratories (Pennsylvania, USA). Normalization to check for the variation in loading of the samples was performed using GAPDH (Santa Cruz Biotechnology, California, USA) as the housekeeping protein.

References

[1] Li Fong Seet, Y.F.T., Li Zhen Toh, Stephanie WL Chu, Ying Shi Lee, Subbu S Venkatraman, Tina T Wong, *Targeted therapy for the post-operative conjunctiva: SPARC silencing reduces collagen deposition.* Br J Ophthalmol, 2018. **102**(10): p. 1460–1470.

[2] Lorber, B.F., Frédéric Bailly, Marc Roy, Hervé Kern, Daniel, *Protein Analysis by Dynamic Light Scattering: Methods and Techniques for Students.* Biochemistry and Molecular Biology Education, 2012. **40**(6): p. 372-382.

[3] Ltd, M.I., *Zeta Potential Theory*, in *Zetasizer Nano Series*. p. 16.1-16.12.

[4] Barbara L Dutrow, C.M.C. *X-ray Powder Diffraction (XRD)*. 2018; Available from: https://serc.carleton.edu/research_education/geochemsheets/techniques/XRD.html.

[5] Natassia Lona Batista, P.O., Gérard Bernhart, Mirabel Cerqueira Rezende, Edson Cocchieri Botelho, *Correlation between degree of crystallinity, morphology and mechanical properties of PPS/carbon fiber laminates.* Materials Research, 2016. **19**(1): p. 195-201.

[6] Suryanarayana, C., *Mechanical behavior of emerging materials.* Materials Today, 2012. **15**(11): p. 486-498.

[7] P.Cheremisinoff, N., in *Chromatographic Techniques*, N. P.Cheremisinoff, Editor. 2008, Elsevier Inc.: Westwood, New Jersey, U.S.A. p. 1-15.

[8] Tomoko Hashimoto, T.K., Takeshi Nagasaki, Akira Murakami and Tetsuji Yamaoka, *Quantitative comparison between poly(L-arginine) and poly(L-lysine) at each step of polyplex-based gene transfection using a microinjection technique.* Sci. Technol. Adv. Mater., 2012. **13**(015009): p. 1-8.

[9] Desjardins, P.C., Deborah, *NanoDrop microvolume quantitation of nucleic acids.* Journal of Visualized Experiments : JoVE, 2010(45): p. 2565.

[10] Database, J.S.E. 2018, JoVE Cambridge, MA.

[11] David B. Willams, C.B.C., *Transmission Electron Microscopy*. 2nd ed. 2009, New York, USA: Springer. 804.

[12] Xupeng Mu, H.L., Lianlian Fan, Shaohua Yan, and Kebang Hu *Efficient Delivery of Therapeutic siRNA with Nanoparticles Induces Apoptosis in Prostate Cancer Cells.* Journal of Nanomaterials, 2018. **2018**: p. 1-10.

Chapter 4

Results and Discussion

The chapter reports the characterization and optimization of the layer by layer (LbL) nanoparticles (NPs) system. The aim of this study is to maximize the total amount of siRNA that can be loaded in the LbL NPs system to cause an effective and prolonged gene silencing effect over 21 days. Various parameters of the LbL NPs system were evaluated and it was observed that the particles coated with the highest PLR molecular weight (M_w) and optimized with additional siRNA layers contained the greatest total siRNA content. These particles were also observed to release the highest amount of siRNA (in PBS medium, pH 7.40). The selected multilayered NPs system was tested for its cell viability and the particles cellular internalization was investigated. Finally, the study proceeded to investigate the amount of free siRNA released within cells and also on their gene silencing effect. It was observed that the system was able to effectively deliver siRNA into the cells/cytoplasm to cause an efficient and prolonged gene silencing effect over 21 days.

4.1 Introduction

The aim of the report is to maximize the total siRNA content encapsulated in the multilayered nanoparticles (NPs) system to cause an effective and prolonged gene silencing effect. Characterization of the NPs to examine their size and zeta potential were measured utilizing the Malvern zetasizer. X-ray diffraction (XRD) was employed to identify the percent crystallinity present in the HAp core material. Gel permeation chromatography (GPC) was carried out to determine the average molecular weight distribution of the poly-L-arginine (PLR) polyelectrolyte in solution. Transmission Electron Microscopy (TEM) imaging was done to confirm the shape morphology of the particles. Cell viability assay was investigated to assess the toxicity of the LbL NPs system. Following that, to increase the amount of siRNA loaded within the particle, different PLR/siRNA coating amount were investigated. The release behavior of the LbL NPs system loaded with PLR of different M_w and the system loaded with additional siRNA layers will be investigated. This is to observe and select the optimal NPs system that releases the most siRNA at each time interval (over 28 days). The NPs system that is selected will then be used for the subsequent *in vitro* studies. *In vitro* qualitative and quantitative cellular internalization studies will be carried out to observe the LbL NPs internalization into HuRPF cells. The amount of free siRNA within the HuRPF cells and the amount of *SPARC* knockdown in HuRPF cells over 21 days were evaluated.

4.2 Characterization studies of LbL NPs

4.2.1 X-ray powder diffraction (XRD)

The XRD technique was utilized to evaluate the elemental composition and percent crystallinity of the HAp core material. The data was collected and interpreted by Match! and TOPAS software from the FACTS laboratory.

The XRD data processed with Match! showed that HAp was made up of calcium (Ca), phosphorus (P), oxygen (O) and hydrogen (H). The respective elements and intensities

match the reference pattern of HAp as retrieved from the ICSD database (ICSD entry no.: 04-010-6315).

The percent crystallinity of HAp was calculated by the TOPAS software to be at 78.30 % by dividing the area under the diffraction peak by the area under the amorphous hump. Figure 4.1 below illustrates the XRD patterns of the HAp (<200 nm) powder sample:

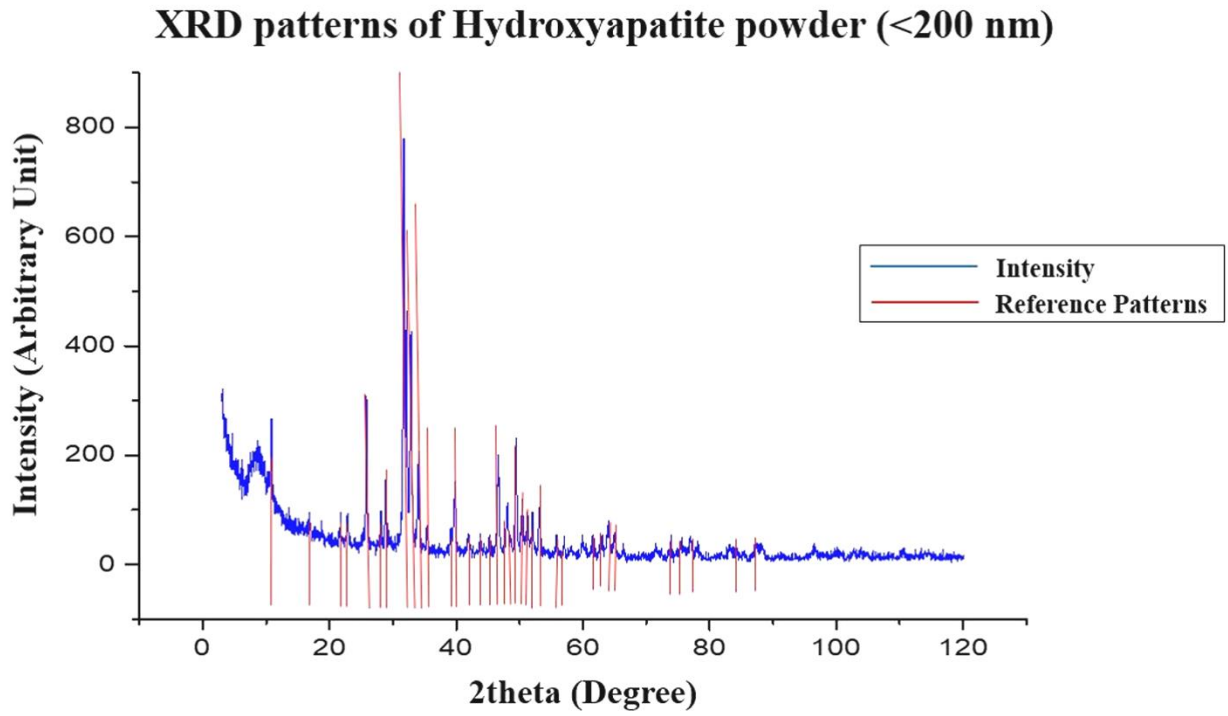

Figure 4.1: XRD patterns of HAp (<200 nm) powder sample (blue) with the reference patterns (red) included. The percent crystallinity was found to be at 78.30 %. The sample was run for 55 minutes at room temperature over 2theta degree range of 0 - 120°. The data was collected and interpreted by Match! and TOPAS software from the FACTS laboratory.

From Figure 4.1, it was ascertained that the HAp nanopowder [$Ca_5(OH)(PO_4)_3$] procured from Sigma-Aldrich (USA) consists of the exact elemental compositions as HAp according to the XRD data. Furthermore, the percent crystallinity of HAp core material was found to be at 78.30 %, which indicates that the material was mainly crystalline. This is a

characteristic of a hard and strong material. The remaining 21.70 % of the sample was found to be amorphous, indicating that there are portions of the constituents in the material arranged in a disorderly manner. The amorphous regions allow the material to be more flexible and soluble than their crystalline counterparts. Hence, the crystalline regions provide HAp with high mechanical strength while the amorphous regions enhance the flexibility and solubility of the material. These properties allow HAp to undergo the various processing steps (i.e. maximum speed used on vortex mixer) during the layer by layer fabrication preventing the deformation of the particles.

4.2.2 Gel permeation chromatography (GPC)

Gel permeation chromatography (GPC) was carried out to determine the average molecular weight distribution of the various poly-L-arginine (PLR) (procured from Sigma-Aldrich). PLR molecular weight (with the analysis provided by Sigma-Aldrich) of 5000 – 15 000 Da, 15 000 – 70 000 Da and >70 000 Da was used in this study. The average molecular weight analysis on the various PLR polyelectrolytes was determined by using the Agilent 1260 Infinity GPC/SEC system (with comparison against the Agilent EasiVial PEG/PEO standard calibration kit). The average molecular weight (M_w) distribution of PLR, the calculated PDI, degree of polymerization (DP) and charge per molecule of the respective PLR is as illustrated in Table 4.1 below:

Table 4.1: Parameters of the poly-L-arginine (PLR) used. M_w and Mn represents the weight average and the number average molecular weight respectively. PDI represents the polydispersity index and DP represents the degree of polymerization of the respective PLR.

Mw of PLR provided by Sigma-Aldrich (Da)	Mw of PLR (Da)*	Mn of PLR (Da)*	PDI (Mw/Mn)*	Degree of polymerization (DP)	Ratio of Charge per molecule of PLR/siRNA
5000 – 15 000	10053 ± 23.64	7584 ± 3962.20	1.33 ± 0.69	48	1
15 000 – 70 000	37649.67 ± 3796.37	31066.67 ± 3559.24	1.21 ± 0.18	198	5
>70 000	166090.70 ± 766.55	48540 ± 12852.99	3.42 ± 0.91	309	7

*Determined by GPC.

The same kind of polymer can differ largely in terms of molecular weight solely due to the different number of repeating units. Hence, the molecular weight of polymers is given as averages determined by the GPC system. There are two commonly determined values by GPC: the weight average molecular weight (M_w) which is calculated from the weight fraction distribution of molecules with different sizes. As the larger molecules weigh more than the smaller molecules, the calculated weight average M_w would be skewed towards the higher M_w of macromolecules in the sample that contributes to the averaging process while it puts aside those with a smaller M_w. This means that a very small amount of the larger molecules can have a huge influence towards the weight average M_w calculation of the sample. The number average molecular weight (Mn) as determined by GPC takes into account all the molecules of the polymer (all molecular weights contribute significantly) in the averaging process (in which the total weight of the molecules in the sample is divided by the total number of molecules that the sample contains). The Mn takes into consideration the total number of molecules regardless of size that are present in the sample [1]. Therefore, the weight average M_w is always greater than the number average molecular weight (Mn) since it takes into consideration not only the number of molecules of each of the polymer present in the sample, but also the mass of the respective polymers.

Table 4.1 shows the M_w and Mn determined by GPC for the various PLR used in this study. The M_w for PLR 5000 – 15 000 Da was found to be at 10053 ± 23.64 Da, with Mn of 7584

± 3962.20 Da. The M_w for PLR 15 000 – 70 000 Da was found to be at 37649.67 ± 3796.37 Da, with Mn of 31066.67 ± 3559.24 Da. The M_w for PLR >70 000 Da was found to be at 166090.70 ± 766.55 Da, with Mn of 48540 ± 12852.99 Da.

The degree of polymerization (DP) relates to the average number of the monomer unit in the polymer chain and it is calculated by dividing the number average molecular weight (Mn) of the polymer by the molecular weight of a single repeating unit/monomer. The molecular weight of L-arginine is 157 Da. The formula to calculate the DP of its respective polymer is as given below:

$$\text{DP of PLR} = \frac{\text{Mn of PLR}}{157\ \text{Da}}$$

The relation between DP and molecular weight (Mn) of the polymer is given by the multiplication of DP and the molecular weight of a single repeating unit/monomer [2]. DP relates to the average numbers of the repeated monomer unit, with each unit carrying one positive charge in the guanidinium group. This in turn correlates to the number of charges per molecule of the respective PLR which will be further explained in the later part of this section with regards to the values calculated from Table 4.1. Chain entanglement (ability of polymer chains to become entangled with one another) is another important factor contributing to the physical properties of the polymer. The degree of chain entanglement increases as the polymer chain gets longer or as the molecular weight of the polymer increases, which contributes to its strength and flexibility [3]. Whereas, a shorter polymer chain is weak and brittle but it becomes strong and pliable above certain length. This is a factor that could be taken into consideration in deciding the most suitable type of PLR (i.e. based on the length of polymer chain and molecular weight) to be used. This ensures the ability of the PLR to exhibit strong nucleic acid binding and promotes efficient cellular entry. It was observed that a minimum of 4 to 8 PLR repeating units were needed to effectively condense nucleic acids and to trigger the cellular internalization (an increase in the repeating units would lead to an increase in transfection efficiency) [4].

PLR >70 000 Da showed the highest DP at 309 among the three different PLR M_w polypeptides as listed in Table 4.1. Since the DP corresponds to the number of positive charges on the polymer, this means that there are 309 positive charges on the PLR >70 000 Da polypeptide. This also meant that PLR >70 000 Da has the longest polymer chain (compared to the repeating units of the lower PLR M_w). This increases its nucleic acid binding ability, increasing the total siRNA content in the particles. This also helps in condensing the nucleic acids (i.e. siRNA) more effectively, hence reducing the overall particle size. Smaller-sized particles can undergo cellular entry significantly faster as compared to bigger-sized particles, to trigger an increased transfection efficiency. Being the highest PLR M_w, the chain entanglement of PLR >70 000 Da would be greater which gives the polymer more strength and flexibility.

With the information listed in Table 4.1, the charge per molecule of PLR can be calculated based on the ratio of charge per molecule of PLR and of the siRNA. For instance, PLR >70 000 Da had a total number of 309 positive charges per molecule and siRNA (consist of 21 base-pairs) possess 1 negative charge per base/molecule at its phosphate group. Hence, for a double helix siRNA there would be a total number of 42 negative charges per molecule of siRNA. From this, the ratio of the charge per molecule of PLR >70 000 Da to the charge per molecule of siRNA would be 7:1. This means that each molecule of PLR is able to bind to 7 molecules of siRNA. Similarly, for PLR 15 000 – 70 000 Da, there are a total number of 198 positive charges per molecule. Therefore, the ratio of the charge per molecule of PLR 15 000 – 70 000 Da to the charge per molecule of siRNA would be 5:1, meaning that each molecule of PLR is able to bind to 5 molecules of siRNA. For the PLR 5000 – 15 000 Da, there are a total number of 48 positive charges per molecule, so the ratio of the charge per molecule of PLR 5000 – 15 000 Da to the charge per molecule of siRNA would be 1:1. This means that each molecule of PLR is able to bind to 1 molecule of siRNA. Thus, PLR >70 000 Da has the ability to bind to more siRNA as compared to the PLR polypeptides with a lower M_w as listed in Table 4.1. This explains the capability for the LbL NPs coated with PLR >70 000 Da to possess the highest amount of total siRNA content, which will be evaluated with experimental data under the section of 4.2.4 below.

4.2.3 Effect of poly-L-arginine (PLR) and siRNA amount on LbL NPs

It was hypothesized that loading different amounts of PLR in each layer and an increased amount of siRNA per layer would lead to a higher total siRNA content in the LbL NPs. To affirm this, 3 layered LbL NPs (using PLR >70 000 Da) were fabricated with different amounts of PLR loading (0.50 mg and 2 mg of PLR in either the inner or outer layer of the NPs) and with an increased amount of siRNA loading per layer (1.20 nmol and 2.40 nmol of siRNA per layer of the NPs). The particles fabricated were of the following configurations as illustrated in Table 4.2 below with their respective size and zeta potential of the LbL NPs, and also for the total amount of siRNA content in the respective LbL NPs configurations:

Table 4.2: Total amount of siRNA content, size and zeta potential of the LbL NPs with different amount of PLR loaded and with an increased amount of siRNA loaded per layer.

LbL NPs configuration	Size (nm) ± STDEV	PDI ± STDEV	Zeta potential (mV) ± STDEV	Amount of siRNA content (pmol)
HAp|PLR(0.5 mg)|siRNA(1.2nmol)|PLR(0.5 mg)*^	314.03 ± 4.23	0.18 ± 0.02	38.80 ± 0.20	542.79 ± 7.98
HAp|PLR(2 mg)|siRNA(1.2nmol)|PLR(0.5 mg)*	298.97 ± 3.56	0.35 ± 0.10	35.17 ± 2.42	517.79 ± 30.22
HAp|PLR(0.5 mg)|siRNA(1.2nmol)|PLR(2 mg)*	310.90 ± 0.72	0.24 ± 0.03	35.33 ± 0.74	543.74 ± 5.47
HAp|PLR(0.5 mg)|siRNA(2.4nmol)|PLR(0.5 mg)^	313.50 ± 0.44	0.26 ± 0.01	32.43 ± 0.38	547.44 ± 14.02

* LbL NPs coated with different amounts of PLR. ^ LbL NPs loaded with different amounts of siRNA.

Table 4.2 shows that the size and zeta potential did not increase when more amount of PLR was loaded in the LbL NPs system. The size of HAp was 184.83 (± 7.08) nm with zeta potential of -1.56 (± 0.04) mV. The size and zeta potential of NPs loaded with more amount of PLR did not increase probably because of the maximum neutralization of the HAp

charge. Hence, there was no changes in the size and zeta potential when an increased amount of PLR was loaded.

In order to compare and verify the total siRNA amount present in the particles, the total siRNA contents of the various particles were released and quantified with Nanodrop. Briefly, 1 mg of each of the particles were dispersed in 0.25 % trypsin-EDTA solution, vortexed then shaken at 1500 rpm overnight at 37 °C in the thermoshaker to disassemble the particles (releasing all the siRNA contents). The anova statistical analysis was carried out to compare the total amount of siRNA present in the various particles loaded with 1.20 nmol of siRNA and different amounts of PLR, as listed in Table 4.2 (denoted by *). The *p*-value was found to be 0.22, which implies there were no significant differences. Therefore, this concludes that more PLR coating on the LbL NPs will not affect the thickness and loading of siRNA in the particles. Further, 0.50 mg of PLR coating per layer for every 1 mg of HAp used was the optimized amount for maximum PLR coating on the LbL NPs. Hence, 0.50 mg of PLR per layer would be used for the fabrication of the LbL NPs in the subsequent studies.

As observed from Table 4.2, the size of the NPs did not increase with more amount of siRNA loaded in the LbL NPs and the zeta potential did not increase for the NPs loaded with higher amount of siRNA. It could be due to the washing steps during the LbL NPs fabrication to wash away uncoated PLR before the fabrication of the next layer onto the NPs. In the process, certain amounts of PLR could have been washed away (which is also reported in literatures regarding the loss of composites by the many necessary washing steps during the layer by layer fabrication [5]). Hence, the PLR that have been coated onto the NPs binds to only 1.20 nmol of siRNA and the remaining uncoated siRNA could have been washed away before the fabrication of the next layer of PLR.

In order to verify that the amount of total siRNA content present in the particles are similar, the total siRNA contents of the various particles were released and quantified with Nanodrop. The anova statistical analysis was carried out and the *p*-value was found to be at 0.64, in which a *p*-value >0.05 means that the data has no significant differences.

Therefore, this concludes that by loading more amount of siRNA in each siRNA layer did not increase the total siRNA content in the particle and that the coating amount of 1.20 nmol siRNA used was apparently the optimal amount for siRNA loading. Additionally, it was reported that the LbL NPs loaded with 1.20 nmol siRNA is sufficient to elicit gene silencing effect for a minimum period of 2 weeks [6], and the aim of this thesis is to ultimately deliver a sufficient amount of siRNA into the cell cytoplasm to cause an efficient and prolonged gene silencing effect. Hence, 1.20 nmol siRNA per layer would be used for the fabrication of the LbL NPs in the subsequent studies.

4.2.4 Effect of poly-L-arginine (PLR) M_w on LbL NPs

Since the effect of poly-L-arginine (PLR) and siRNA amount did not show significant increase to the total siRNA content in the LbL NPs, further investigations were done to coat the LbL NPs with different PLR molecular weight (PLR 5000 – 15000 Da, PLR 15 000 – 70 000 Da and PLR >70 000 Da) for increasing the total siRNA content in the particles. This is to validate if there will be any effect on the LbL NPs by using different PLR M_w possessing different degree of polymerization.

According to the GPC data from Table 4.1, it was observed that PLR >70 000 Da shows the highest degree of polymerization (DP) at 309 among the three different PLR M_w polypeptides and that for every 1 molecule of PLR >70 000 Da, it could bind to 7 molecules of siRNA (based on calculations). Also, it was mentioned in literatures that the degree of chain entanglement increases as the polymer chain/repeating units gets longer, contributing to the strength and flexibility of the polymer. The polymer with the longest chain length will be able to increase its nucleic acid (i.e. siRNA) binding ability. Therefore, referring back to Table 4.1, PLR >70 000 Da seems to be the best candidate (as compared to PLR 5000 – 15 000 Da and PLR 15 000 – 70 000 Da) for the ability to bind to more amount of siRNA which could increase the overall total amount of siRNA in the LbL NPs. To affirm this, 3 layered LbL NPs were fabricated with different PLR M_w which were of the following configurations as illustrated in Table 4.3 below with their respective size and zeta potential

of the LbL NPs, and also for the total amount of siRNA content in the respective LbL NPs configurations:

Table 4.3: Total amount of siRNA content, size and zeta potential of the LbL NPs coated with different PLR M_w per layer.

LbL NPs configuration (HAp | PLR | siRNA | PLR)	Size (nm) ± STDEV	PDI ± STDEV	Zeta potential (mV) ± STDEV	Amount of siRNA content (pmol)
3 layered NPs loaded with PLR 5000 – 15 000 Da	445.67 ± 1.88	0.28 ± 0.06	33.77 ± 0.45	495.72 ± 29.77
3 layered NPs loaded with PLR 15 000 – 70 000 Da	394.27 ± 13.80	0.29 ± 0.15	33.30 ± 0.00	519.81 ± 22.48
3 layered NPs loaded with PLR >70 000 Da	314.03 ± 4.23	0.18 ± 0.02	38.80 ± 0.10	584.32 ± 3.33

Table 4.3 shows that the size of the NPs decreases with higher PLR M_w coated on the LbL NPs but the zeta potential did not increase when PLR 5000 – 15 000 Da and PLR 15 000 – 70 000 Da was coated on the LbL NPs system. However, the zeta potential for LbL NPs coated with PLR >70 000 Da increased as compared to the LbL NPs coated with PLR 5000 – 15 000 Da and PLR 15 000 – 70 000 Da. This would further validate the GPC data and explanation from Table 4.1 that PLR >70 000 Da having more repeating units (possessing the highest DP) and thus the longer polymer chain (as compared to PLR 5000 – 15 000 Da and PLR 15 000 – 70 000 Da) is able to increase its ability to bind to more siRNA through electrostatic interactions and to condense the siRNA more effectively which reduces the overall particle size as shown from Table 4.3 with the size of 314.03 ± 4.23 nm for 3 layered NPs coated with PLR >70 000 Da.

Experiments were done to compare and verify if the total amount of siRNA present in the 3 layered LbL NPs coated with PLR >70 000 Da contains the most siRNA (as compared to the 3 layered LbL NPs coated with PLR 5000 – 15 000 Da and PLR 15 000 – 70 000 Da). The total siRNA contents of the various particles were released and quantified with the microplate reader (the siRNA used in this experiment will be labelled with 6FAM GFP) and the samples are compared against a series of 6FAM siRNA of known concentrations,

with Ex/Em of 480/520 nm. The anova statistical analysis was carried out to compare the three particles coated with different PLR M_w and the *p*-value was found to be at 0.01, in which a *p*-value <0.05 means that the data has significant differences.

However, the total amount of siRNA content for 3 layered LbL NPs coated with PLR 5000 – 15 000 Da and PLR 15 000 – 70 000 Da does not show significant differences as it could be due to their low DP. The lower M_w of PLR which possess a lower DP results in a decrease on its nucleic acid binding ability, thus the lesser total siRNA content in the particles. Furthermore, PLR 5000 – 15 000 Da possessing the shortest repeating units would have a decreased ability to bind and condense the siRNA layer effectively. Hence, making the larger sized particle at 445.67 (± 1.88) nm as compared to the particle coated with PLR 15 000 – 70 000 Da with the size of 394.27 (± 13.80) nm.

All in all, the 3 layered LbL NPs coated with PLR >70 000 Da has longer repeating units which can bind to more amount of siRNA (1 molecule of PLR can bind to 7 molecules of siRNA) hence the highest amount of total siRNA content at 584.32 (± 3.33) pmol as compared to the 3 layered LbL NPs coated with PLR 5000 – 15 000 Da (1 molecule of PLR can bind to 1 molecule of siRNA) with total siRNA content of 495.72 (± 29.77) pmol and the 3 layered LbL NPs coated with PLR 15 000 – 70 000 Da (1 molecule of PLR can bind to 5 molecules of siRNA) with total siRNA content of 519.81 (± 22.48) pmol. However, before deciding on the PLR M_w that should be used for coating on the LbL NPs for subsequent *in vitro* studies, the release behavior (in PBS medium) of the particles coated with the different PLR M_w were investigated as shown in 4.2.6.

4.2.5 Effect of additional siRNA layer on LbL NPs

In order to further increase siRNA loading in the particles to achieve a more prolonged and sustained gene silencing effect, additional layers of siRNA can be fabricated on the LbL NPs system. The LbL NPs coated with PLR >70 000 Da and loaded with increasing layers of 6FAM-labelled siRNA was fabricated in 3 layered LbL NPs configuration (containing 1 layer of siRNA), 5 layered LbL NPs configuration (containing 2 layers of siRNA) and 7

layered LbL NPs configuration (containing 3 layers of siRNA). The size, zeta potential and the total amount of siRNA content in the respective LbL NPs configurations are shown in Table 4.4:

Table 4.4: Total amount of siRNA content, size and zeta potential of the 3, 5 and 7 layered LbL NPs coated with PLR >70 000 Da.

LbL NPs configuration	Size (nm) ± STDEV	PDI ± STDEV	Zeta potential (mV) ± STDEV	Amount of siRNA content (pmol)
HAp | PLR | siRNA | PLR (3 layered NPs)	314.03 ± 4.23	0.18 ± 0.02	38.80 ± 0.10	584.32 ± 3.33
HAp | PLR | siRNA | PLR | siRNA | PLR (5 layered NPs)	421.63 ± 1.12	0.23 ± 0.06	40.53 ± 0.23	976.00 ± 16.63
HAp | PLR | siRNA | PLR | siRNA | PLR | siRNA | PLR (7 layered NPs)	431.30 ± 1.25	0.37 ± 0.02	42.13 ± 2.12	1112.94 ± 14.28

From Table 4.4, it is observed that there was a slight increase in size and zeta potential with additional layers of siRNA fabricated on the LbL NPs. The size of 3 layered NPs (containing 1 layer of siRNA) was 314.03 (± 4.23) nm, 5 layered NPs (containing 2 layers of siRNA) was 421.63 (± 1.12) nm and the 7 layered NPs (containing 3 layers of siRNA) was 431.30 (± 1.25) nm. The zeta potential of 3 layered NPs was 38.80 (± 0.10) nm, 5 layered NPs was 40.53 (± 0.23) nm and the 7 layered NPs was 42.13 (± 2.12) nm. The slight increase in size and zeta potential was a result of additional layers coated on the LbL NPs.

In order to compare and verify the total siRNA amount present in the 3 layered, 5 layered and 7 layered LbL NPs as shown in Table 4.4, the total siRNA contents of the various particles were released and quantified with the microplate reader (the siRNA used in this experiment was labelled with 6FAM GFP and the samples were compared against a series of 6FAM siRNA of known concentrations, with Ex/Em of 480/520 nm). The anova statistical analysis shows that the 3, 5 and 7 layered LbL NPs has significant differences (p-value = 0.004) in their total siRNA content. The 3 layered (3L) LbL NPs had an average amount of 584.32 (± 3.33) pmol of total siRNA content, 5 layered (5L) LbL NPs had an

average amount of 976.00 (± 16.63) pmol of total siRNA content and the 7 layered (7L) LbL NPs had an average amount of 1112.94 (± 14.28) pmol of total siRNA content.

The results show that 7L LbL NPs have 14.03 % more siRNA content than the 5L LbL NPs while the 7L LbL NPs have 90.47 % more siRNA content than the 3L LbL NPs. Hence, it could be deduced that 7L LbL NPs which contains 3 layers of siRNA have the highest content of total siRNA in the LbL NPs as compared to the 5L and 3L LbL NPs having 2 layers and 1 layer of siRNA respectively. High siRNA content in the LbL NPs could possibly deliver efficient and prolonged gene silencing effect. However, before deciding on which of the multilayered LbL NPs that should be used for subsequent *in vitro* studies for an efficient and prolonged gene silencing effect, the release behavior (in PBS medium) of the particles coated with 1 layer of siRNA (3L LbL NPs), 2 layers of siRNA (5L LbL NPs) and 3 layers of siRNA (7L LbL NPs) were investigated as shown in 4.2.7.

4.2.6 siRNA release behavior of NPs fabricated with different PLR M_W

The fabrication of 3 layered LbL NPs loaded with different PLR M_w (PLR 5000 – 15 000 Da, PLR 15 000 – 70 000 Da and PLR >70 000 Da) as discussed in 4.2.4 were utilized for the study on the 6FAM-labelled siRNA release behavior over 28 days. The release study was conducted using MWCO of 100kD dialysis tubing containing 1mg HAp worth of the respective particle samples and was placed in a glass container filled with 10 mL of PBS (pH 7.40). The glass container was placed in the thermoshaker, shaking overnight at 50 rpm at 37 °C over a period of 28 days with the stipulated time intervals of day 1, day 3, day 5, day 7, day 14, day 21 and day 28. At the respective time intervals, readings were measured using the microplate reader (compared against a series of 6FAM siRNA of known concentrations, with Ex/Em of 480/520 nm) and the glass container were replenished with fresh 10 mL PBS (pH 7.40) for the subsequent timepoints.

The cumulative release profile of 3 layered LbL NPs loaded with different PLR M_w (PLR 5 – 15 kDa, PLR 15 – 70 kDa and PLR >70 kDa) are as illustrated in Figure 4.2 below:

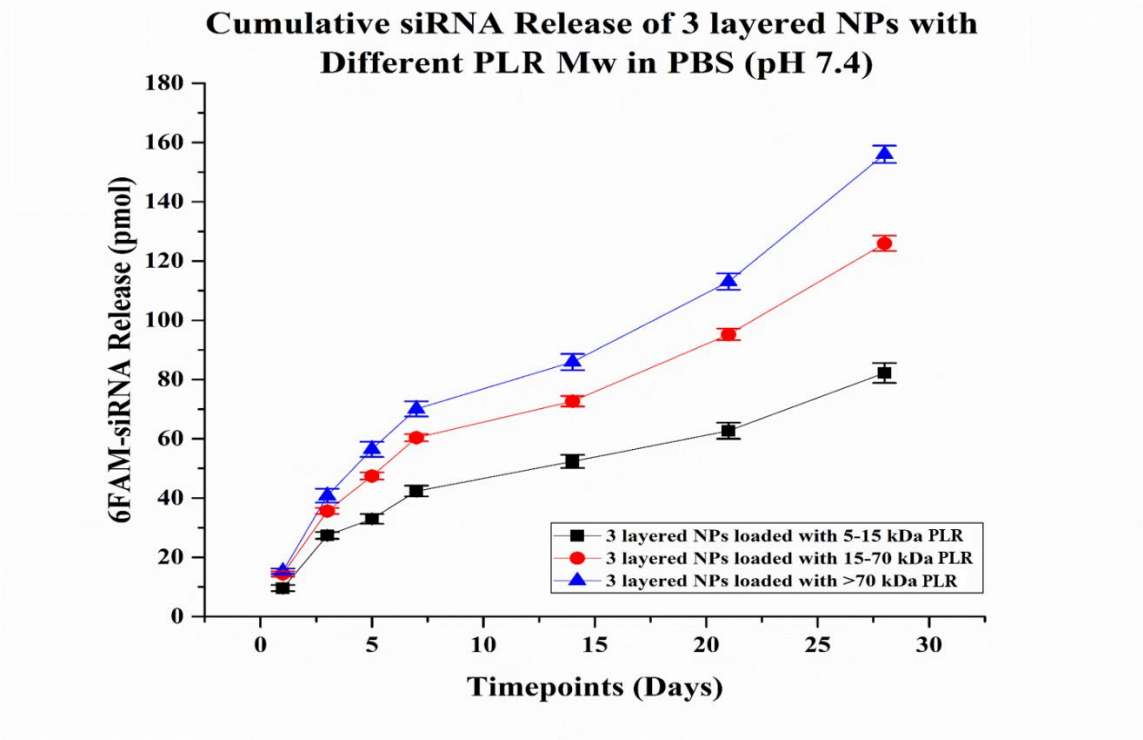

Figure 4.2: Cumulative siRNA release profile of 3 layered LbL NPs loaded with different PLR M_w (PLR 5 – 15 kDa, PLR 15 – 70 kDa and PLR >70 kDa) in PBS (pH 7.40) medium over a period of 28 days. At the respective timepoint (days 1, 3, 5, 7, 14, 21 and 28), the samples were collected and measured with the microplate reader to observe the amount of 6FAM siRNA release (compared against a series of 6FAM siRNA of known concentrations, with Ex/Em of 480/520 nm). The samples in the dialysis tubing that were submerged in the glass container was replenished with fresh 10 mL PBS (pH 7.40) for the subsequent timepoints. All samples were prepared and readings measured in triplicates.

The 6FAM siRNA release profile as observed from Figure 4.2 shows that the particles loaded with different PLR M_w (PLR 5 – 15 kDa, PLR 15 – 70 kDa and PLR >70 kDa) exhibits gradual release of siRNA over 28 days. From Figure 4.2, the initial burst release of 6FAM siRNA for all the respective 3 layered LbL NPs loaded with different PLR M_w were observed at day 1. However, the burst release of 6FAM siRNA at day 1 for the 3 layered LbL NPs loaded with PLR 5 – 15 kDa were 9.60 (± 1.04) pmol which was 1.94 % of the total amount of siRNA loaded. The burst release of 6FAM siRNA at day 1 for the 3 layered LbL NPs loaded with PLR 15 – 70 kDa were 14.40 (± 0.90) pmol which was 2.77 %

of the total amount of siRNA loaded. The burst release of 6FAM siRNA at day 1 for the 3 layered LbL NPs loaded with PLR >70 kDa were 15.30 (± 0.90) pmol which was 2.62 % of the total amount of siRNA loaded. This showed that the initial burst release of siRNA at day 1 did not cause a huge amount of siRNA release all at once and the respective NPs were still able to release siRNA gradually over 28 days.

The 3 layered LbL NPs loaded with PLR 5 – 15 kDa released an average of 82.19 (± 3.36) pmol of 6FAM siRNA while the 3 layered LbL NPs loaded with PLR 15 – 70 kDa released an average of 125.93 (± 2.57) pmol of 6FAM siRNA and the 3 layered LbL NPs loaded with PLR >70 kDa released an average of 156.01 (± 2.89) pmol of 6FAM siRNA by day 28. The anova statistical analysis was conducted and the *p*-value is 0.01 which indicates that there is significant difference in the amount of siRNA release of the 3 layered LbL NPs loaded with different PLR M_w. This showed that the 3 layered LbL NPs loaded with PLR >70 kDa has a higher amount of siRNA release over 28 days as compared to the 3 layered LbL NPs loaded with PLR 5 – 15 kDa and PLR 15 – 70 kDa respectively.

Figure 4.3 below illustrates the cumulative siRNA percent release of the 3 layered NPs loaded with different PLR M_w:

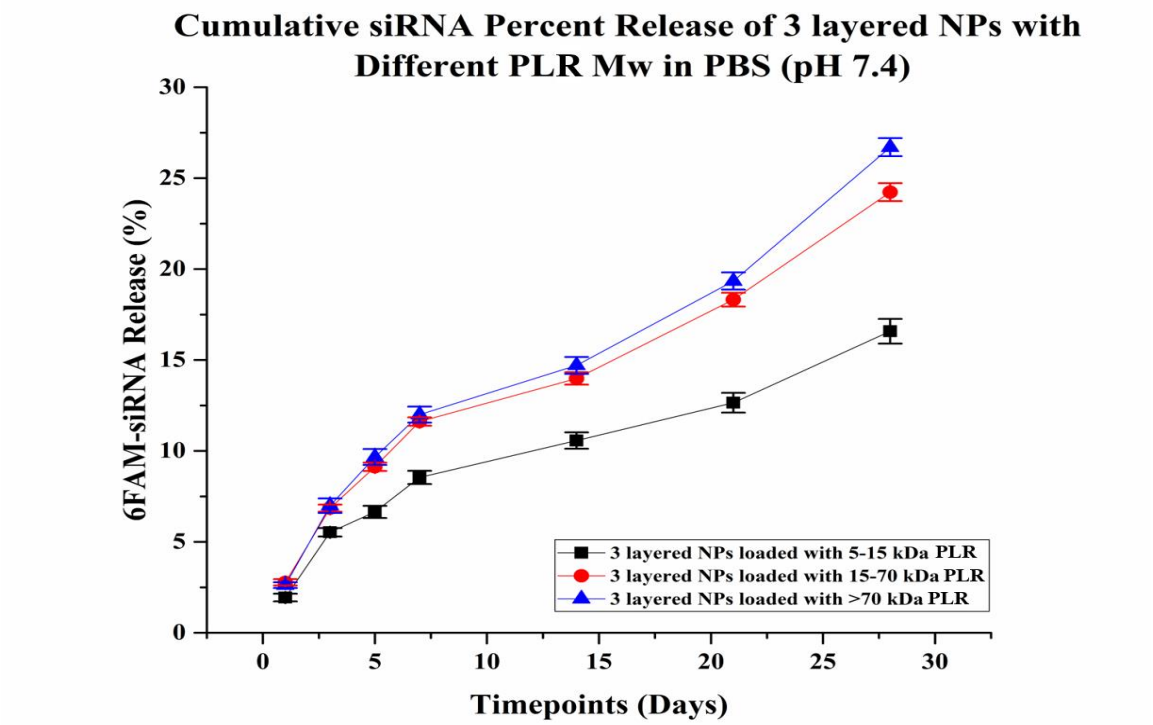

Figure 4.3: Cumulative siRNA percent release of 3 layered LbL NPs (loaded with different PLR M_w) in PBS (pH 7.40) medium over a period of 28 days. At the respective timepoint (days 1, 3, 5, 7, 14, 21 and 28), the samples were collected and measured with the microplate reader to observe the amount of 6FAM siRNA percent release (compared against a series of 6FAM siRNA of known concentrations, with Ex/Em of 480/520 nm). The samples in the dialysis tubing that were submerged in the glass container was replenished with fresh 10 mL PBS (pH 7.40) for the subsequent timepoints. All samples were prepared and readings measured in triplicates.

Figure 4.3 shows the cumulative siRNA percent release of 3 layered LbL NPs loaded with various PLR M_w in PBS (pH 7.40). The 3 layered NPs loaded with PLR 5 – 15 kDa releases siRNA at 16.58 (± 0.68) %, 3 layered NPs loaded with PLR 15 – 70 kDa releases siRNA at 24.23 (± 0.49) % and the 3 layered NPs loaded with PLR >70 kDa releases siRNA at 26.70 (± 0.50) % by day 28. This shows that the 3 layered NPs loaded with various PLR M_w could potentially be longer than 28 days. The anova statistical analysis was conducted and the *p*-value is 0.01 which indicates that there is significant difference in the percentage siRNA release of the 3 layered LbL NPs loaded with various PLR M_w.

The 3 layered LbL NPs loaded with PLR >70 kDa would be the preferred particle to be used for the subsequent studies due to the fact that it had the ability to bind to more siRNA during the layer by layer fabrication. In the process, it could load the most amount of total siRNA content in the particle, hence resulting in the release of more amount of siRNA at each time interval. Releasing more amount of siRNA at each time interval could benefit the ultimate aim of achieving a more effective gene silencing effect [7, 8].

4.2.7 siRNA release behavior of NPs fabricated with additional siRNA layers

The fabrication of 3 layered (containing 1 layer of siRNA), 5 layered (containing 2 layers of siRNA) and 7 layered (containing 3 layers of siRNA) LbL NPs loaded with PLR >70 000 Da as discussed in 4.2.5 were utilized for the study on the 6FAM-labelled siRNA release behavior over 28 days.

The cumulative release profile of 3 layered, 5 layered and 7 layered LbL NPs are as illustrated in Figure 4.4 below:

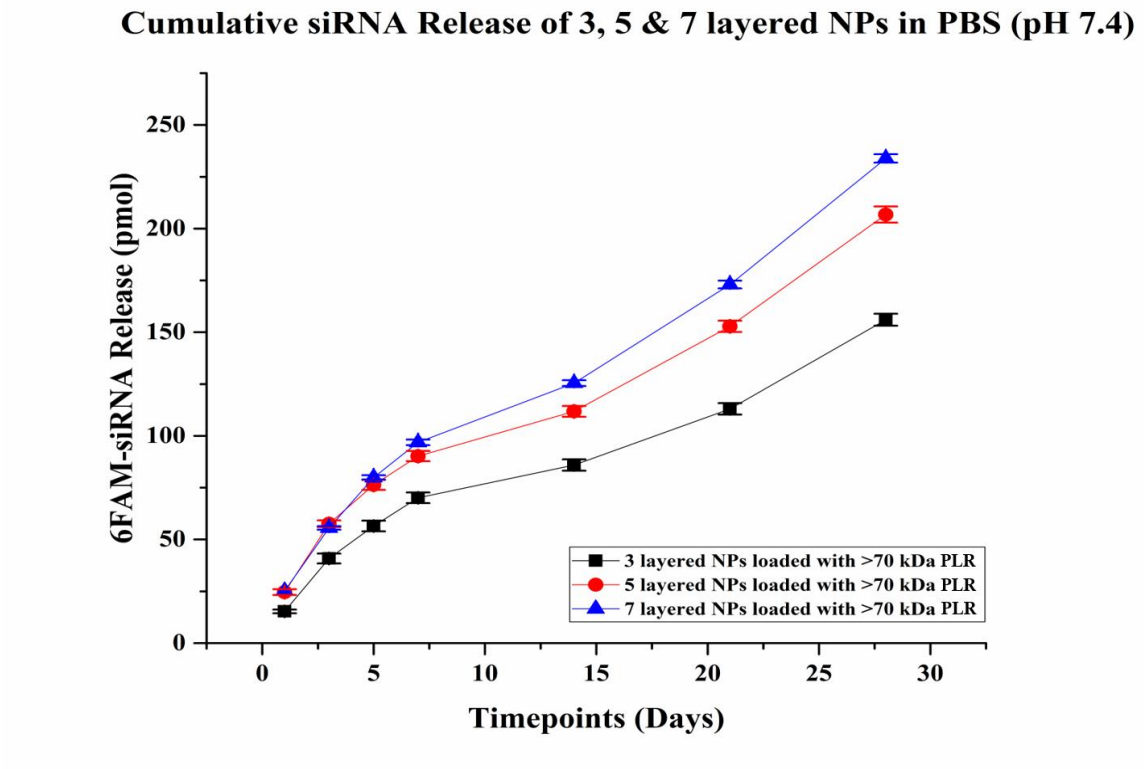

Figure 4.4: Cumulative siRNA release profile of 3 layered, 5 layered and 7 layered LbL NPs (loaded with PLR M_w >70 kDa) in PBS (pH 7.40) medium over a period of 28 days. At the respective timepoint (days 1, 3, 5, 7, 14, 21 and 28), the samples were collected and measured with the microplate reader to observe the amount of 6FAM siRNA release (compared against a series of 6FAM siRNA of known concentrations, with Ex/Em = 480/520 nm). The samples in the dialysis tubing that were submerged in the glass container was replenished with fresh 10 mL PBS (pH 7.40) for the subsequent timepoints. All samples were prepared and readings measured in triplicates.

The 6FAM siRNA release profile as observed from Figure 4.4 shows that the 3 layered, 5 layered and 7 layered LbL NPs exhibit gradual release of siRNA over 28 days. From Figure 4.4, the initial burst release of 6FAM siRNA for the 3 layered, 5 layered and 7 layered LbL NPs were observed at day 1. However, the burst release of 6FAM siRNA at day 1 for the 3 layered LbL NPs were 15.30 (± 0.90) pmol which was 2.62 % of the total amount of siRNA loaded. The burst release of 6FAM siRNA at day 1 for the 5 layered LbL NPs were 24.59 (± 1.37) pmol which was 2.52 % of the total amount of siRNA loaded. The burst release of 6FAM siRNA at day 1 for the 7 layered LbL NPs were 25.20 (± 0.00) pmol which was 2.26 % of the total amount of siRNA loaded. This showed that the initial burst release of siRNA at day 1 did not cause a huge amount of siRNA release all at once and the respective NPs were still able to release siRNA gradually over 28 days. The similar burst release of siRNA observed on day 1 could be attributed to the degradation of the outermost PLR layer, releasing the outermost siRNA layer, which could have happened at the same pace. Also, the strong binding efficiency between the negatively charged siRNA and the highly positively charged PLR layer results in the low initial burst release of the 3, 5 and 7 layered LbL NPs.

The 3 layered LbL NPs (containing 1 layer of siRNA) released an average of 156.01 (± 2.89) pmol of siRNA, the 5 layered LbL NPs (containing 2 layers of siRNA) released an average of 206.77 (± 3.91) pmol of siRNA while the 7 layered LbL NPs (containing 3 layers of siRNA) released an average of 233.85 (± 2.04) pmol of siRNA by day 28. The anova statistical analysis shows that the 3, 5 and 7 layered LbL NPs has significant

differences (*p*-value = 0.01) in their release profile. This showed that the 7 layered LbL NPs has a higher amount of siRNA release over 28 days as compared to the 3 layered LbL NPs and the 5 layered LbL NPs.

Figure 4.5 below illustrates the cumulative siRNA percent release of the 3, 5 and 7 layered NPs:

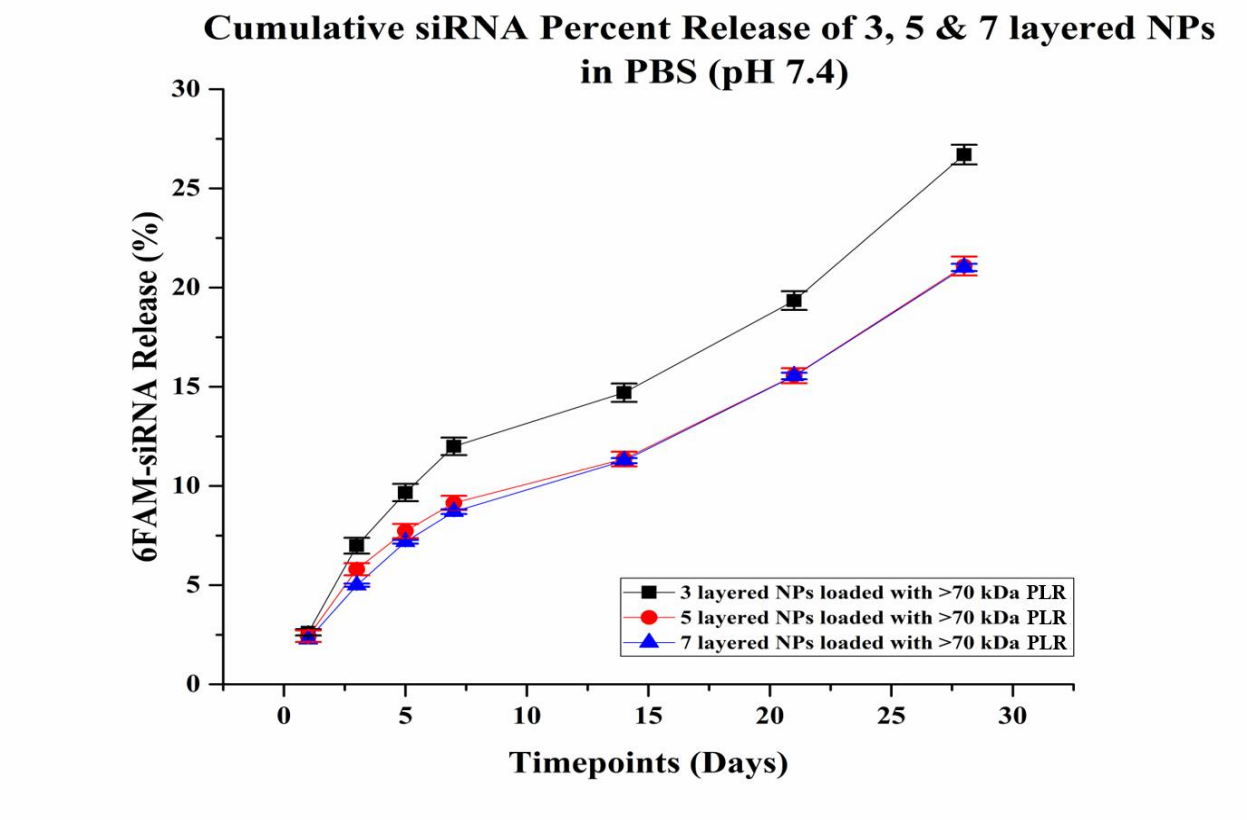

Figure 4.5: Cumulative siRNA percent release of 3, 5 and 7 layered LbL NPs (loaded with PLR M_w >70 kDa) in PBS (pH 7.40) medium over a period of 28 days. At the respective timepoint (days 1, 3, 5, 7, 14, 21 and 28), the samples were collected and measured with the microplate reader to observe the amount of 6FAM siRNA percent release (compared against a series of 6FAM siRNA of known concentrations, with Ex/Em of 480/520 nm). The samples in the dialysis tubing that were submerged in the glass container was replenished with fresh 10 mL PBS (pH 7.40) for the subsequent timepoints. All samples were prepared and readings measured in triplicates.

Figure 4.5 shows the cumulative siRNA percent release of the 3, 5 and 7 layered LbL NPs in PBS (pH 7.40). The 3 layered NPs releases siRNA at 26.70 (± 0.50) %, 5 layered NPs releases siRNA at 21.09 (± 0.47) % and the 7 layered NPs loaded with PLR >70 kDa releases siRNA at 21.01 (± 0.18) % by day 28. This shows that the cumulative siRNA percent release of 3, 5 and 7 layered NPs could potentially be longer than 28 days. The anova statistical analysis was conducted and the *p*-value is 0.89 for the percent release of 3 layered, 5 layered and 7 layered NPs which means that there were no significant difference comparing the 3, 5 and 7 layered NPs. There was no significant difference as well for the percent release comparing the 3 layered and 5 layered NPs with *p*-value of 0.82 and the percent release of 5 layered and 7 layered NPs with *p*-value of 0.96. This could be due to the total percentage of siRNA release per layer, as the percentage contribution by each layer would decrease inverse proportionally with the increase in the number of layers. Also, as observed from the graph, the 3 layered NPs releases a higher percentage of siRNA as compared to the 5 layered and 7 layered NPs over 28 days. Hence, this could further validate the percentage contribution by each layer decreasing inverse proportionally with the increase in number of siRNA layers loaded in the NPs. Since the 3 layered NPs consist of only 1 layer of siRNA, the percentage of siRNA release would be exhausted first before the 5 layered NPs (containing 2 layers of siRNA) and the 7 layered NPs (containing 3 layers of siRNA).

All in all, the 7 layered LbL NPs would be the preferred particle to be used for the subsequent *in vitro* studies because it could load the most amount of total siRNA content in the particle. This could be due to the 7 layered NPs having 3 layers of siRNA in the LbL NPs which further increases the total amount of siRNA content in the particle, hence resulting in the release of more amount of siRNA at each time interval. Releasing more amount of siRNA at each time interval could benefit the ultimate aim of achieving a more effective gene silencing effect [7, 8]. This further affirms that by fabricating additional layers of siRNA on the LbL NPs system, it increases the total siRNA content in the particles, releases a higher amount of siRNA at each time intervals which could potentially achieve a more extended and effective gene knockdown *in-vitro*.

4.2.8 Transmission electron microscope (TEM) imaging

To observe the shape morphology of the fabricated LbL NPs, TEM imaging was employed. The images of HAp (core material) NPs, 3 layered, 5 layered and 7 layered LbL NPs were as shown in Figure 4.6 below:

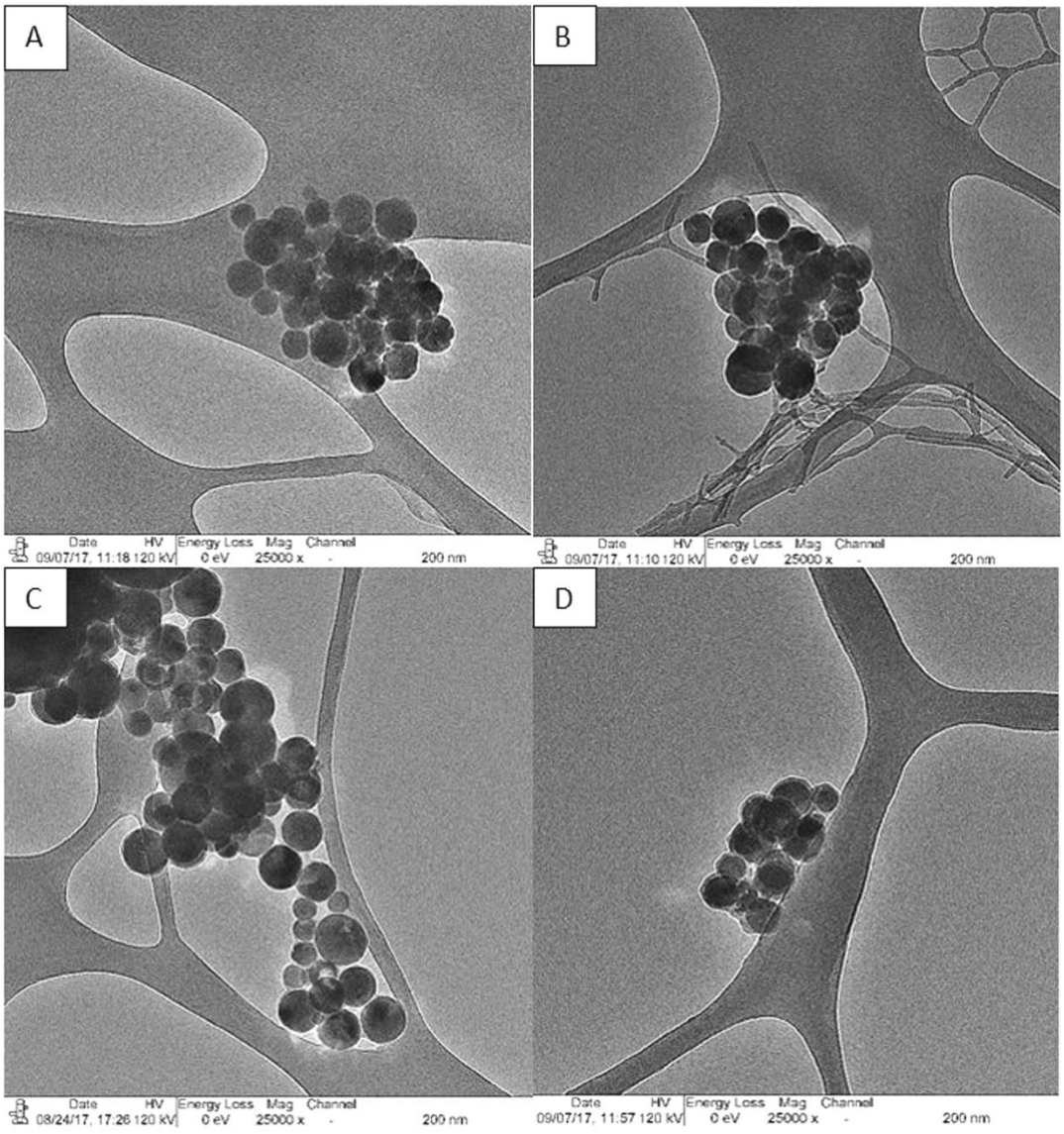

Figure 4.6: TEM images of (A) HAp only NPs, (B) 3 layered LbL NPs, (C) 5 layered LbL NPs and (D) 7 layered LbL NPs.

The TEM images as observed from Figure 4.6 show that the NPs are in spherical shape morphology which would lead to a higher cellular entry as compared with NPs of other shape morphology due to the membrane wrapping that occurs during the nanoparticles entry into the cells as mentioned in the literatures [9, 10].

4.3 *In vitro* toxicity study

In order to assess the cell viability on Human Retroperitoneal Fibroblast (HuRPF) cells treated with 7 layered LbL NPs, MTT (methyl-thiazolyldiphenyl-tetrazolium bromide) assay was employed. This is to ensure that the 7 layered LbL NPs will not exhibit toxic effects on the HuRPF cells before the start of any cell related experiments for the subsequent *in vitro* studies. Based on a previous study, 108 μg of the particles was selected as the dosage for their *in vivo* experiments (treatment for every 30 000 cells after dispersing NPs in 5 μL PBS), which takes into consideration the maximum amount that could be injected into the subconjunctival of mouse models [6, 11]. However, in this study, *in vitro* experiments will only be conducted using HuRPF cells (not taking into consideration the maximum volume of the NPs treated to the cells). Hence, based on the previous study on utilizing 30 000 cells which were dispersed in 5 μL PBS, the subsequent *in vitro* experiments in the current study utilizing 50 000 HuRPF cells would have to be treated with 8 μL of the 7L LbL NPs. With that, from freeze drying of the 7 layered LbL NPs utilizing 2 mg worth of HAp (which is equivalent to 50 μL of 7L LbL NPs) was then weighed. The weight of 7L LbL NPs was found to be at $8.07*10^{-4}$ g. Since 8 μL of the 7L LbL NPs will be used, therefore 129 μg of the particles (dispersed in 8 μL cell culture medium) will be the selected dosage for subsequent *in vitro* studies.

For the MTT cell viability study, the 7 layered LbL NPs were added to 500 HuRPF cells at varying doses of 258 μg, 129 μg and 64.5 μg. The cells were then incubated with the NPs over a span of 2 days (24- and 48-hour time intervals). At the respective time intervals, the cells were assayed for their cell viability with MTT by measuring the fluorescence intensities of the cells using the microplate reader with an absorbance wavelength of 595

nm. The viability of cells was then calculated in comparison with the control (cells without treatment of NPs). The data is shown in Figure 4.7 below:

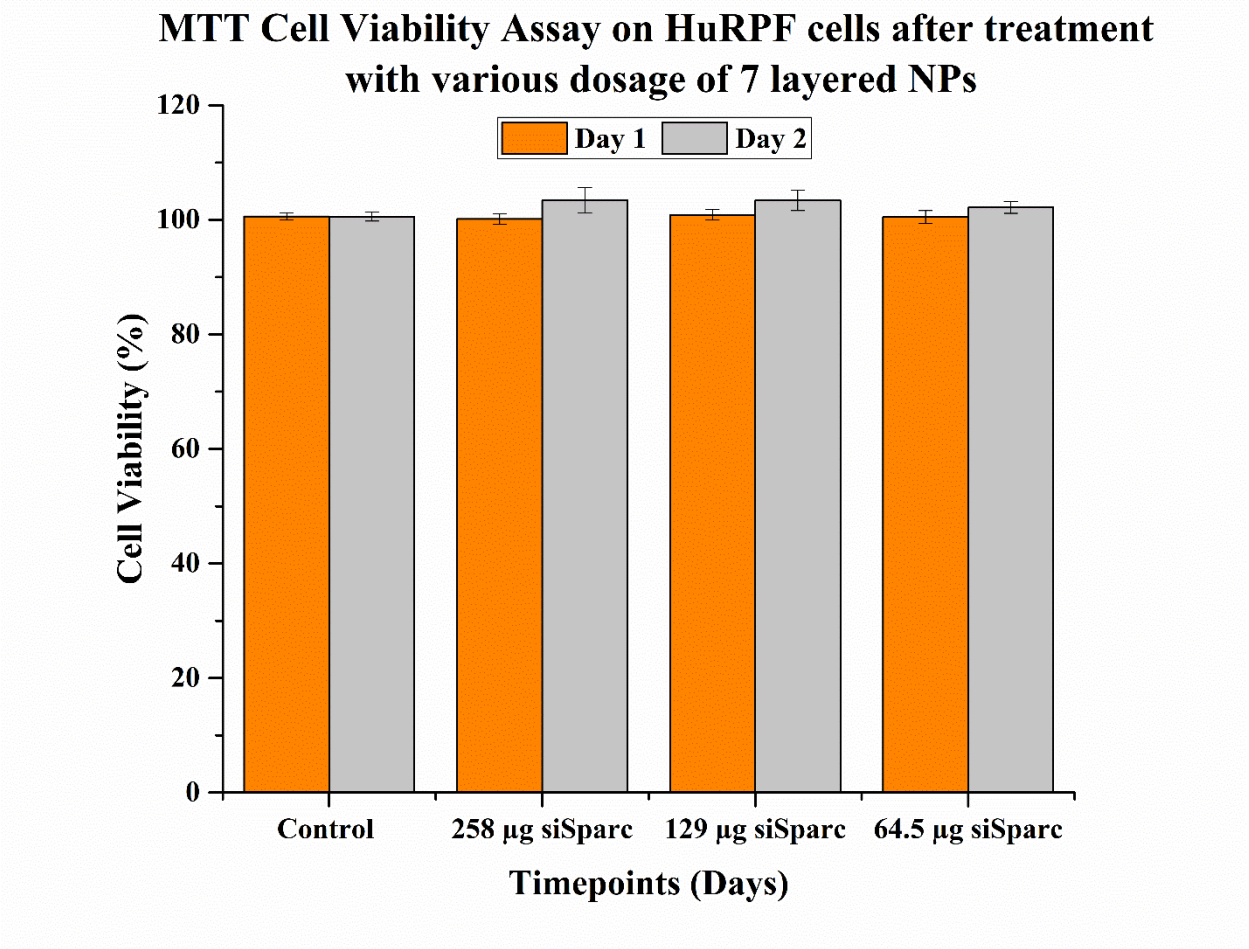

Figure 4.7: MTT assay tracking the cell viability of 500 HuRPF cells after treatment with 7 layered LbL NPs at dosages of 258 µg, 129 µg and 64.5 µg over a span of 2 days (siSPARC = NPs loaded with SPARC siRNA). Measurements were taken using the microplate reader with an absorbance wavelength at 595 nm. All samples were prepared and readings measured in triplicates.

From Figure 4.7, it was observed that the 7 layered LbL NPs incubated with the various dosages did not exhibit any toxic effects on the HuRPF cells over the span of 2 days (24- and 48-hour time intervals). Therefore, 129 µg of the particles (dispersed in 8 µL cell culture medium) will be safe to use as the selected dosage for subsequent *in vitro* studies.

4.4 *In vitro* cellular entry of LbL NPs

After selecting the dosage of 7L LbL NPs treatment for HuRPF cells and made sure that it will not elicit toxic effects to the cells, further cell related experiments could be initiated. In order to check whether if the particles are able to enter into the cells, confocal laser scanning microscopy (CLSM) was employed as the *in vitro* qualitative study of LbL NPs cellular internalization. 12.9 μg (based on the selected dosage of 129 μg 7L LbL NPs treatment to 50 000 HuRPF cells) of the 7 layered FITC-labelled HAp LbL NPs were added to 5000 HuRPF cells in the 4-wells covered glass chambers and incubated overnight at 37 °C with 5 % CO_2. The samples were then imaged after 24 hours of incubation to observe the internalization of NPs in HuRPF cells and the samples were compared against the control cells (without NPs treatment).

Following this, Guava flow cytometry will be conducted for the quantification of 7L 6FAM siRNA loaded LbL NPs internalization into the HuRPF cells over various time intervals of day 1, day 3, day 5, day 7, day 14 and day 21. 129 μg of the 7L 6FAM-labelled siRNA LbL NPs was added to 50 000 HuRPF cells and at the respective time interval, the cells were trypsinized and incubated with 0.40 % trypan blue for 7 minutes at room temperature. Next, the cells will be spun down at 650 RCF for 5 minutes at 10 °C. The supernatant was then removed and the cell pellet was resuspended in PBS and quantified using the Guava flow cytometry. Trypan blue was used to quench the fluorescence present in dead cells and the 6FAM fluorescence that are bound onto the surface of HuRPF cells. Since trypan blue is unable to penetrate into live cells, hence the flow cytometry system will only pick up and measure the true 6FAM fluorescence signal within the cells (which in turn corresponds to the quantity of particles in the HuRPF cells) at the various time intervals. The samples were compared against the control cells (without any treatment of particles).

With the qualitative and quantitative study, it provides an insight of ensuring that the particles have indeed entered into the cells and to provide the percentage of cells with the 7L LbL 6FAM siRNA loaded NPs over the various time intervals. Following this, further

in vitro studies could be done to quantify the amount of free siRNA release within the cells and also the gene knockdown efficiency over 21 days.

4.4.1 *In vitro* qualitative cellular entry of LbL NPs

The CLSM images for *in vitro* qualitative cellular internalization of the 7 layered LbL NPs with FITC-labelled HAp internalization into HuRPF cells and the control cells (without NPs treatment) were as illustrated in Figure 4.8 below:

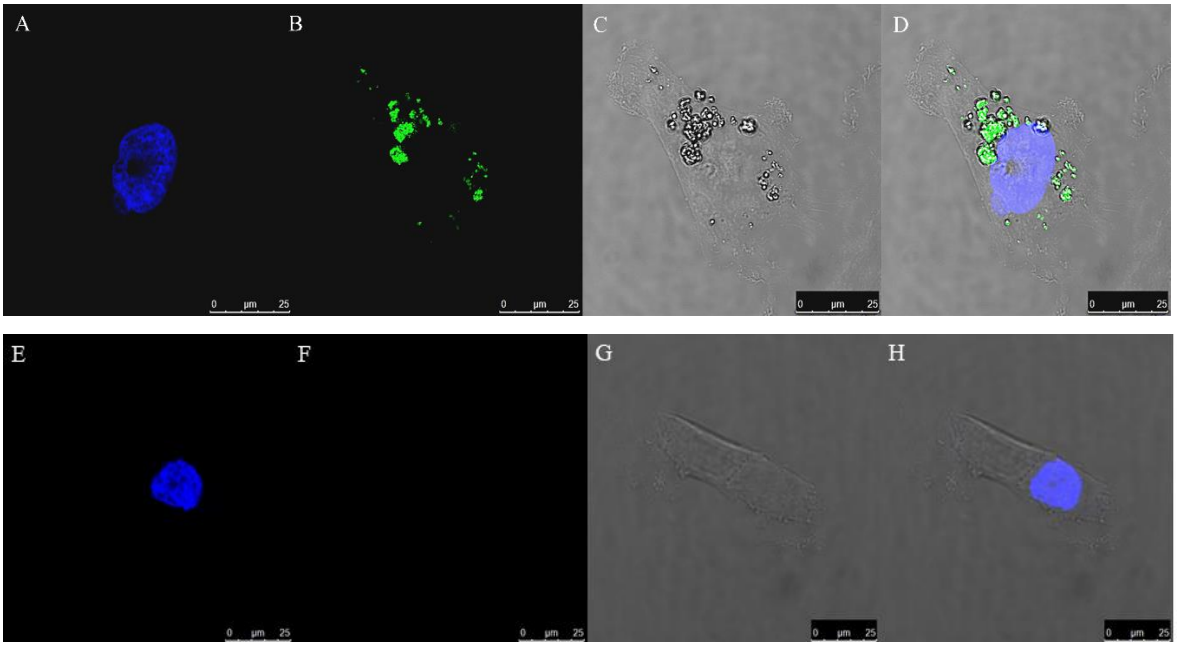

Figure 4.8: Confocal microscopic images of the cellular entry of 7 layered LbL NPs with FITC-labelled HAp and the control cells (without NPs treatment). (A) The cell nuclei were visualized by the staining of vectashield with DAPI. (B) Green fluorescence from the 7 layered LbL NPs with FITC-labelled HAp. (C) Brightfield image of the HuRPF cells. (D) Internalization of 7 layered LbL NPs with FITC-labelled HAp in the HuRPF cells as shown in the overlay image. (E-H) Control cells (without NPs treatment). The respective images of the blue channel, green channel, brightfield image and overlay image are presented. All the images were taken at 40X magnification and 4.3X zoom. The sample cells were compared against control cells (without NPs treatment).

In order to verify the cellular entry of the particles, 7 layered LbL NPs with FITC-labelled HAp were added to HuRPF cells and incubated overnight. The cells were then imaged on the next day by CLSM and the internalization of particles were observed showing green FITC signals.

4.4.2 *In vitro* quantitative cellular entry of LbL NPs

The *in vitro* quantitative cellular entry of 7 layered 6FAM siRNA loaded LbL NPs was done to investigate the percentage of cells containing the 7 layered 6FAM siRNA loaded LbL NPs over various time intervals of day 1, day 3, day 5, day 7, day 14 and day 21. Figure 4.9 below shows the flow cytometry analysis of the percentage of cells containing the 7 layered 6FAM siRNA loaded LbL NPs over 21 days:

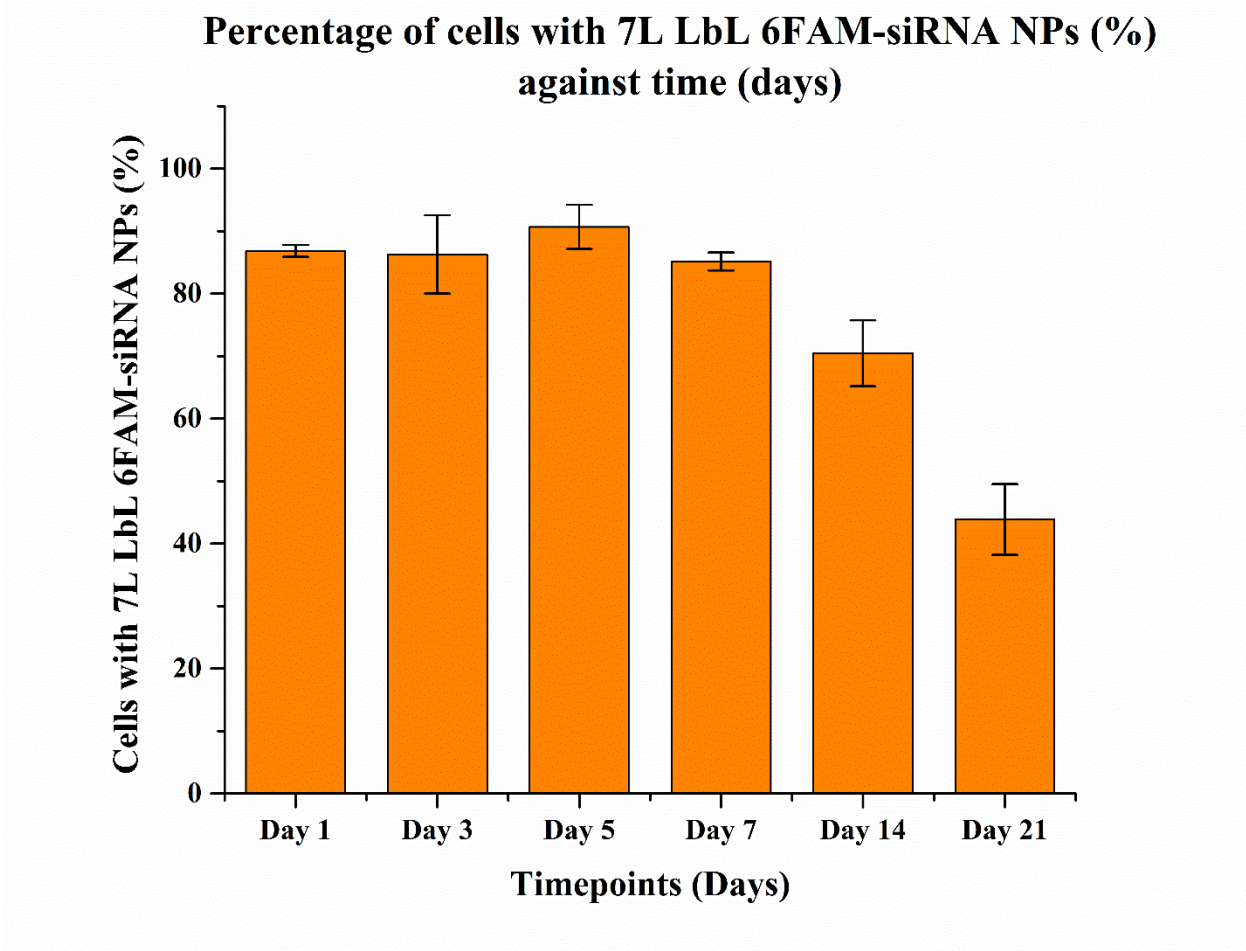

Figure 4.9: Flow cytometry analysis of HuRPF cells containing the 7 layered 6FAM siRNA loaded LbL NPs at the respective time interval of day 1, day 3, day 5, day 7, day 14 and day 21. There were 80 % to 90 % of cells containing the 6FAM siRNA loaded LbL NPs for 7 days before a sudden drop was experienced in the cells containing the 6FAM siRNA loaded LbL NPs from day 7 to day 21. All samples were prepared and readings measured in triplicates.

Prior to the flow cytometry test, trypan blue was added to the HuRPF cells to quench the fluorescence present in dead cells and the particles bound onto the cell surface. Hence, the flow cytometer would only measure the fluorescence signal within the cells. The presence of LbL NPs within the cells indicate the successful cellular entry of LbL NPs.

From Figure 4.9, it shows that the percentage of cells containing LbL NPs were of similar amounts (80 % to 90 %) from day 1 to day 7. From the data, it was evident that the particles fabricated could easily penetrate the fibroblast cells as seen in the extremely high percentage of cells with particles just one day post particle dosing. That could be attributed to the highly positive PLR external coatings of the particles, enabling efficient attraction towards the negatively charged cellular membranes and subsequent entry into the cells. The high percentage of cells containing the particles within the first 7 days could be due to dynamic cellular internalization of the 7L 6FAM siRNA loaded LbL NPs which could already be significantly observed within the first hour post incubation [12, 13].

From the data, it was then observed that there was a sudden drop (from day 7 to day 21) in the percentage of cells with the LbL NPs at about 70 % on day 14 and a further drop at about 40 % on day 21. There could be two major reasons attributing to the dip in percentage cells with particles. Firstly, the drop could be due to loss in the HAp NPs. Upon successful cellular entry into the fibroblast cells, possibly via endocytosis, most of the particles could have ended up within early endosomes with slightly acidic pH environment internally. These endosomes will eventually mature into late endosomes with increasing pH internally and fuse with enzymes enriched lysosomes. Hence, to escape digestion, most of the highly positive charged LbL NPs could accumulate within the endosomes and collectively weaken

the endosomal membranes to form pores big enough for their escape into the cytoplasm. Understandably, some of the particles could have been unable to escape and eventually got digested by the lysosomes, contributing to the loss in particles within the cell population. Another possible reason for loss in the HAp NPs could be that some of the siRNA released has been utilized for gene silencing. The particles that manage to escape the endosomes will start releasing siRNA once in the cytoplasm. These siRNA available within the cytoplasm could complementarily bind to mRNA to inhibit protein synthesis. More siRNA could have also been utilized for gene silencing when cells regenerate mRNA in response to the dip in mRNA levels within them.

Secondly, another reason for the dip in percentage of cells with particles could be due to cell division. A review by Treuel *et al.* states that the NPs dilution effect that occurs during cell division will distribute the particles from the parent cells to the daughter cells (the presence of NPs within cells will be split between the daughter cells). There are 4 phases in the cell cycle during which the cell grows or undergo cell division. The G1/post-mitotic phase (initiation of cell growth), the S/synthesis phase (replication of DNA), the G2 phase (period of cell growth and synthesis of proteins in preparation of mitosis), and the M/mitotic phase (period of cell division). The authors has observed that once after the cell division phase (with NPs exposure), the cells showed a reduced NPs concentration as compared to other phases, and when the cells that have divided began populating the S phase, the NPs concentration within the cells were found to be reduced again [14]. Therefore, in relation to the current study, it further explains the sudden drop in the percentage of HuRPF cells containing 6FAM fluorescence from day 7 to day 21. Further *in vitro* experiments such as the amount of free siRNA presence within the cells and the percentage of SPARC knockdown over a 21 days period were investigated.

4.5 Amount of free siRNA within HuRPF cells and immunoblotting assay

The quantitative cell penetration study showed the percentage of cells with particles over 21 days. However, it does not provide information on the amount of NPs/siRNA within the cells. It will be interesting to find out the amount of free siRNA that are present within the

cells over 21 days and whether the siRNA is being used up for gene silencing of *SPARC*. Also, the amount of siRNA that is remaining in the particles can also be evaluated. By investigating the amount of free siRNA within the cells for the respective time interval, coupled with the immunoblotting assay to find out whether siRNA was being used up for gene silencing, it could shed light on when and how the multilayered nanoparticles internalize into cells to release free siRNA within cells. The behavior of free siRNA release inside the cells as compared with the behavior of siRNA release in PBS medium (pH 7.40) could also be investigated.

In this study, the cell lysis buffer would be utilized to break down the cell membrane, releasing the free siRNA within cells which will be measured over 21 days. Furthermore, in a study conducted by Lakatos *et al.* have also utilized lysis buffer in their experiments to incubate labelled RNAs in the lysis buffer for various tests (i.e. electrophoretic mobility shift assays) [15]. Before proceeding with the experiment to examine the amount of free siRNA within cells, preliminary tests have to be done to ensure that the lysis buffer will not degrade the siRNA and also the LbL NPs system. Figure 5.0 below shows the standard curve for both the 6FAM siRNA dispersed in PBS medium and also in the lysis buffer. The gradients (y = mx) obtained from both the standard curve remained similar which suggest that the lysis buffer will not degrade the 6FAM siRNA.

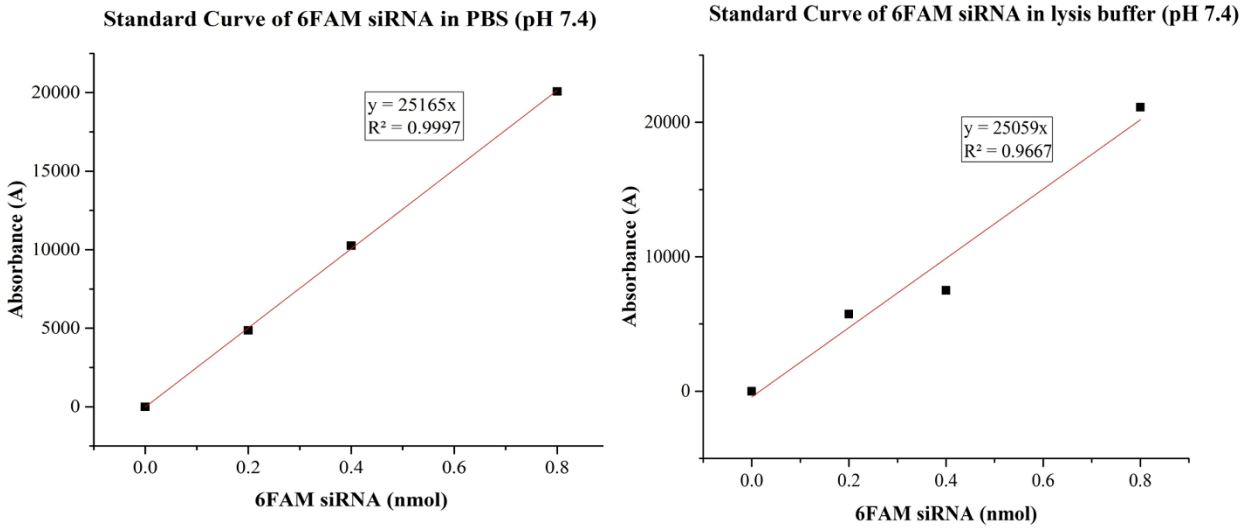

Figure 5.0: Effect of 6FAM siRNA in PBS and in the lysis buffer. The gradients (y = mx) remained similar for both the standard curve which suggest that the lysis buffer will not degrade the 6FAM siRNA.

Next, the 3 layered LbL NPs loaded with 1 layer of 6FAM siRNA was fabricated and immediately digested in lysis buffer, and incubated in two different batches. One of the batches was incubated in lysis buffer for 5 minutes while the other batch was incubated in lysis buffer for 10 minutes, at room temperature. Both of the batches were then spun down at 15 000 rpm for 5 minutes and the supernatant collected for measurements using the microplate reader (Ex/Em = 480/520 nm). All samples were measured and compared against the control (lysis buffer only). Anova statistical analysis is employed to find out if there were any significant differences between the control (containing lysis buffer only) and the 3L LbL NPs loaded with 6FAM siRNA incubated in lysis buffer for 5 minutes and for 10 minutes. The results showed that the incubation of particles in lysis buffer for 5 minutes did not show any significant differences (p value = 0.59) between the control (lysis buffer only) and sample (incubation of NPs in lysis buffer for 5 minutes). The incubation of particles in lysis buffer for 5 minutes achieved an average measured fluorescence intensity of 44.33 (± 0.58) a.u. for the control and 44.67 (± 2.52) a.u. for the sample respectively. The incubation of particles in lysis buffer for 10 minutes also did not show any significant differences (p value = 0.09) between the control (lysis buffer only) and sample (incubation of NPs in lysis buffer for 10 minutes), with the average measured fluorescence intensity of 44.33 (± 0.58) a.u. for the control and the average measured fluorescence intensity of 39.33 (± 1.53) a.u. for the sample.

Following this, it affirms that the lysis buffer will not degrade the siRNA and the LbL NPs system. Hence, the experiment was initiated to evaluate the amount of free siRNA within cells by using lysis buffer to break up the cell membrane releasing the free siRNA within cells at the stipulated time interval of day 1, day 3, day 5, day 7, day 14 and day 21. 8 μL of the 7 layered 6FAM siRNA loaded LbL NPs were added into 50 000 HuRPF cells which was cultured in 6-wells plate and incubated at 37 °C with 5 % CO_2. The HuRPF cells were then processed and the cell membrane were lysed to retrieve the free siRNA at the

respective time intervals (compared against the control cells, without any treatment of particles) which were measured by the microplate reader (Ex/Em = 480/520). All samples were compared against a series of 6FAM siRNA standard curve (Tecan measurements to be taken of 6FAM siRNA of known concentrations). After the measurement of free siRNA within the cells, the cell pellets containing the remaining NPs will be dispersed in 0.25 % trypsin-EDTA, shaking overnight using the thermoshaker at 37 °C. This would disassemble the LbL NPs system for measuring the remaining siRNA on the particles (Ex/Em = 480/520) at the respective time interval. Figure 5.1 below illustrates the data on the amount of free siRNA within cells, the amount of siRNA remained in the NPs and also the calculated amount of siRNA that were being consumed/degraded over 21 days. The total amount of loaded siRNA was 618.13 (± 3.97) pmol.

▪Total amount of loaded siRNA: 618.13 ± 3.97 pmol

Timepoint (Days)	1	3	5	7	14	21
Amount of siRNA remained in NP (%)	37.63 ± 3.89	18.91 ± 3.19	8.01 ± 0.53	10.97 ± 2.33	1.52 ± 0.13	0.85 ± 0.68
Amount of free siRNA within cells (%)	46.06 ± 4.98	59.29 ± 1.81	47.93 ± 1.93	27.82 ± 2.81	9.43 ± 0.65	2.79 ± 0.17
Amount of siRNA consumed/degraded (%)	16.31 ± 6.30	21.80 ± 3.65	44.07 ± 2.00	61.21 ± 3.66	89.05 ± 0.87	96.36 ± 0.94

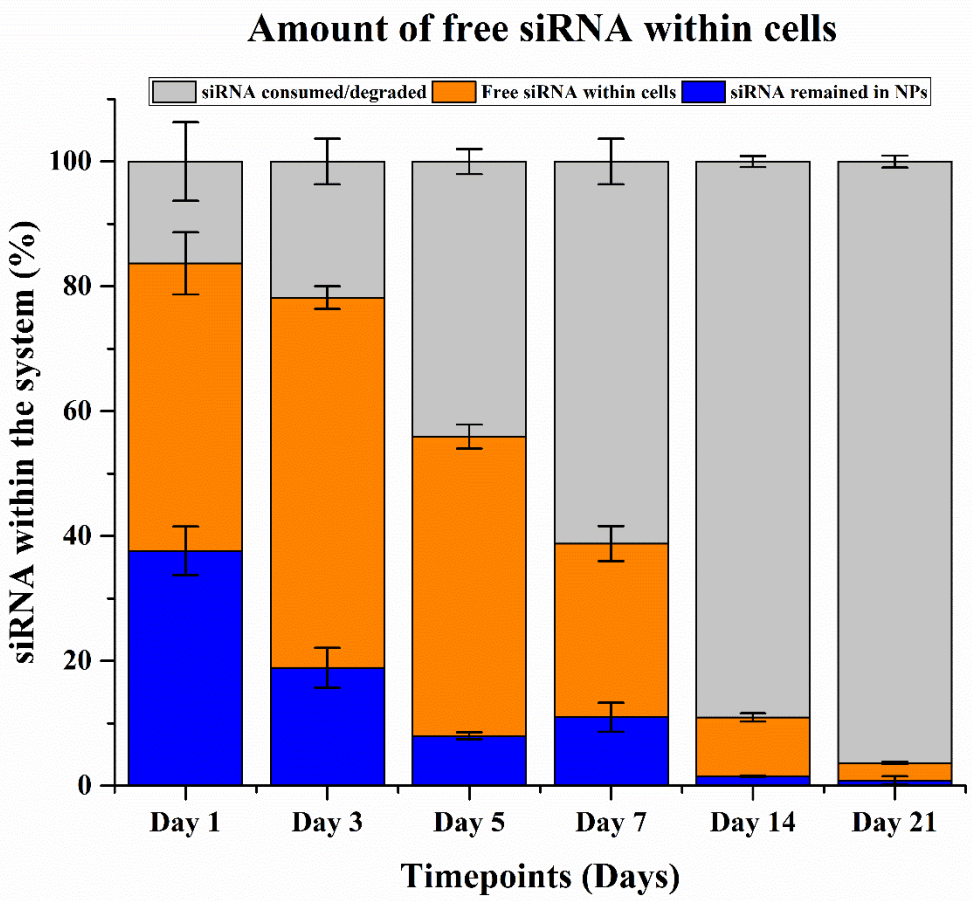

Figure 5.1: Graphical representation of the amount of free siRNA within cells (represented by the orange bar) after the treatment of 7 layered 6FAM siRNA loaded LbL NPs to HuRPF cells at the respective time interval of day 1, day 3, day 5, day 7, day 14 and day 21. The siRNA remained in NPs (represented by the blue bar) and the siRNA consumed/degraded (represented by the grey bar) at each time interval could also be evaluated. The total amount of siRNA loaded in 50 000 HuRPF cells was 618.13 (± 3.97) pmol. The samples were collected and measured with the microplate reader (compared against a series of 6FAM siRNA of known concentrations, with Ex/Em of 480/520 nm). All samples were prepared and readings measured in triplicates.

Thereafter, the immunoblotting assay was employed to assess the percentage of *SPARC* knockdown over the stipulated time interval of day 1, day 3, day 5, day 7, day 14 and day 21. This would correlate to the amount of free siRNA within cytoplasm (site of action for

gene silencing) over 21 days. 8 μL of the respective 7 layered SPARC-siRNA loaded LbL NPs (siSparc-LbL) and the 7 layered SCRAM-siRNA loaded LbL NPs as the negative control (siScram-LbL) were added into 50 000 HuRPF cells which was cultured in 6-wells plate and incubated at 37 °C with 5 % CO_2. Figure 5.2 (A) below illustrates the protein separation and antibody treatment over 21 days using the Biorad Chemidoc system. It showed the intensity of the respective SPARC protein bands (43 kDa) with the siScram-LbL negative control compared against the siSparc-LbL samples which were normalized against the GAPDH housekeeping protein (37 kDa) to correct for variation in loading. Figure 5.2 (B) illustrates the percentage knockdown of *SPARC* over 21 days.

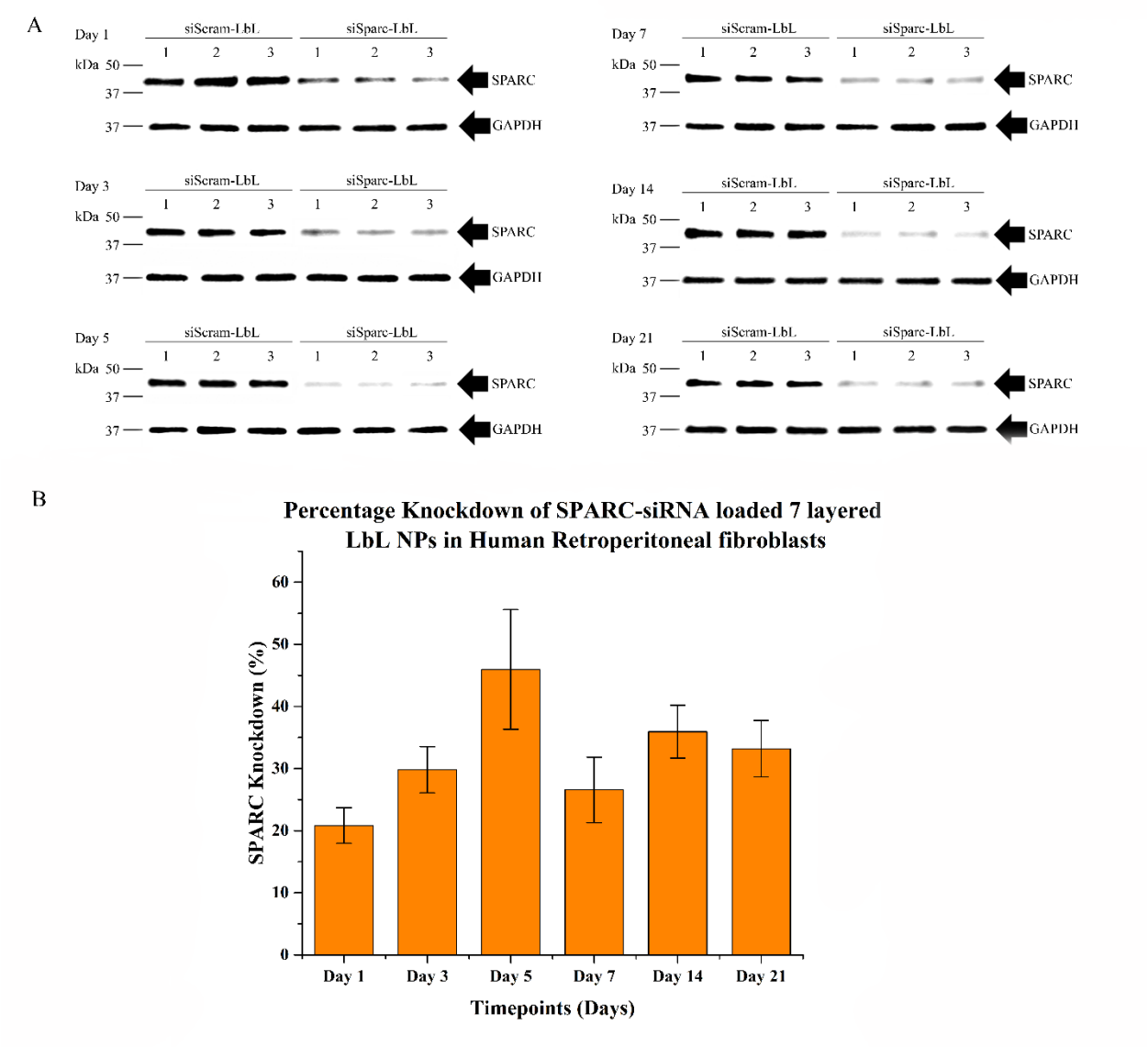

Figure 5.2: Immunoblotting analysis of 7 layered siRNA loaded LbL NPs in HuRPF cells at the respective time interval of day 1, day 3, day 5, day 7, day 14 and day 21. (A) Protein separation and antibody treatment over 21 days using Biorad Chemidoc system. siScram-LbL was added into 50 000 HuRPF cells as a negative control in comparison with the siSparc-LbL sample that was added into 50 000 HuRPF cells. (B) Percentage knockdown of *SPARC* over 21 days. All samples were prepared and readings measured in triplicates.

Figure 5.1 shows the amount of free siRNA that was present within the cells over 21 days. The amount of free siRNA present within the cells on day 1 was 46.06 (± 4.98) %. As

mentioned previously, after the particles has entered into the cells (endocytosis), they will most probably end up in endosomes which will eventually fuse with lysosomes to digest any foreign materials. Most of the particles could escape from the endosomes via pore formation (highly positively charged particles) [6]. These particles would finally end up in the cytoplasm to start release free siRNA. The amount of free siRNA within the cytoplasm on day 1 was only 46.06 (± 4.98) % probably because some of the particles could still be trying to escape from the endosomes while some were still dynamically entering the cells. The remaining siRNA (37.63 (± 3.89) %) could be accounted for in the LbL NPs (unreleased). The unaccounted siRNA (16.31 (± 6.30) %) could be due to the digestion by lysosomes or could have been utilized for gene silencing. As seen from Figure 5.2 (B), the knockdown of *SPARC* was already 20.82 (± 2.87) % at day 1. This amount of gene silencing is considered impressive considering that it was only one day post particle dosing where a lot of particles are still trying to dynamically enter into the cells and some other particles trying to escape from endosomes.

Following this, the amount of free siRNA on day 3 has increased to 59.29 (± 1.81) % probably because most particles should have escaped from the endosome into the cytoplasm, actively releasing free siRNA. The release of free siRNA on day 3 was the highest and the remaining siRNA (unreleased) has reduced to 18.91 (± 3.19) %. With a higher level of free siRNA in the cytoplasm, it could logically result in more gene silencing effect. Indeed, according to the immunoblotting assay, there was an increase in the knockdown activity. The knockdown of *SPARC* increased to 29.80 (± 3.72) % on day 3. The unaccounted siRNA (digestion by lysosome or consumed for gene silencing) increased slightly as compared to day 1 at 21.80 (± 3.65) %. As most particles that could escape from the endosomes into the cytoplasm should have already done so by day 3, the increase in percent of unaccounted siRNA compared to day 1 should largely be due to siRNA consumed for gene silencing. This correlates to the slight increase in the knockdown of *SPARC*.

The amount of free siRNA on day 5 has dropped to 47.93 (± 1.93) %. This slight drop in the free siRNA level could be due to particles (released into the cytoplasm) releasing

siRNA slower than siRNA that was utilized for the knockdown effect. The remaining siRNA (unreleased) in the LbL NPs has further reduced to 8.01 (± 0.53) % on day 5. The level of free siRNA available in the cytoplasm on day 5 was still relatively high to elicit an extensive gene silencing of *SPARC.* Indeed, according to the immunoblotting assay, the percentage of *SPARC* knockdown has increased extensively to 45.97 (± 9.64) % on day 5. In addition, the unaccounted siRNA (digestion by lysosome or consumed for gene silencing) increased further as compared to day 3 at 44.07 (± 2.00) %. The large increase should largely be attributed to more siRNA consumed for gene silencing activity. This correlates to the extensive knockdown of *SPARC* which was the highest in fact throughout the 21 days gene silencing study.

Figure 5.1 shows that there was a drastic drop in the amount of free siRNA on day 7 at 27.82 (± 2.81) %. This could be due to cell division and mRNA (messenger RNA, RNA molecules that direct protein synthesis) regeneration. As it was already day 7 into the study, cell division should have at least occurred once for every cell. During cell division, parent cells which contain particle and free siRNA could inherit them to their daughter cells. Hence, the same amount of particles/siRNA was then split into many cells (NPs dilution effect). That could result in some cells having undetectably small amounts of siRNA out of the detectable range of the microplate reader used. The mRNA regeneration in the cells occur periodically to replenish mRNA levels within cells for protein synthesis. Since it has been already 7 days, it was likely that mRNA regeneration has occurred at least once. The spike in mRNA could reduce the free siRNA levels in the cells largely. Another reason for the dip in free siRNA levels in the cells at day 7 could be due to disassembly behavior of the particles within the cells.

After the cellular entry and the endosomal escape of LbL NPs, the outermost PLR layer would be degraded gradually, exposing the outermost siRNA layer to the cytoplasm [6]. The siRNA layer would then continuously release siRNA into the cytoplasm. It was estimated that by day 7, most of the siRNA from the outermost siRNA layer could be close to exhaustion, probably contributing to the drastic decrease in free siRNA level by day 7.

The adjacent PLR layer must first be degraded before the inner second siRNA layer could be expose to further release siRNA into the cytoplasm.

Nonetheless, the level of free siRNA in the cytoplasm on day 7 were still high enough to elicit significant gene silencing of *SPARC* as proven by the immunoblotting assay from Figure 5.2 (B), showing the percentage of *SPARC* knockdown of 25.76 (± 7.21) % on day 7. The unaccounted siRNA (digestion by lysosome or consumed for gene silencing) further increased as compared to day 5 at 61.21 (± 3.66) %. This correlates to the existing gene silencing of *SPARC*.

There was a further decrease in the amount of free siRNA on day 14 at 9.43 (± 0.65) % and on day 21 at 2.79 (± 0.17) %. It was probably because within this period, a few rounds of cell division and mRNA regeneration could have happened, leading to the drop in the amount of siRNA at day 14 and day 21 as explained above. However, it is important to note that remarkably, there was still free siRNA present within the cytoplasm even at day 14 and day 21 into the study. Hence, gene silencing of *SPARC* could be still sustained. This is evident from the immunoblotting assay from Figure 5.2 (B) which shows percentage of *SPARC* knockdown at 35.95 (± 4.26) % on day 14 and 33.17 (± 4.54) % on day 21. The increased in gene silencing percent from day 7 could be due to the inner siRNA layer of the particles being exposed to the cytoplasm, sustaining siRNA release to prolong knockdown of *SPARC* on day 14 and day 21. The percentage of *SPARC* knockdown was not only consistent at 35.95 (± 4.26) % on day 14 and at 33.17 (± 4.54) % on day 21, but also extensive considering that it was already three weeks into the study conducted with a single dosage of particles. This evidently showed that the developed multilayered siRNA loaded particle could indeed sustained release of siRNA within the cytoplasm and elicit prolonged gene silencing effect with just a single application over 3 weeks. The unaccounted siRNA (digestion by lysosome or consumed for gene silencing) on day 14 and day 21 further increased as compared to day 7 at 89.05 (± 0.87) % and 96.36 (± 0.94) % respectively. This correlates to the significant gene silencing of *SPARC*.

All in all, it is important to note that a total amount of 618.13 (± 3.97) pmol of siRNA was loaded in the 7 layered NPs system. Over the 21 days period of the study, free siRNA was found to be present in the cells/cytoplasm which leads to a significant percentage of *SPARC* knockdown. The reason to such an observation could be due to the material properties of PLR (which was coated in the bilayers of the LbL NPs system). PLR has unique properties such as possessing a high loading capacity for siRNA, has a high transfection efficiency and also it is highly positively charged. Therefore, it could protect the NPs from lysosomal enzymes through extensive pore formation [6] which allows the NPs to escape from the endosome to the cell cytoplasm, to provide sustained and prolonged release of siRNA for its mode of action (to silence the gene of interest).

The release profile of siRNA within the cells at the respective time interval of day 1, day 3, day 5, day 7, day 14 and day 21 could also be evaluated. The amount of siRNA that were consumed/degraded (refer to Figure 5.1) can be calculated from the subtraction of 'the amount of free siRNA within cells' with 'the amount of siRNA remaining in the LbL NPs' by 100 %.

The calculated cumulative/consumed percentage siRNA release profile within the cells on day 1 was 62.37 (± 3.89) %, followed by an increase to 81.09 (± 3.19) % on day 3 and 91.99 (± 0.53) % on day 5. There was a drop in the release profile at 89.03 (± 2.33) % on day 7 but the release profile increased on day 14 at 98.48 (± 0.13) % and remained similar at 99.15 (± 0.68) % on day 21.

The *in vitro* siRNA release profile within the cells could be compared with the siRNA release profile in PBS (pH 7.40) release medium from Figure 4.4. The cumulative percentage of siRNA release in PBS (pH 7.40) release medium on day 1 was 2.26 (± 0.00) %, followed by 5.00 (± 0.08) % on day 3, 7.18 (± 0.09) % on day 5, 8.70 (± 0.12) % on day 7, 11.27 (± 0.13) % on day 14 and 15.54 (± 0.17) % on day 21. The respective graphical representation for the cumulative/consumed percentage siRNA release profile within the cells and the cumulative percentage of siRNA release in PBS (pH 7.40) release medium is shown in Figure 5.3 below:

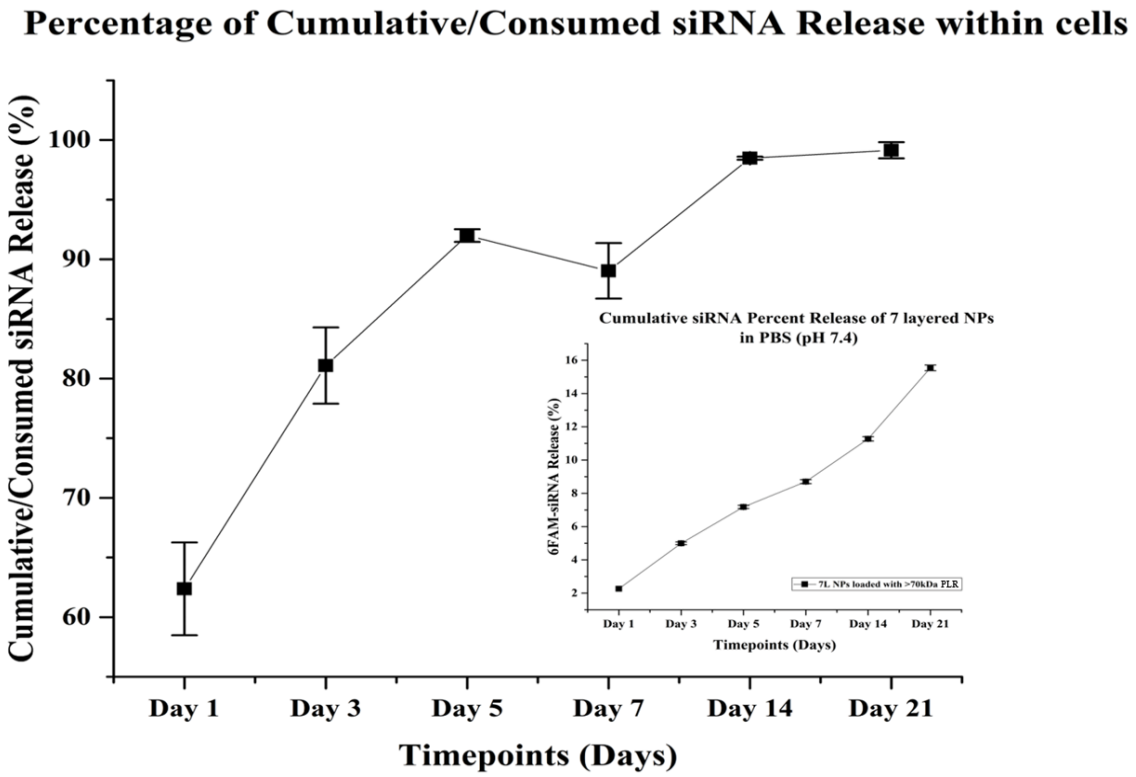

Figure 5.3: *In vitro* cumulative/consumed siRNA release profile within the cells and the cumulative siRNA release profile in PBS (pH 7.40) release medium. The release of siRNA in the cells was higher than the release of siRNA in PBS (pH 7.40) release medium. This could be due to certain interaction of the cellular components in the cytoplasm with the particle system. Hence, induces the higher release profile within the cells. However, the release behavior (within the cells and in PBS medium) were similar over 21 days. All samples were prepared and readings measured in triplicates.

Figure 5.3 shows that the *in vitro* cumulative/consumed siRNA release within the cells were higher than the cumulative release of siRNA in PBS (pH 7.40) release medium. This could be due to the cellular entry and the endosomal escape of LbL NPs resulting in faster defoliation of the outermost PLR layer, exposing the outermost siRNA layer to the cytoplasm and continuously release siRNA. In a study conducted by Jaganathan *et al.*, an investigation was done to observe the release profile of LbL siRNA nanovectors (SNV) in

simulated cytoplasmic and endosomal environments. It was found that the various cellular components present in the cells (cell cytoplasm consists of the fluid known as cytosol and also various ions and organic molecules, salts, enzymes and organelles) might have induced the higher amount of siRNA release in the cytoplasm simulated environment [16]. It was suggested that the cytoplasm is a highly reductive environment and the components from SNV may undergo redox reactions which trigger the release of siRNA from particles [17, 18]. The higher cumulative/consumed siRNA release profile within the cells is essential as the amount of free siRNA (observed from Figure 5.1) found within the cells could then be utilized for a significant gene silencing effect as observed in Figure 5.2.

The cumulative/consumed siRNA release profile within cells showed (taking into consideration the amount of siRNA consumed/degraded) an increase in the release of siRNA from day 1 to day 5 but experienced a drop in the release profile from day 5 to day 7. This could be further explained from the previous data from Figure 5.1 and Figure 5.2 that during the first 5 days, NPs could have internalized into the cells (escaping from endosome into the cytoplasm) releasing free siRNA in the cytoplasm. The free siRNA present in the cytoplasm could be used for the knockdown of *SPARC,* with the most knockdown effect observed on day 5. From day 5 to day 7, the drop in the release profile could be due to cell division and the mRNA regeneration process that were occurring. Hence, leading to the lower amount of siRNA within the cells and also the drastic drop in the amount of SPARC knockdown. Also, on day 7 the outermost siRNA layer of the NPs could have been defoliated/exhausted, leading to the decrease in siRNA release within cells. This can be referred to the defoliation study previously conducted by Tan *et. al.* in which the authors found that the LbL NPs have been detached from the system by day 9 starting from the outermost layer which suggests LbL NPs disassembly through the layer by layer 'onion effect' [6]. From the current study, it proves that the outermost layer of the LbL NPs could be defoliated/exhausted before day 9. The siRNA release profile within cells has increased from day 7 to day 21. This observation could indicate that the inner layer of siRNA could be exposed to the cytoplasm and also it is important to note that the amount of free siRNA within cells at day 14 and day 21 could still cause a significant knockdown of *SPARC*. Furthermore, the siRNA release profile within cells at day 14 and

day 21 remained similar and the knockdown activity shows similar percentage of SPARC gene silencing as well. This suggest the potential of the LbL NPs system in achieving a sustained release of free siRNA in the cytoplasm at day 14 and day 21.

Further, the cumulative/consumed percent siRNA release within cells could be correlated to the cumulative percent siRNA release in PBS (pH 7.40) based on the steepness of their respective release profile. From Figure 5.3, the respective release profile experienced the same steepness from day 1 to day 5. The LbL NPs could have entered into cells and was releasing siRNA as observed from the release profile of the cumulative/consumed percent siRNA release within cells. Whereas the siRNA release in PBS (pH 7.40) was observed that the outermost siRNA layer could be exposed and released into the PBS medium from day 1 to day 5. However, the release profile was shifted from day 5 to day 7 for both the cumulative/consumed percent siRNA release within cells and the cumulative percent siRNA release in PBS (pH 7.40). The cell division and mRNA regeneration could be happening between day 5 to day 7 for the cumulative/consumed percent siRNA release within cells. Whereas the outermost layer of the LbL NPs could have been defoliated/exhausted between day 5 to day 7 as observed from the shift in the release profile of the cumulative percent siRNA release in PBS (pH 7.40). Following this, from day 7 to day 21, the release profile of the cumulative/consumed percent siRNA release within cells and the release profile of the cumulative percent siRNA release in PBS (pH 7.40) have both increased. This could indicate that most of the outermost layer of the LbL NPs has been detached, exposing the inner siRNA layer in the cells and also in the PBS (pH 7.40) medium.

This indicates that the 7 layered LbL NPs (containing 3 layers of siRNA) could enter into cells, escaping from endosome into the cytoplasm to release siRNA via the disassembly of LbL NPs through a layer by layer ‘onion effect’ (starting with the outermost layer). Hence, leading to the efficient and prolonged gene silencing effect over 21 days with just a single application. This serve to advance the field of non-viral gene therapy as the multilayered NPs system could be utilized as a suitable vector to increase the delivery efficiency and prolong its effect to combat against various diseases (i.e. fibrosis) that requires sustained

intervention. Further, according to a previous study by Tan *et al.*, the NPs were investigated for their release profile in a release medium (PBS pH 7.40)[6] but the study was lacking as the release environment/behavior in PBS medium might not be similar to the environment inside the cells since proteins, ions and organic molecules would be present. Also, there were no studies done to elucidate the amount of siRNA release inside the cells over the stipulated time intervals. Here, for the first time, the study was done to provide comprehensive investigation on the multilayered delivery system releasing siRNA inside the cells/cytoplasm to cause an effective and prolonged gene silencing effect over 21 days with just a single application.

References

[1] Ward, T.C., *Molecular weight and molecular weight distributions in synthetic polymers.* Journal of Chemical Education, 1981. **58**(11): p. 867-879.

[2] Alfred Rudin, P.C., in *The Elements of Polymer Science & Engineering*. 2013, Elsevier: USA. p. 1-62.

[3] Yam, K.L., *Encyclopedia of Polymer Science and Technology*. 4th ed, ed. H.F. Mark. Vol. 15. 2010, USA: John Wiley & Sons, Inc.

[4] Hua Lu, J.W., Ziyuan Song, Lichen Yin, Yanfeng Zhang, Haoyu Tang, Chunlai Tu, Yao Lin and Jianjun Cheng, *Recent advances in amino acid N-carboxyanhydrides and synthetic polypeptides: chemistry, self-assembly and biological applications.* Chem. Commun., 2014. **50**(2): p. 139-155.

[5] Xinna Zhao, K.M., Tifeng Jiao, Ruirui Xing, Xilong Ma, Jie Hu, Hao Huang, Lexin Zhang and Xuehai Yan, *Fabrication of Hierarchical Layerby-Layer Assembled Diamond-based Core-Shell Nanocomposites as Highly Efficient Dye Absorbents for Wastewater Treatment.* Scientific Reports, 2017. **7**(44076): p. 1-13.

[6] Yang Fei Tan, Y.S.L., Li-Fong Seet, Kee Woei Ng, Tina T. Wong and Subbu Venkatraman, *Design and in vitro release study of siRNA loaded Layer by Layer nanoparticles with sustained gene silencing effect.* Expert Opinion on Drug Delivery, 2018. **15**(10): p. 937-949.

[7] Betul Bozdogan, O.A., Ekin Çelik, Mustafa Turk and Emir Baki Denkbas, *Novel layer-by-layer self-assembled peptide nanocarriers for siRNA delivery.* RSC Adv., 2017. **7**: p. 47592–47601.

[8] Cheol Am Hong, H.Y.S.a.Y.S.N., *Layer-by-layer siRNA/poly(L-lysine) Multilayers on Polydopamine-coated Surface for Efficient Cell Adhesion and Gene Silencing.* Scientific Reports, 2018. **8**(7738): p. 1-7.

[9] Chithrani BD, G.A., Chan WC, *Determining the size and shape dependence of gold nanoparticle uptake into mammalian cells.* Nano Lett. , 2006. **6**(4): p. 662-668.

[10] Chithrani BD, C.W., *Elucidating the mechanism of cellular uptake and removal of protein-coated gold nanoparticles of different sizes and shapes.* Nano Lett. , 2007. **7**(6): p. 1542–1550.

[11] Li Fong Seet, Y.F.T., Li Zhen Toh, Stephanie WL Chu, Ying Shi Lee, Subbu S Venkatraman, Tina T Wong, *Targeted therapy for the post-operative conjunctiva: SPARC silencing reduces collagen deposition.* Br J Ophthalmol, 2018. **102**(10): p. 1460–1470.

[12] Stephanie E. A. Gratton, P.A.R., Patrick D. Pohlhaus, J. Christopher Luft, Victoria J. Madden, Mary E. Napier, and Joseph M. DeSimone, *The effect of particle design on cellular internalization pathways.* PNAS, 2008. **105**(33): p. 11613–11618.

[13] Seung Koo Lee Dr., M.S.H., and Ching-Hsuan Tung Dr. [Prof.], *Layered nanoprobe for long-lasting fluorescent cell label.* Small, 2012. **8**(21): p. 3315–3320.

[14] Lennart Treuel, X.J.a.G.U.N., *New views on cellular uptake and trafficking of manufactured nanoparticles.* J R Soc Interface, 2013. **10**(82): p. 1-14.

[15] Lorant Lakatos, T.C., Vitantonio Pantaleo, Elisabeth J Chapman, James C Carrington, Yu-Ping Liu, Valerian V Dolja, Lourdes Fernandez Calvino, Juan Jose Lopez-Moya and Jozsef Burgyan, *Small RNA binding is a common strategy to suppress RNA silencing by several viral suppressors.* The EMBO Journal, 2006. **25**(12): p. 2768–2780.

[16] Hamsa Jaganathan, S.M., Srimeenakshi Srinivasan, Bhuvanesh Dave, Biana Godin, *Design and In Vitro Evaluation of Layer by Layer siRNA Nanovectors Targeting Breast Tumor Initiating Cells.* PLOS ONE, 2014. **9**(4): p. 1-8.

[17] Zhao E, Z.Z., Wang J, Yang C, Chen C, Gao L, Feng Q, Hou W, Gao M, Zhang Q., *Surface engineering of gold nanoparticles for in vitro siRNA delivery.* Nanoscale, 2012. **4**(16): p. 5102-9.

[18] Tan SJ, K.P., Roh YH, Kahn JS, Luo D., *Engineering Nanocarriers for siRNA Delivery.* Small, 2011. **7**(7): p. 841-56.

Chapter 5

Future Work

Moving forward, the modification of HAp NPs could be employed to increase the overall negative surface potential of the core material. This is to compensate the loss of subsequent polyelectrolyte layer from the necessary washing steps during the fabrication process. In this thesis, the designed multilayered LbL NPs system is loaded with SPARC siRNA which has the potential to reduce fibrosis as discussed from various studies. The designed layer by layer NPs system could be utilized to deliver other types of therapeutic agents (such as a different kind of siRNA) for gene silencing. The NPs system could also be loaded with the different types of siRNA per layer to target the many undesirable proteins which may be produced sequentially over the stipulated time intervals with just a single application. From the gene knockdown effect as observed in this thesis, further experiments could be carried out to correlate with the data. For instance, to examine the mRNA levels in the cell cytoplasm at the respective time interval by utilizing the quantitative PCR (QPCR) technique. This information should show a correlation with the gene knockdown study. With a higher amount of knockdown activity in the cell cytoplasm, the mRNA level is expected to decrease. In vivo studies could be investigated to observe the effect of the multilayered LbL NPs on diseased animals and if the results are desirable, the multilayered LbL NPs system could potentially be introduced into the clinical trials in future.

5.1 Modification of HAp core material to increase polyelectrolyte loading

The increase in the number of siRNA layers proves that more siRNA can be loaded in the LbL NPs which results in a higher, prolonged and sustained rate of release. Modifications to the HAp core material could be incorporated in the current system to further improve the loading of the polyelectrolyte layer which might be loss due to the necessary washing steps during the fabrication process. For instance, by increasing the net negative surface potential of the core material, HAp NPs could potentially attract more positively charged PLR polyelectrolytes. Hence, this could balance out the loss of certain amount of the PLR layer during the fabrication process. An increase in the positively charged polyelectrolyte layer could in turn further increase the total siRNA capacity in the LbL NPs system. This could also compensate the loss of certain amount of siRNA during the washing steps. HAp NPs could be coated with sodium carboxymethyl cellulose, SCMC (a polymer with highly net negatively charged surface potential) for this purpose [1]. Building upon this proposition, HAp NPs could be coated with SCMC and subject to zeta potential and size measurement followed by the subsequent fabrication steps to form the 7 layered SCMC-coated HAp LbL NPs.

5.2 Fabrication of multilayered NPs loaded with different types of siRNA per layer

In the current study, the multilayered NPs system were loaded with SPARC siRNA to cause the gene silencing of SPARC which in turn would lead to the reduction of fibrosis at the site of injury. However, in order to target the many undesirable proteins which may be produced sequentially over different time intervals, various types of siRNA could be loaded into each layer of the multilayered NPs system. This could be done to target various diseases at the same time with just a single application. For instance, the various undesirable protein interactions (such as amyloid fibers and oligomers) causes the onset of several diseases such as Huntington's disease, cystic fibrosis and Alzheimer's disease [2-4]. The amyloid precursor protein (APP) and β-secretase activity have been found to associate with the various neurodegenerative diseases and the amyloid precursor protein (APP) siRNA and β-secretase siRNA were found to initiate the gene silencing of APP and β-

secretase [5, 6]. Hence, the multilayered NPs system can be employed to load the respective siRNA into each of the layers to target against the undesired proteins over the stipulated time intervals. The flexibility and effectiveness of the multilayered NPs system to cater to a wide variety of applications would enhance its significance in nanomedicine.

5.3 Investigation by quantification of mRNA

In this study, the 7 layered LbL NPs (siSparc-LbL and siScram-LbL) was utilized to investigate the effect of siRNA release within the cell cytoplasm to cause a significant gene silencing effect over 21 days. The same experiment (utilizing the 7 layered siSparc-LbL and 7 layered siScram-LbL) should be repeated for the quantification of mRNA which can be measured by utilizing the quantitative PCR (qPCR) technique. qPCR is a technique used for the quantification of nucleic acids (i.e. messenger RNA, mRNA) in a sample and it allows the mRNA to be screened concurrently [7]. This information is important as it could in turn be correlated to the amount of gene knockdown in the cell cytoplasm. The mRNA level in the cell cytoplasm is expected to be decreased with a higher amount of the knockdown activity. The correlation between these experiments would further affirm the effectiveness of the 7 layered LbL NPs system by releasing siRNA consistently in the cell cytoplasm for a prolonged gene silencing effect.

5.4 *In vivo* studies on diseased models

Various particle characterization and *in vitro* studies has been employed to increase the total siRNA loading capacity and to evaluate the effectiveness of the 7 layered LbL NPs system. The investigations from these studies showed that it is possible to increase the loading of therapeutic agents by the simple modification of the particle system. Also, the particle system was observed to exhibit prolonged release of siRNA *in vitro* (both in PBS medium and within the cells). The effectiveness of the multilayered NPs system was validated by the ability to cause an efficient and prolonged knockdown effect over 21 days. Therefore, *in vivo* experiments should be performed to test the effect of the same multilayered NPs system on diseased animal model. For instance, since mouse and humans

share the similar genomes [8], *in vivo* studies could be carried out using mouse models. This is to investigate the efficacy of the particle system to deliver siRNA in living organism as compared to the *in vitro* studies. Other observations from the *in vivo* studies can be evaluated as well, such as the murine toxicology and pharmacology studies to ensure safe dosages of the therapeutic agents administered. If the *in vivo* studies using the 7 layered LbL NPs system is successful, the system could potentially be introduced into the clinical trials in future.

5.5 Conclusion

The interim conclusion to this thesis by fabricating the LbL NPs system utilizing HAp NPs as the core material, with PLR as the polyelectrolyte (PE) layer, is based on the experiments motivated at incorporating more SPARC siRNA into the system. The ultimate aim is to maximize the total siRNA loading capacity and to achieve an effective and prolonged gene silencing of SPARC. The effect of PLR and siRNA amount on the LbL NPs did not show significant difference to the total siRNA content. The utilization of different PLR M_w shows that the 3 layered NPs loaded with PLR >70 000 Da exhibits the highest total siRNA content. Additional siRNA layer was coated on the LbL NPs system. It was observed that the 7 layered NPs containing 3 layers of siRNA showed the highest total siRNA content. This suggest that the additional siRNA layers can help in maximizing the total siRNA content in the LbL NPs system. TEM images reveal that the NPs are morphologically spherical and the cell viability assay suggest that the dosage selected were not toxic to HuRPF cells. The release study in PBS medium (pH 7.40) over 28 days concludes the highest release amount and fastest release rate in the 3 layered NPs loaded with PLR >70 000 Da. The 3, 5 and 7 layered NPs loaded with PLR >70 000 Da was examined for their release profile over 28 days in PBS medium (pH 7.40). The 7 layered NPs exhibits the highest release amount and fastest release rate. Releasing more amount of siRNA at each time interval could result in a more effective and prolonged gene silencing effect. With that, the 7 layered NPs system was selected as the optimal particle to be used for subsequent *in vitro* experiments. The particles internalization into HuRPF cells was confirmed by CLSM. The flow cytometry shows the percentage of cells containing LbL 6FAM-siRNA

NPs detected within the cells over 21 days. Following this, the amount of free siRNA release within cells and also the gene knockdown efficiency was investigated over 21 days. The data shows that the amount of free siRNA release within cells causes an efficient and prolonged gene silencing of SPARC over 21 days. This validates the effectiveness of the 7 layered LbL NPs system which has the potential in delivering an efficient and prolonged gene silencing effect for 21 days with just a single application. The flexibility and effectiveness of the multilayered NPs system could be utilized to cater to various disease targets. For instance, the modification of HAp NPs could be employed to increase the overall negative surface potential of the core material. The designed particle could be used to deliver other types of therapeutic agents (such as a different kind of siRNA) for gene silencing. It could also be loaded with different types of siRNA per layer to target against the many undesirable proteins with just a single application. Further studies to investigate the mRNA levels in cell cytoplasm should be examined which could in turn correlate with the gene knockdown study. *In vivo* studies should be employed to test the effect of the multilayered NPs system on diseased animals and if the results are desirable, it could potentially enter into clinical trials.

References

[1] Grzadka, E., *The Adsorption Layer in the System: Carboxymethylcellulose/Surfactants/NaCl/MnO2.* J Surfact Deterg, 2012. **15**(4): p. 513–521.

[2] Mileidy W. Gonzalez, M.G.K., *Chapter 4: Protein Interactions and Disease.* PLOS Computational Biology, 2012. **8**(12): p. 1-11.

[3] Martin L. Duennwald, S.J., Flaviano Giorgini, Paul J. Muchowski, and Susan Lindquist, *A network of protein interactions determines polyglutamine toxicity.* PNAS, 2006. **103**(29): p. 11051-11056.

[4] Jucker, D.E.a.M., *The amyloid state of proteins in human diseases.* Cell, 2012. **148**(6): p. 1188–1203.

[5] Oded Singer, R.A.M., Edward Rockenstein, Leslie Crews, Nicole G Coufal, Fred H Gage, Inder M Verma & Eliezer Masliah, *Targeting BACE1 with siRNAs ameliorates*

Alzheimer disease neuropathology in a transgenic model. Nature Neuroscience, 2005. **8**(10): p. 1343-1349.

[6] Yann Senechal, P.H.K., John F. Cryan, Francois Natt and Kumlesh K. Dev, *Amyloid precursor protein knockdown by siRNA impairs spontaneous alternation in adult mice.* Journal of Neurochemistry, 2007. **102**(6): p. 1928–1940.

[7] Medrano, M.L.W.a.J.F., *Real-time PCR for mRNA quantitation.* BioTechniques, 2005. **39**(1): p. 75-85.

[8] Richard J. Murala, E.W.M., Hamilton Smitha, George L. Gabor Miklosb, Ron Widesc, Aaron Halperna, Peter W. Lia, Granger Suttona, Joseph H. Nadeaud, Steven L. Salzberge, Robert Holta, Cheryl A. Evansa, Fu Lua, Kendra Biddicka, Vivien Bonazzia, Arthur Delchera, Xiangqun H. Zhenga, Mark Yandella, Doug Ruschf, William Majorosa, Jeff Hoovera, Jian Wanga, J. Craig Venterf, Mark D. Adams, *A preliminary comparison of the mouse and human genomes.* International Congress Series, 2002. **1246**(C): p. 169–181.